TABLE OF CONTENTS

Page

LIST OF TABLES

Page

LIST OF FIGURES

Page

LIST OF ABREVIATIONS

AC	Alternative current
AF	Active filter
APF	Active power filter
CHB	Cascaded H-Bridge
DC	Direct current
DQ	Synchronous reference frame
EV	Electrical vehicle
FC	Flying Capacitor
HB	Half Bridge
HSR	High-speed railway
HSTs	High speed train system
IEEE	Institute of Electrical and Electronics Engineering
IGBT	Insulated gate bipolar transistor
KVL	Kirchhoff's Voltage Law
LVF	Low voltage fluctuation
NPC	Neutral Point Clamped
PCC	Point of common coupling
PFC	Power Factor Correction
PI	Proportional Integral
PLL	Phase Locked Loop
PQ	Instantaneous Reactive Power Theory

PV	Photovoltaic
PWM	Pulse width modulation
RMS	Root Mean Square
SAF	Shunt active filters
SAPF	Shunt Active Power Filter
SMC	Sliding Mode Control
SPS	Sim Power System
SPWM	Sinusoidal pulse width modulated
SRF	Synchronous reference frame
THD	Total harmonic distortion
TPSS	Traction power supply system
UPOC	Unified power quality conditioner
UPS	Uninterruptable power supplies
VSC	Voltage source converter
VSI	Voltage source inverter

INTRODUCTION

Over the past few decades, and since the introduction of power electronics, power quality has become a great preoccupation. As defined by world standards, power quality is identified as the "physical characteristics of the electrical supply provided under normal operating conditions that do not disrupt or disturb the user processes" (Khadkikar et Chandra, 2008) The spread of power electronics systems used in a number of various nonlinear producing loads degrades the electric supply networks' power quality, especially at the level of end users. Common instances of those comprise household equipment, office machinery and computers, adjustable speed drives (ASDs), uninterruptible power supplies (UPS) and industrial furnaces. These converters generate harmonic currents that cause malfunctions and failures of protection systems, equipment overheating, noise, vibration and interferences with communication systems. Therefore, with the objective of mitigating the harmonic pollution within power systems, the IEEE (Institute of Electrical and Electronics Engineers) and IEC (international Electro technical Commission) have come up with regulating guidelines, standards IEEE 519 and IEC 61000 in an attempt to govern the accepted limits of injected (Standard, 2004)

Table 1.1 IEEE519 harmonic current limits

I_{sc} / I_{L1}	h<11	11≤h<17	17 ≤ h < 23	23 ≤ h < 35	35 ≤ h	THD (%)
< 20	4.0	2.0	1.5	0.6	0.3	5.0
20 - 50	7.0	3.5	2.5	1.0	0.5	8.0
50 - 100	10.0	4.5	4.0	1.5	0.7	12.0
100 - 1000	12.0	5.5	5.0	2.0	1.0	15.0
> 100	15.0	7.0	6.0	2.5	1.4	20.0

This project's main purpose is to build a configuration can be used in the near future to allow electric vehicle chargers to be offered in the residential group's integrating solar or wind energy to support a grid. The configuration can be extended to supply the electrification

railway systems. A configuration that is used as an interface from a single phase to the three-phase power grid and loads including five-level dc/ac converter uses Leblanc transformer/Scott transformer. Both converters enable compensating harmonics, reactive power and load imbalances, the link between two single-phase sources and a three-phase source. A control is also developed to achieve these objectives, a technique of balancing of the currents allowed to balance the two currents in the secondary of the Leblanc transformer is proposed, which has an impact on the balance of current on the side of the three-phase network at the primary of the Leblanc transformer.

The aim of using Le-Blanc transformer is to link the single-phase power to electric railway from the general grid of three-phase system. Nowadays one of the major problems in the railway traction system in terms of network's power quality caused by (AC) electrified is voltage and current. There are numerous methods that are and can be used to decrease such unbalance issues.

Four contributions of the project research are carried out, it concern:

- Proposed configuration for residency group integrating a charging electric vehicle supported by a PV solar from three phases main grid to multiple single phases;
- Configuration for railway train integrating a PV solar, Leblanc transformer with power quality improvement;
- Developed control to improve to balance a current in the grid side;
- Review of different control applied to single-phase inverter.

The present project's study is mainly about the introduction of two single-phase five level inverters scheme in the secondary of the Leblanc transformer/Scott transformer to improve power quality in the grid side. The present's thesis is organized as per the following:

In chapter one is presented a literature review for different topologies and mitigation techniques, multilevel inverter, control, different transformer connection and the most special winding connection for balance and unbalance load for power quality issue.

The second chapter includes, a review different kinds of control topologies such as nonlinear control systems, pq control theory and dq control, as well as an analysis the stability of the control system. Validation by simulation of different controls including the design and simulation result showing the different power elements, like the, DC bus voltage and bus capacitor are comprised and link inductor.

Chapter 3 will present a comparison between two different kinds of transformers connection, which is Scott and Leblanc transformer design and Simulation.

Chapter 4 is about applying the integration of Leblanc transformers to supply different utilities such as railway traction with PV solar that connects to the three-phase system via a Leblanc transformer and electrical plug vehicles also by using a Leblanc connection as well as a layout of the simulation findings, including a five-level inverter.

Last of all, a general conclusion on the simulation findings ends the project.

CHAPTER 1

LITERATURE REVIEW

1.1 Introduction

Before 1960, the design of the stage wave cascaded H-Bridge multilevel inverter had made the multilevel inverter technology happen, attempting to create a new control method for generating a surge wave in the output of inverter (Mcmurray, 1971). That cascaded H-bridge inverter's circuit loop was presented in (Bedford et Hoft, 1964), followed by a Diode Clamped Converter, in 1970 (Baker, 1980) However, all of these attempts were only applied in low power energy.

In the 1980s the Cascade H-Bridge (CHB) and Neutral Point Clamped (NPC) were introduced in medium applications (Baker, 1981; Nabae, Takahashi et Akagi, 1981). Then during the 1990s, the low-voltage Flying Capacitor (FC) inverter, which had been created in the 1960s, was revisited for medium- and high-power voltage applications. The authors discuss high-voltage power conversion. They go through and compare conventional series connection and three-level voltage source inverter methods. They present a new versatile multilevel commutation cell, proving that it's a safer and an easier to control structure, and that it produces purer output waveforms. They also explain the way this method can be used for either choppers or voltage-source inverters and can also be broadened to be used for any number of switches (Meynard et Foch, 1992).

Around the same time as the commercialization of 4500 V gate turn-off (GTO) thyristors (mid 1980s), there was the launch of medium-voltage motor drive as an example of the application of those devices (Wu, Converters et Drives, 2006). Later on, during the late 1990s, the fabrication of insulated gate bipolar transistors (IGBT) and gate commutated thyristors (GCT) evolved from high power switch development (Steimer et al., 1997).

Because of their simple gate-control, snubber less operation, and low power loss, these switches were then commonly used inside both medium and high power inverters (Wu, Converters et Drives, 2006)

An important characteristic of multilevel inverters is that, through the use of medium-voltage equipment, they can help industries and renewable energy resources provide high power applications. In fact, he interesting features of these multi-level inverters have attracted researchers as well as industries' attention. Some of their major advantages are as per the following (Kouro et al., 2010)

- Reduced distortion of output voltage, as a result of the multiple levels of the output waveform;
- Reduced the voltage by switches that leads to lower dv/dt (voltage stress);
- Lower common mode voltage, a useful feature for motor drives;
- Lower switching losses, by reason of lower switching frequency.

Multilevel inverters of different types have been presented and constructed, most of them for power applications high-voltage and medium (Franquelo et al., 2008) for the reason that a it is not possible to connect a sole power switch directly to grid in case of a medium-voltage.

1.2 Multi-Level Converters Topologies

Many industrial applications necessitate power capabilities from medium power to high power. For example, motor drives and utility applications need medium voltage and megawatt levels of power. In medium to high-voltage power applications, multi-level converters can be a convenient alternative, due to the fact that the rating limitations of power electronic components disallow connecting for only one power semiconductor switch. They also represent a convenient choice for renewable energy systems. Thus, in the past years, a number of multi-level topologies have emerged.(Khomfoi et Tolbert, 2007; Tolbert et Peng, 2000)

There are a different multilevel inverter topologies have been presented (Franquelo et al., 2008; Kouro et al., 2010; Rodriguez, Jih-Sheng et Fang Zheng, 2002) according to the following steps.

1.2.1 The Cascade H-Bridge

Generally utilized in power drives such as high or medium-voltage (Wu, Converters et Drives, 2006). The cascaded H-Bridge multilevel inverter comprises multiple units of single-phase H-Bridge inverters serially connected in each phase. The figure (1.1 a) shows one phase of a seven-level cascaded H-Bridge that contains 3 single-phase H-Bridge cells in each phase(Malinowski et al., 2010). In a Cascaded H-Bridge multilevel inverter, of each phase has an output voltage that can be calculated as: Van=V1+V2+V3.

Two types of Cascaded H-Bridge exists: H-Bridges having equal DC sources and H-Bridges having unequal DC sources, as per description below.

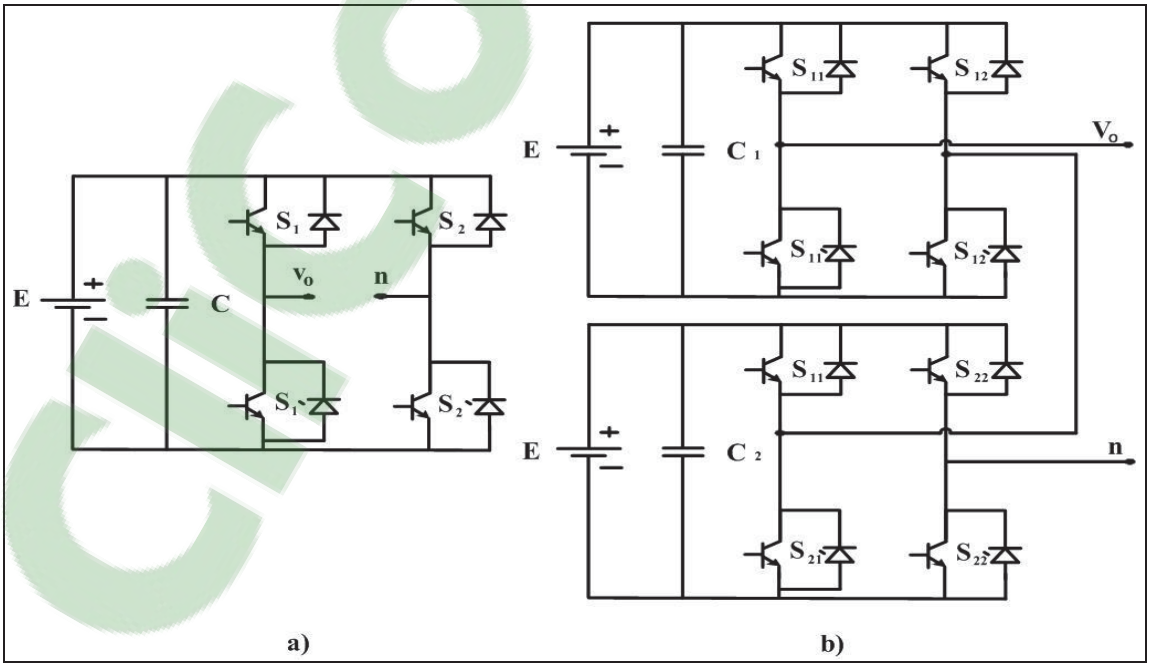

Figure 1.1 a) three-Level b) five-level Single-phase cascade H-Bridge
Taken from Sotoodeh (Sotoodeh, 2014)

This topology was developed prior to the other two basic topologies and has a totally dissimilar configuration. Figure (1.1 b) shows the structure of the three-level and five-level cascaded H-Bridge converter. Each DC source connects to an H-bridge converter. Each H-bridge converter' AC outputs are serially connected in such a way that the combination voltage waveform sums up the inverter outputs.

1.2.2 The Neutral Point Clamped

A Neutral Point Clamped multilevel invert's leg is seen in Figure (1.2) which was originally proposed by (Nabae, Takahashi et Akagi, 1981) after which the three-level Neutral Point Clamped found numerous applications and usages in many industries (Rodriguez et al., 2010)

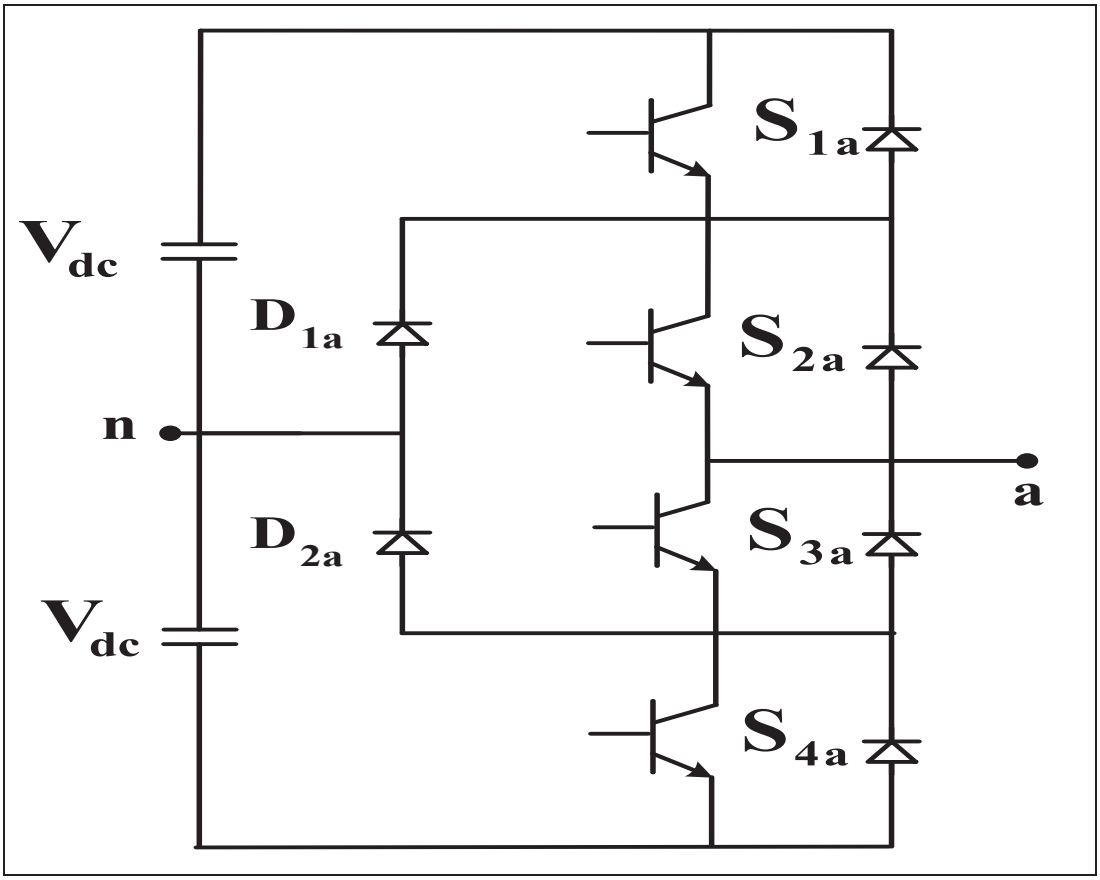

Figure 1.2 Five Level Neutral Point Clamped for single Phase
Taken from Vahedi (Sotoodeh, 2014)

“The clamped diodes (D1a, D2a) are linked to the DC capacitors’ neutral point, resulting in adding a zero level to the output voltage. Therefore, in a three-level Neutral Point Clamped, the output voltage is constituted of -Vdc, 0 and +Vdc. When S1a and S2a are ON, the output is + Vdc. When S3a and S4a are ON, the negative voltage appears at the output which is -Vdc. Finally, if S2a and S3a are ON, the voltage at the point (a) will be 0. S3a complements S1a and the same for S2a and S4a. As an example, when S1a is ON, S3a is OFF. This topology’s main advantage is in the fact that it is flexibly controllable by space vector modulation (Lewicki, Krzeminski et Abu-Rub, 2011; Rojas, Ohnishi et Suzuki, 1995) additionally to PWM. With this characteristic the Neutral Point Clamped becomes a multilevel inverters’ topology that is favored by researchers, for them to develop its control strategy, by presenting and testing a number of different methods of control (Bor-Ren et Ta-Chang, 2004; Das et Narayanan, 2012). However extensively utilized in applications, of high power the Neutral Point Clamped topology is seen as having the following drawbacks balancing the capacitors voltages and unequal loss distribution among switches”.(Vahedi, 2016)

1.2.3 The Diode-Clamped (DC) Topology

The diode-clamped multilevel inverter is among the main multilevel inverter topologies. The single-phase types of these inverters have been characterized as not having redundant states. Significantly, such states are suitable for reducing devices switching frequency throughout the inverter operation, and hence for reducing switching power losses and targeted to electromagnetic distortion influence. They also enhance other features of inverter performance for example enabling capacitor voltage balancing. It consists in using a number of diodes that will obstruct small DC sources. Single-phase three-level and configuration of a five-level diode-clamped inverter are drawn in Figures (1.3 a) and (1.3 b),respectively (Chaulagain et Diong, 2016)

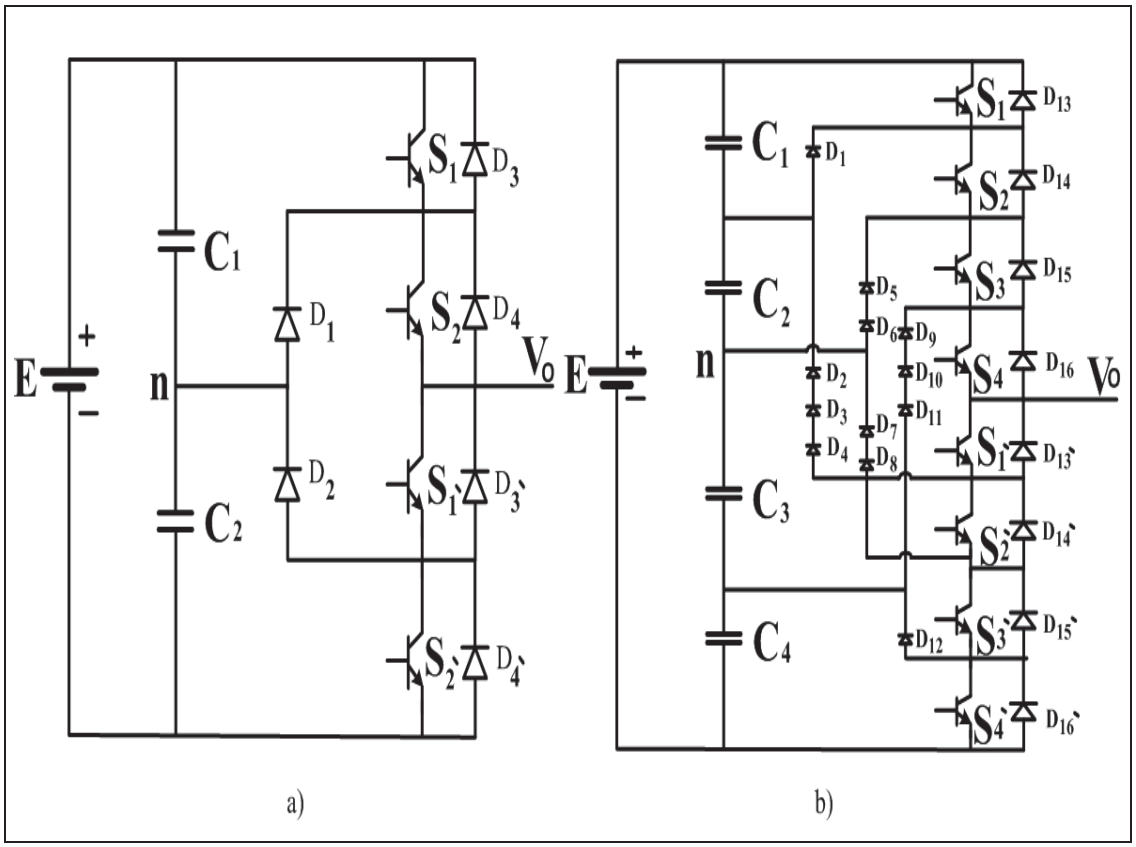

Figure 1.3 a) Single-phase three-level b) Single-phase five-level topology
Taken from Sotoodeh (Sotoodeh, 2014)

“Extending the DC topology to a collective number of level configurations is easy. In a three-level diode-clamped inverter, the DC bus voltage is separated by capacitor banks into two steps of the same voltage. The inverter’s functioning is simple. The DC topology’s name derives from the voltage between two switches being attached through the clamping diodes. When switches (S1,S2) are on and (S1‘,S2‘) are off, the inverter’s output voltage is equal to the voltage of C1, which is equal to(+E)/2. Similarly, when switches (S1,S2) are off and (S1‘,S2‘) are on, the inverter’s output voltage is equal to C2’s voltage, which is equal to (-E)/2. When (S2, S1‘) are on and (S1, S2‘) are off, the inverter’s output voltage is equal to 0. In a five-level diode-clamped inverter, the DC bus voltage is divided into four steps of the same voltage. Here, the number of diodes needed to clamp the voltage changes point after point. Each diode is set to supply voltage blocking across one capacitor. For example, only one diode represents D1, while three diodes equal to D1 represent D1’, diodes that are in

series because they must obstruct voltage through capacitors C2, C3 and C4; in other words, it allows using one diode with higher blocking capacity or three diodes placed in series with same blocking capacity as D1. Considering the diode reverse voltage for a number of level inverters, formulated by V_r=E/(n-1), for a five-level inverter's -diode revers voltage is equal to E/4, therefore proving that raising the number of levels decreases the components' voltage stress".(Vahedi, 2016)

1.2.4 The Flying Capacitor (FC) topology

The Flying Capacitor is another multilevel inverters' topology and it consists of a battery, three capacitors and four semiconductor switches, as seen in Figure 1.4(Escalante, Vannier et Arzande, 2002).

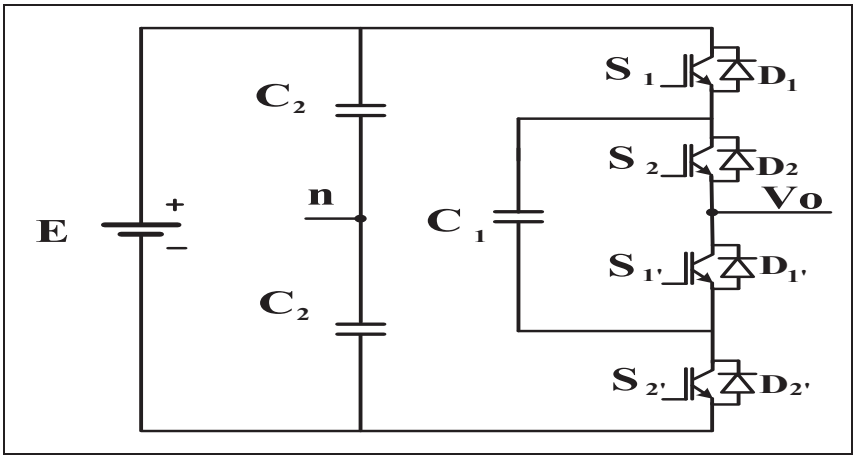

Figure 1.4 One Phase of a Three-Level Flying Capacitor Multilevel Inverter
Taken from Sotoodeh (Sotoodeh, 2014)

In the Flying Capacitor model, a capacitor replaces the clamped diode found in the Neutral Point Clamped. It originates from a two-level inverter in which a capacitor feed each of the two switches. This topology leads to an output which features 3 voltage levels for an output namely –Vdc, 0, +Vdc. Because it uses several capacitors, the Flying Capacitor has restrictions on its use due to its need to have numerous DC capacitors isolators to achieve control of voltage balancing (Wu, Converters et Drives, 2006) Additionally to these topologies, a number of new topologies are recently being applied which are mentioned in

(Kouro et al., 2010). Kouro's topology is similar to the diode-clamped one in which diodes are substituted by capacitors to keep voltage levels the same across DC link capacitors. Figures (1.5 a) and b) show the composition of a single-phase three-level and five-level flying-capacitor inverter. This topology presents a ladder structure of DC dice capacitors, in which each capacitor's voltage is different from the next capacitor's.(Vahedi, 2016)

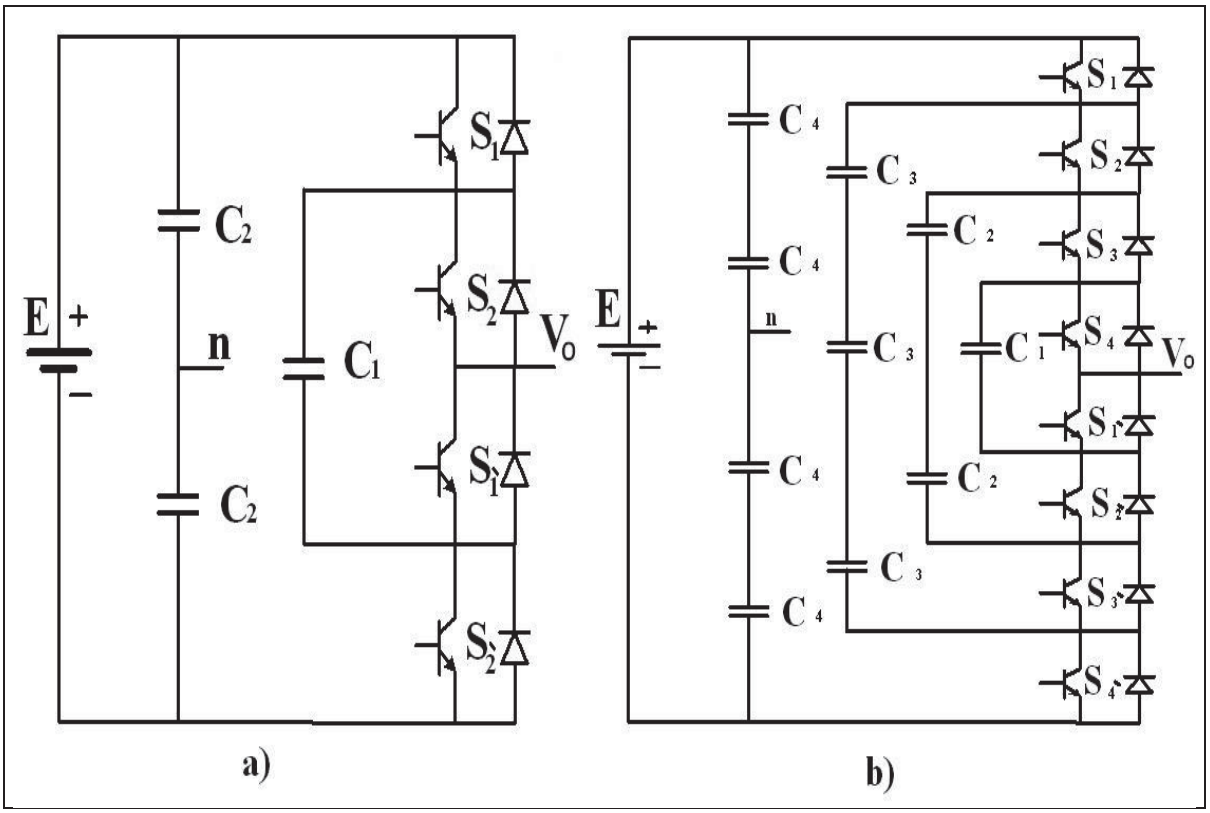

Figure 1.5 a) Single-phase three-level b) Single-phase five-level flying-capacitor topology
Taken from Sotoodeh (Sotoodeh, 2014)

"The three-level flying-capacitor's operation is quite similar to the three-level diode-clamped inverter's operation. When switches (S1,S2) are on and (S1',S2')are off, the inverter's output voltage is equal to $\frac{+E}{2}$ and when switches (S1,S2) are off and (S1',S2') are on, the inverter's output voltage is equal to$\frac{-E}{2}$. When (S1,S1') are on and(S2,S2') are off, the capacitor C1's voltage increases and when(S2,S2') are on and (S1,S1') are off, the capacitor

C1 gets in discharging mode. In the two latter cases, the inverter's output voltage r has value of 0. By switching between these two states, the capacitor C1's charge remains balanced. These two switching states are called intra-phase redundant states, different switch configurations cannot take place in the three-level inverter. S1 and S1' which are the number of switches, should be switched in a complimentary way".(Rodriguez, Jih-Sheng et Fang Zheng, 2002)

1.3 Control applied to the single-phase five level active filters

The Distributed Generation (DG) systems, which rely on renewable energy resources, are essentially sporadic energy sources. Power electronic converters are required as interfaces in order to connect such distributed generation s to the utility grid so that an interface has control synchronization strategies to guarantee the extraction of the maximum achievable power from the primary source as well as its transfer to the grid without compromising the grid's standards of quality.(Khajehoddin et al., 2009) There are several different types of control methods that can be easily used for single-phase five levels active filter.

1.4 Leblanc Transformer

The Leblanc transformer is among the best unbalance mitigation strategies and consists of three transformers two that have three-windings, and one that is with two-winding. The primary windings are the same as the ones found in a regular three-phase transformer, given a delta connection. There are five secondary windings, connected to form into two phases, as seen in Figure (1.6) A Leblanc transformer used nowadays in electric railway systems. It features a special winding connection transformer to generate a single-phase power supply. The balancing and connection schemes are caused by dual secondary loads in the substation of single-phase electrical railway systems where current unbalance can significantly impact the utility supply voltage (Martins, Martins et Pires, 2015). The specially connected Leblanc transformer has an asymmetrical winding structure. Because of its unique winding connection, the Leblanc transformer can change three-phase systems into two-phase or two single power supplies, and thus is considered an attractive alternative for obtaining a two-

phase power system. In fact, the Leblanc transformer performs much better than the Scott transformer with regard to balancing characteristics, maintenance, winding structure high voltage winding connections, and other key factors.

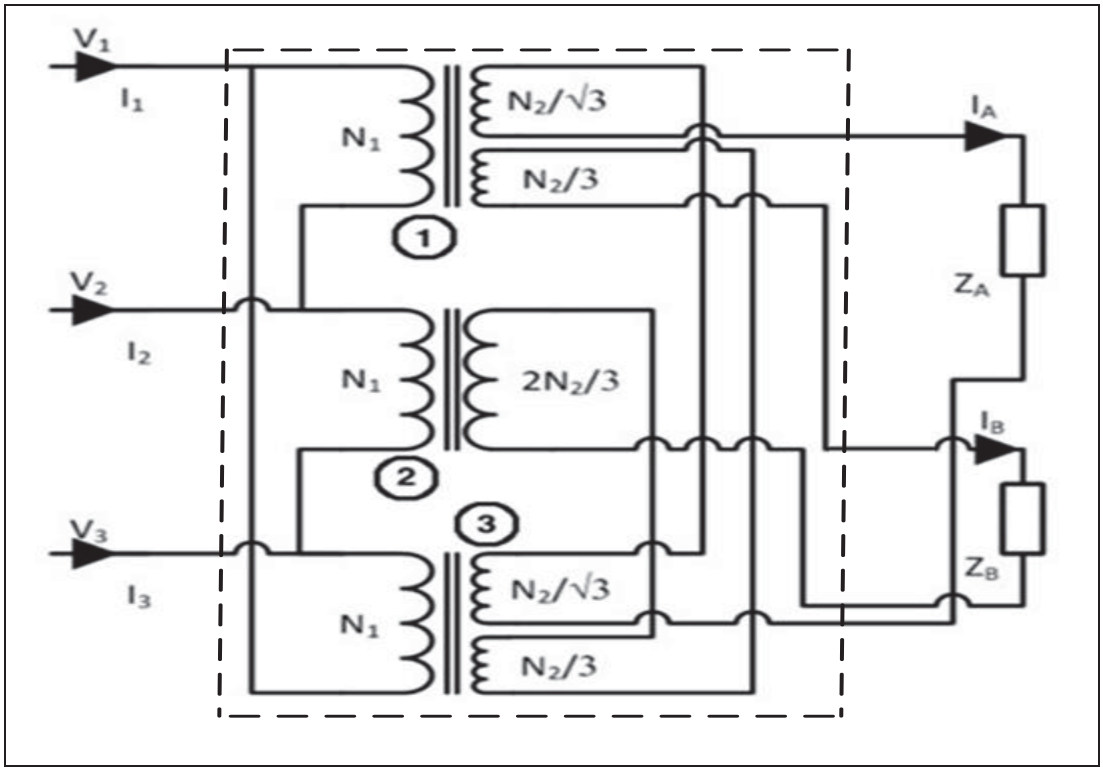

Figure 1.6 The-LeBlanc connexion transformer
Taken from(Martins, Martins et Pires, 2015) (Martins, Martins et Pires, 2015)

1.5 Scott versus blanc Transformer

Like the Leblanc transformer, the Scott transformer is popular for electric rail systems. In cases of two unbalanced single-phase loads, the Scott transformer can change three-phase power supplies into two single-phase ones by reducing the unbalance current, such as in the Tokaido-Shinkansen electric railway (Mochinaga et al., 1991) . It is quite a stress to supply the electrical traction loads on the power supply system.

In general, electric trains use a single-phase AC catenary line for their power supply. In three-phase power systems, single-phase loads are unbalanced. Therefore, when single-phase AC power changes to DC in electric trains, harmonic currents result, along with an unbalanced load. However, each side can be converted to a single-phase load through dividing the catenary line as either outgoing and incoming In this way, there are two equal loads, and the Scott transformer can represent to the three-phase supply system as a single balanced three-phase load, This resolves any imbalance problems. On the other hand, because the two single-phase loads are usually unequal, a certain degree of unbalanced power continues to be drawn by the system through the transformer, but this is less than before. In (Bin-Kwie et Bing-Song, 1996; Chen et Kuo, 1995), the researchers have studied the degree of load unbalance within the three-phase system in the case when two single-phase loads are of different values.

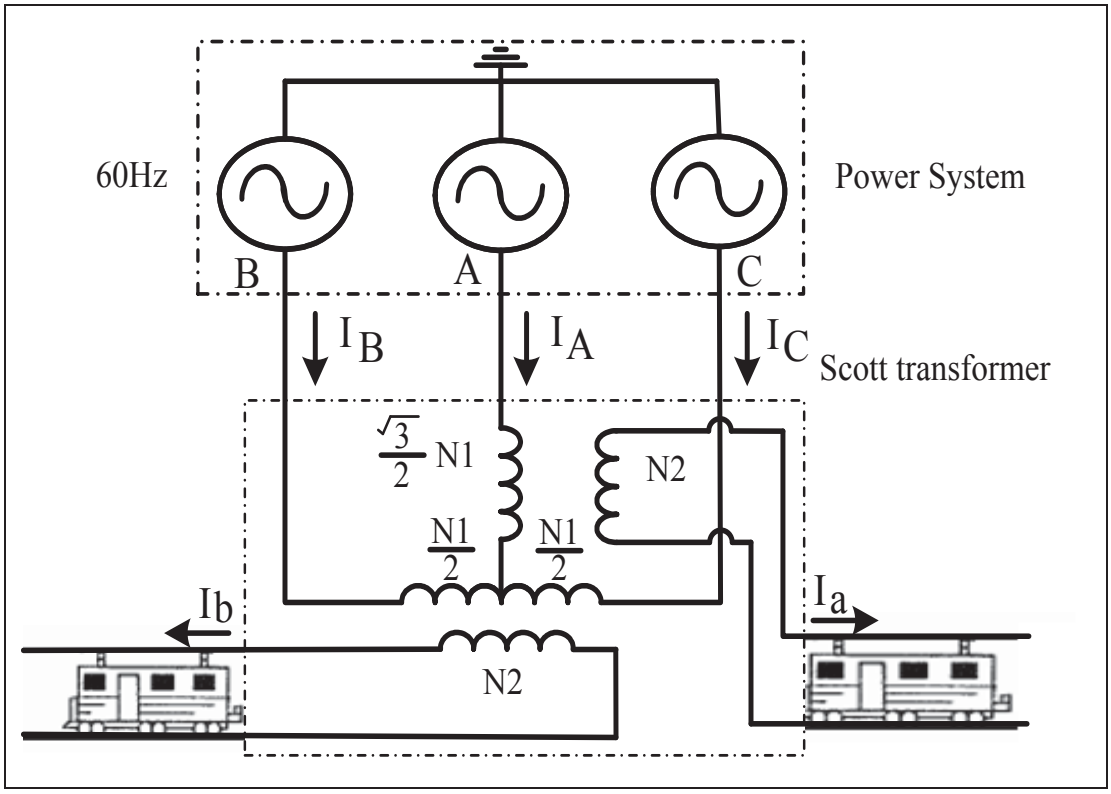

Figure 1.7 Supplying two single-phase electric train by Scott transformer
Taken from (Mazin et Gallant, 2010) (Mazin et Gallant, 2010)

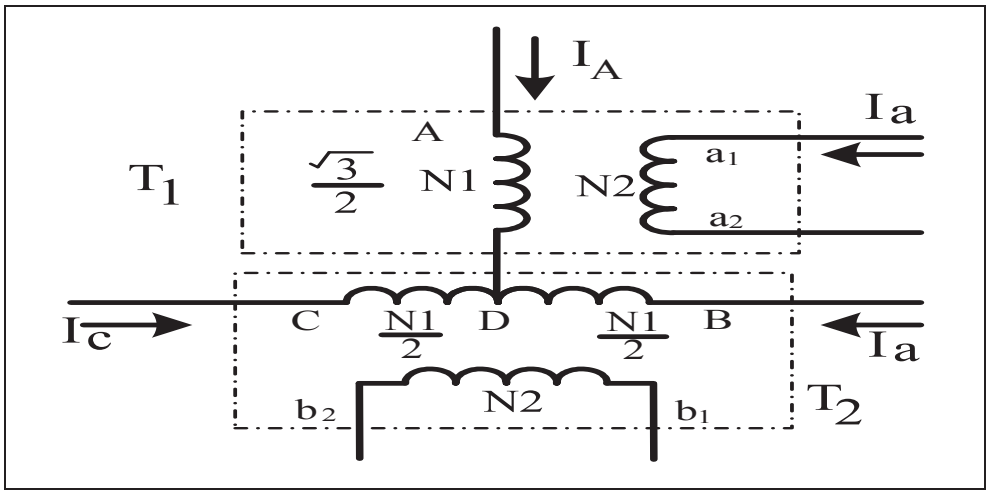

Figure 1.8 The diagram showing the connection of windings for the Scott transformer Taken from(Mazin et Gallant, 2010)(2010)

Scott transformer's special connection makes two unbalanced single-phase loads appear less unbalanced to the power system. One would reflect on whether the Scott transformer would also decrease the harmonic produced by two single-phase loads, an interesting subject that had never been investigated, as revealed by our extensive literature survey. The article's results indicate that Scott transformer does indeed reduce the harmonic introduced into the system by cancelling out the harmonic currents created by the single-phase harmonic loads. The degree of harmonic decrease depends on the harmonic order and the load values. (Mazin et Xu, 2008)

1.6 A single phase to three phase system using Leblanc transformer

The researchers in this paper present a structure for power conversion that changes a single-phase invertor into a three-phase multi-level one. The novel structure utilizes three single-phase voltage source inverters and a Leblanc transformer. Within the power converter, the Leblanc transformer is connected to two single-phase outputs for changing the two-phase voltage into a three-phase one. With this multi-level power conversion construction, a five-level three-phase inverter is obtained. Nonetheless, another type of transformers was also

used: that's how power converters that have special line frequency transformers, such as Scott or Leblanc, were also presented, since they allow deriving a two-phase current from a three-phase source, or vice versa. Two voltages with a 90º phase angle between them are generated by the outputs of the power converters. Using Leblanc transformers allows to provide a three-phase system (Pires et al., 2011)

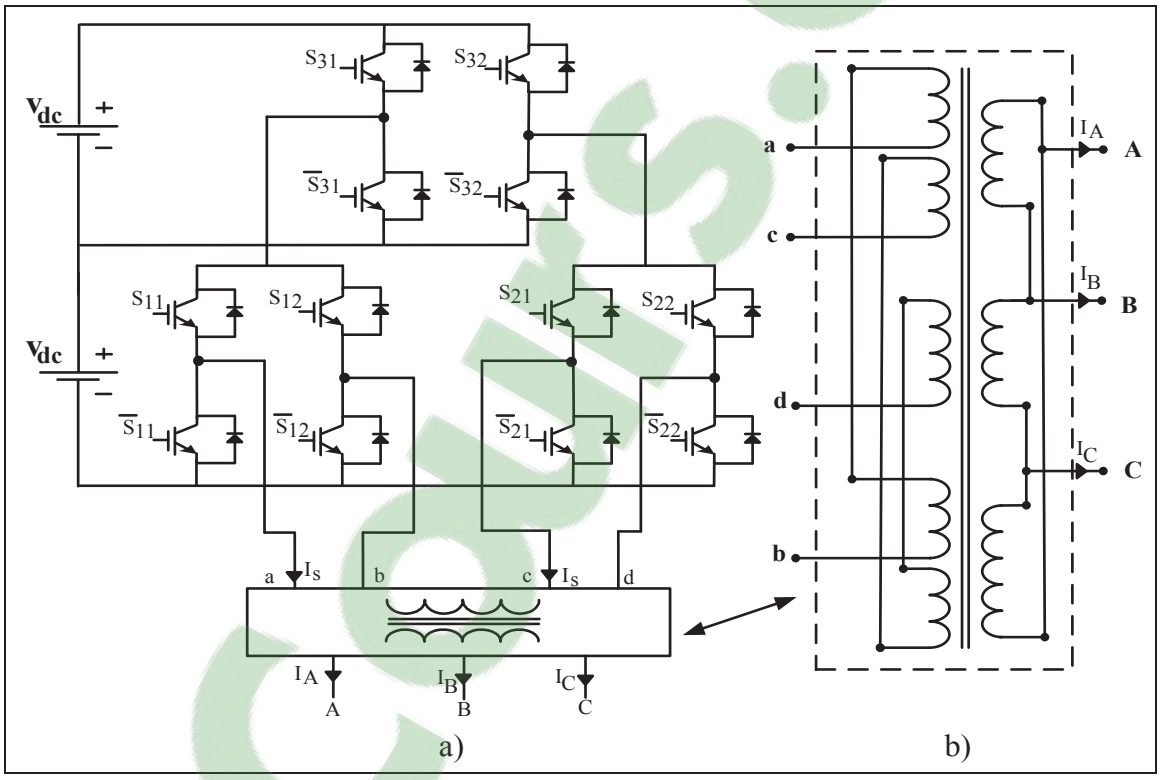

Figure 1.9 a) the conversion structure from a single phase to a three-phase multilevel inverter by using a LeBlanc transformer b) The Connection of the Leblanc transformer
Taken from Pires et al (Pires et al., 2011)

Figure (1.9 a) shows a three-phase multilevel inverter's power conversion structure. In order to have the maximum output voltage this topology utilizes two DC sources and three single-phase voltage source converters. A 2-to-3-phase transformer is used at the voltage source converters' output. A five-level voltage (2V, V, 0,-V,-2V) can be obtained for the output of the power converter structure, given the connection between the three single-phase inverters. However, there is a drawback in using this topology as two of the three inverters have to

resist to 2V (Pires et al., 2011). Figure (1.9 b), depicts a Leblanc transformer, utilizing a three-phase core, which features a winding system. The main windings, which are developed by the power converter that has a 90º phase angle value, are fed by Vcd(t) and Vab(t), while. the secondary windings present as the three-phase systems VT(t), VS(t) and VR(t) (Pires et al., 2011)

1.7 Connection PV solar single phase to three phase system using Leblanc transformer

Using a Leblanc transformer, the authors propose a power conversion structure for grid-connected photovoltaic from single phase to three-phase applications, a structure consisting of a multilevel inverter and a Leblanc transformer. The multilevel power converter employs two single-phase voltage source converters as well as a four-wire voltage source inverter. The Leblanc transformer connects to the multilevel converter's output. The PV system's configuration is dependent on the multi-string technology. The converter's structure can easily create a seven-level output wave form at the multilevel inverter's output.(Pires et al., 2012)

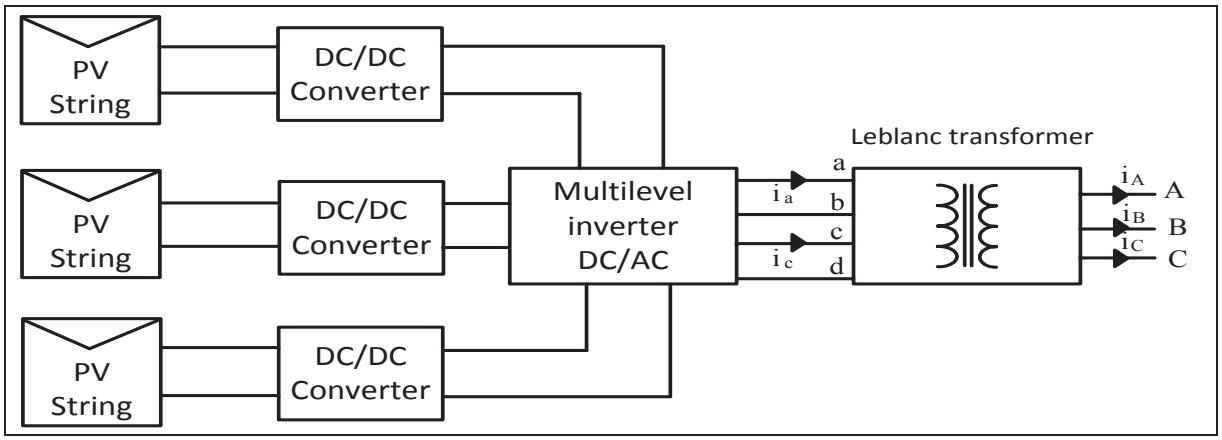

Figure 1.10 The Configuration of photovoltaic system using LeBlanc transformer connected to the grid
Taken from Pires et al (Pires et al., 2011)

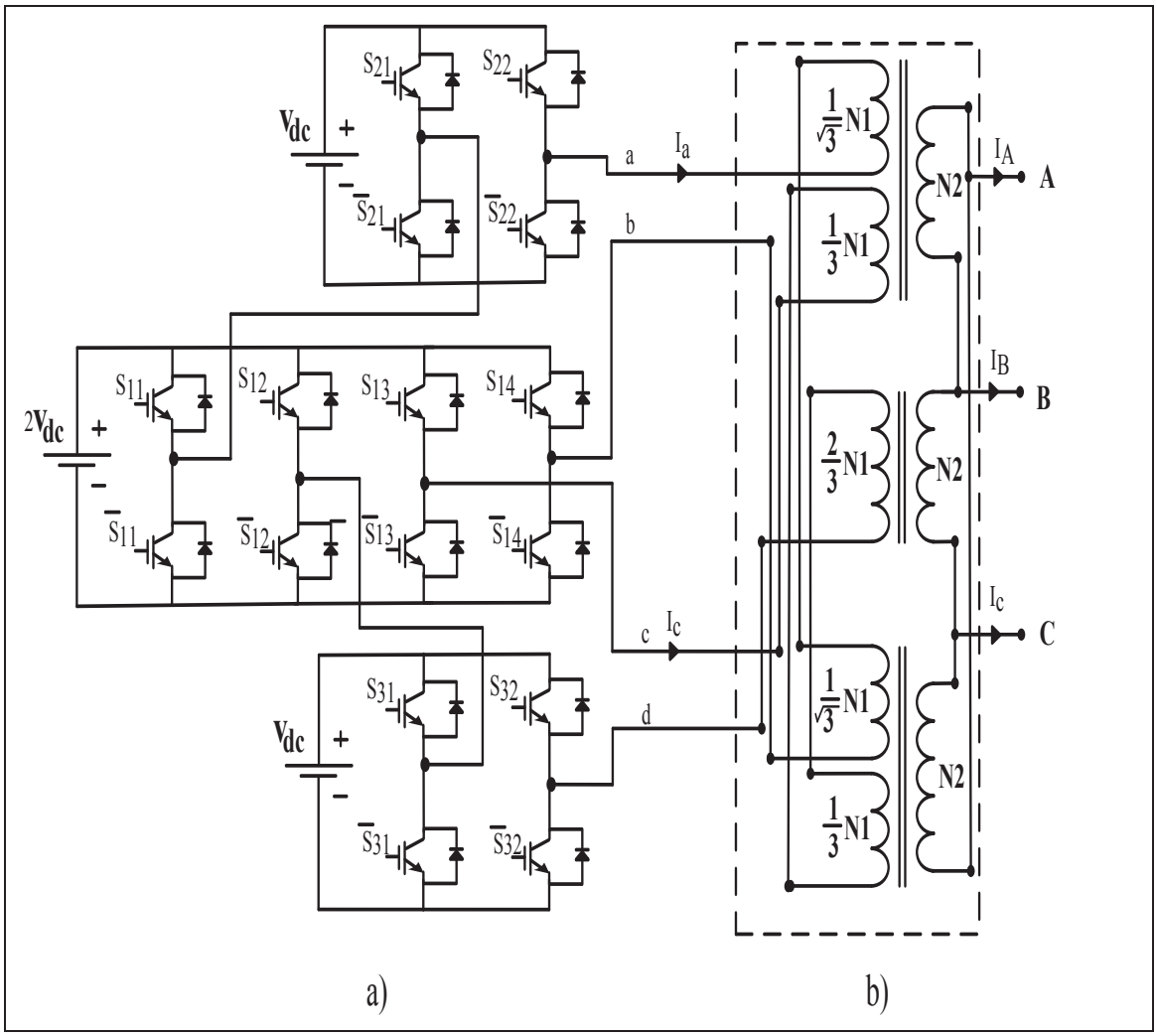

Figure 1.11 a) The Multilevel DC/AC converter connected to Leblanc transformer
b) Leblanc transformer in to model connection scheme
Taken from Pires et al (2011(Pires et al., 2011)

The article presents a multilevel inverter generating two output voltages that must shift by 90 degrees. The Leblanc transformer is utilized to get a three-phase balanced voltage systems at the power converter system's output. The Leblanc connection transformer is an asymmetrical winding transformer, usually used to convert a three-phase voltage system into a two-phase supply, using a special winding connection that is shown in Figure (1.11 b). There are five windings on the primary side, split into two distinct phases, and three delta-connected windings on the secondary side. (Pires et al., 2012)

1.8 Integration of PV solar single phase to three-phase grid using Scott transformer

In.(Dat, Wijnhoven et Driesen, 2012) the researchers introduce a novel topology for a grid-connected PV inverter. This topology was developed as a means to reduce how many switches are used. It is also intended to permit fault-tolerant operations through the incorporation of a Scott transformer as part of the power converter system. A PV power plant connected to the grid is highly vulnerable due to the exposure of its power electronics equipment. Scott transformers are often used to increase the grid-connected PV reliability by the constant operation of the PV system (to compensate for any switch failures in power converters) and decreasing how many switches are used. Three-phase PV inverters can be analyzed during both faulty and normal operations (Dat, Wijnhoven et Driesen, 2012)

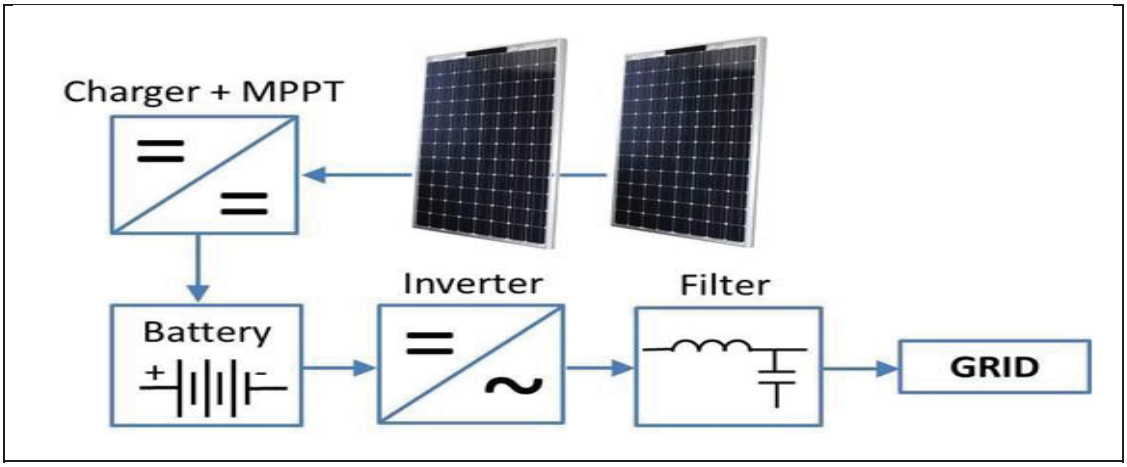

Figure 1.12 Block diagram for a grid connected photovoltaic system
Taken from Dat, Wijnhoven et Driesen (Dat, Wijnhoven et Driesen, 2012)

The power conversion consists of a single phase inverter, electronic switches and a Scott transformer. It uses an LC filter to connect to the grid. A Scott transformer constitutes two separate transformers. It has a special connection as seen in Figure (1.13.) The Scott transformer's structure presented in this article is pretty similar to Scott transformers employed in high-speed railway systems (HSR). There are two single coils or the primary

side represented by V1 − G1 and V2 − G2, and by three-phase windings or the secondary side represented by VA, VB, VC.

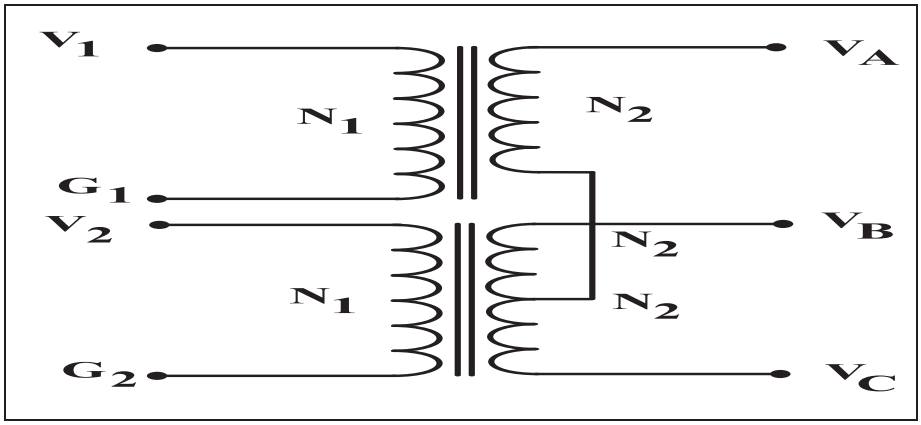

Figure 1.13 Scott connection transformer
Taken from Dat, Wijnhoven et Driesen (Dat, Wijnhoven et Driesen, 2012)

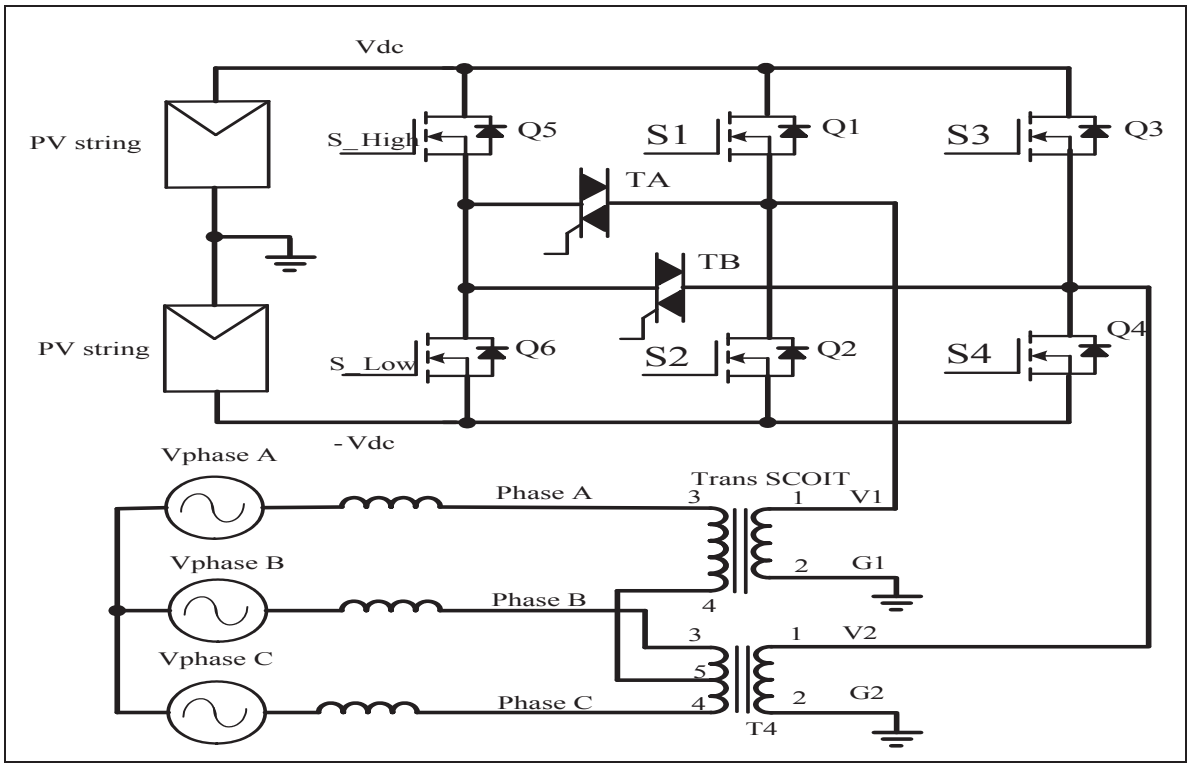

Figure 1.14 Connection diagram of switches in IPM triacs and a Scott transformer
Taken from Dat, Wijnhoven et Driesen (Dat, Wijnhoven et Driesen, 2012)

There are many advantages to the Scott transformer for the fault tolerant operation. First, only four electronic switches in two power legs are needed to make three-phase output currents. The third power leg of a three-phase Integrated Power Electronics Module is hence available as a redundant component for fault-tolerant operations. Second, the Scott transformer's wire connection topology helps obtaining two-phase control signals form a three-phase current feedback. (Dat, Wijnhoven et Driesen, 2012)

1.9 Leblanc transformer application to supply railway traction system

"The article demonstrates that the amount of unbalance caused by single-phase loads provided by the described transformer types depends on the secondary winding's relative loading. As the traction load varies continuously, the phase voltages and the ensuing unbalance will normally reside somewhere. The lowest level of unbalance takes place when the traction load is approximately the same in both transformer windings, a phenomenon that often takes place on a heavily loaded passenger mainline, where a large number of relatively small trains may run at short headway, with almost equal loading in each section. Often, there is only one train provided by the substation at any given moment. Considering the one single-phase transformer as a reference, the two single-phase transformers and the three-phase transformer's asymmetrical connections produce approximately the same level of unbalance for the same load. The Leblanc connections will decrease the unbalance only while all three phases provide the load. The three-phase transformer's symmetrical connection always provide the load from all three phases and is consequently more successful in decreasing the unbalance for the freight railroads type of loading. The author initiated a discussion about how to use special winding three-phase to two-phase transformers, such as modified Woodbridge-connected, Scott connected and Leblanc connected transformers in railway traction systems. The objective of reducing the unbalance issue that includes the typical arrangement for rotary balancing equipment such as induction motors, synchronous compensators and eliminating the negative sequence currents from the three-phase system".(Kneschke, 1985)

CHAPTER 2

REVIEW CONTROL OF SINGLE-PHASE ACTIVE FILTER

2.1 INTRODUCTION

In recent years, applications needing a three-phase system has typically seen the development of Active Power Filters. The electrical grid gets many benefits from the Shunt Active Power Filters in use on single-phase facilities, since these installations have power factor and nonlinear load problems, and since they are significantly responsible, in their total, of the total electric energy consumption. Additional power losses on the electrical grid are caused by harmonics and reactive power drained by single-phase installations. Consequently, mitigating the harmonics at the source contributes in reducing these extra losses and other harmonics generated issues.

The disadvantage from that solution lies in the necessity of numerous Active Power Filters that are distributed in major single-phase facilities. Therefore, it is necessary to place a simple and non-expensive Shunt Active Power Filter on single-phase installations. Furthermore, four simple control theories must be applied on single-phase Shunt Active Power Filters. Results of experimental simulation in comparing the four different control theories are presented and analyzed to determine the best control based on the results. As power electronics were progressing, engineers started to develop electronically controlled devices having nonlinear current consumption, primarily with the objective to increase the energy efficiency and the controllability of advanced production processes.

These devices create harmonics, however, causing increased energy losses and faulty operations in the electrical distribution components. The majority of harmonic sources are derived from single-phase loads in electronic equipment, like printers, copiers and computers. As a means to reduce the effect of harmonics created by these loads, Gyugi and Strycula developed Active Power Filters. In this approach, harmonic distortion in system voltages can be prevented by alleviating harmonics on the customer's side. This is the best

possible way to avoid issues on neighboring facilities and to maintain good electric power quality service. Shunt Active Power Filters can solve harmonic current issues that degrade the voltage waveform on the electrical grid, can also compensate the power factor, and are therefore, nowadays, the best solution.

Overall, Shunt Active Power Filters have more benefits than passive filters, as they do not need a specific harmonic configuration, whereas, Passive Power Filters have to be tuned in every instance. Another advantage of Active Power Filters is their simple installation. They do not require commissioning, and can compensate the power factor and current harmonics right away. This chapter looks at developing suitable controls to apply to Shunt Active Power Filters. This is accomplished, through a comparison of single-phase Shunt Active Power Filters to control approaches (Santos et al., 2009)

2.2 Different controls applied to single-phase active filters

The present chapter introduces a different kind of control which is applicable in single phase active filters like park transformation, PQ control, and synchronous d−q reference frame control, two cases of direct and indirect current control and of sliding mode or nonlinear control. The theory of instantaneous reactive power for the three-phase circuit was introduced by. (Akagi, Kanazawa et Nabae, 1984),in order to determine harmonics from non-sinusoidal voltages and currents. However, it cannot be applied to the single-phase circuit, given that, according to their theory, the instantaneous reactive power is described as the power flows from one phase to another. In general, the distorted wave circuit theory is used to calculate single-phase current and voltage harmonics. An example of this strategy is Fourier analysis which analyzes the repeated waveforms in currents and voltages.

Therefore, there is no precise definition of harmonics in transient states. Practically, the single-phase active filter’s output voltage and current tend to carry an important number of fundamental components, with a tendency to intense fluctuations from the DC bus voltage for the non-periodic load changes. Therefore, the electrolytic capacitor’s large size is needed

for the active filter's DC bus, so to avoid this voltage variation. However, from an economic aspect, it should not be installed, because its large size requires a large space and has a less resistance to the high temperature operation than other types of capacitors. Park transformation strategies are commonly applied to, active power filtering applications for control synchronous d−q reference frames one benefit of this approach is that harmonic/ active/reactive and fundamental active/reactive components which exist within the voltage or current d−q frame. The p−q theory, which is also referred to as the instant active/reactive power technique, has also proven to be useful for three-phase active filters. However, even though the p−q theory and park transformation approaches can be applied in systems described as three-phase three-wire or three-phase four-wire, they cannot be used directly for single-phase systems.

Not long ago, the three-phase p−q theory concept was extended to single-phase system, such as with the direct current control technique, In this method the reference shunt APF current is taken out of the reference compensating current, while in the indirect current control method, the reference source current is taken out of the reference compensating current. The increased use of non-linear and time-varying loads have led to distortion of voltage, current waveforms and increased reactive power demand in AC mains.

Converted into the d-q components in order to separate the fundamental and harmonic components of instantaneous currents (id, iq). One of the main differences between this method and p-q theory is that the d-q method requires calculating the angular position of the source voltages' synchronous reference, using a PLL algorithm. Once the load currents are converted into a synchronous reference, the fundamental and harmonic components are separated, by utilizing a low-pass or high-pass filter.

Additional, Hilbert transforms can be used to enable d-q transformation. Hilbert transforms converts single-phase current or voltage (analytic signals (i.e., complex vectors) instantaneously) Because, for both transient and steady states, the current and voltage main components convert to DC components at the d-q coordinate, current/voltage, harmonics are

obtainable by applying the low-pass filter from the d-q coordinate. The outcome is an economical active filter which features a capacitor that suppresses variations in the DC bus voltage. The reason for this is that the active filter input is able to remove the fundamental power.

2.3 Single phase three level boost control

A single-phase three level boost rectifier was modeled from Space Vector Modulation and d-q transformation was presented in (Salaet et al., 2002). Control loops for controlling the displacement factor of the conductor current for the line voltage (quadrature path) as well as the DC output voltage (direct path) were enabled by the sine variables quadrature and direct decomposition (Salaet et al., 2002). In order to build a simpler PI-based controller, the double line frequency ripple of the output voltage was ignored and the system equation linearized additionally, PFC regulation current loop along with output voltage regulation voltage current loops were applied during controller installations. The researchers also included an overview of the control system for the neutral point voltage's control, known as (charges balancing), but chose to include no more than one. Other voltage sensors for measuring the three-level structure's two capacitor voltages.(Salaet et al., 2002)

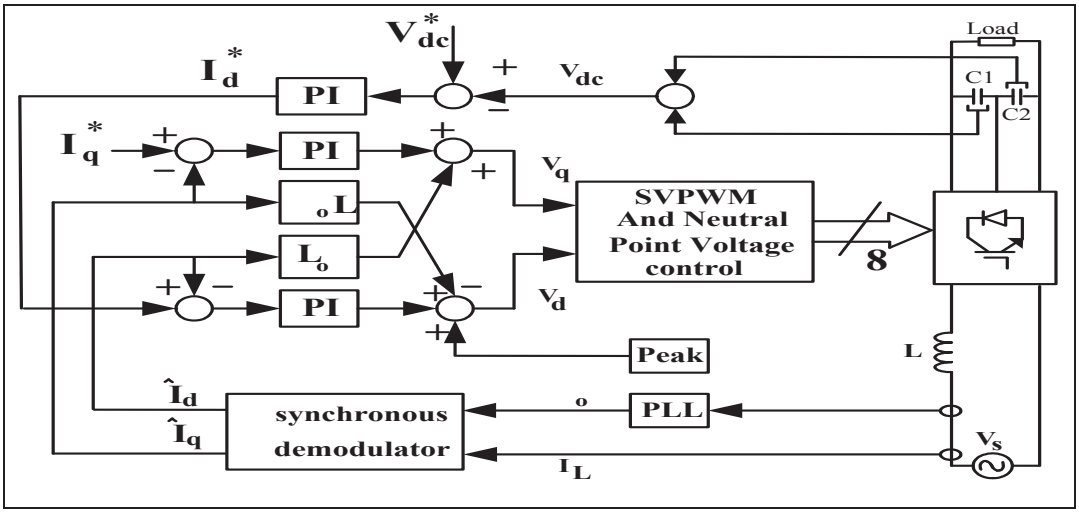

Figure 2.1 Block diagram of the Displacement factor and output voltage control system
Taken from Salaet et al.(Salaet et al., 2002)

2.3.1 Single phase unified power quality conditioner control

In (Khadkikar et Chandra, 2012) applied a single-phase unified power quality conditioner (UPQC) to address any quality issues with power for single-phase systems. The authors suggest using a control method built from synchronous d-q reference frame, in formulating the single-phase system d-q transformation, they used a p-axis, succeeding in attaining, as DC variables. The fundamental component for non-linear load currents as well as distorted supply voltage The researchers also investigate single-phase load current and supply voltage for a d-q frame for real rather than simulated hardware systems, with the overall aim to reduce. harmonics for load current as well as the supply voltage (Khadkikar et Chandra, 2012)

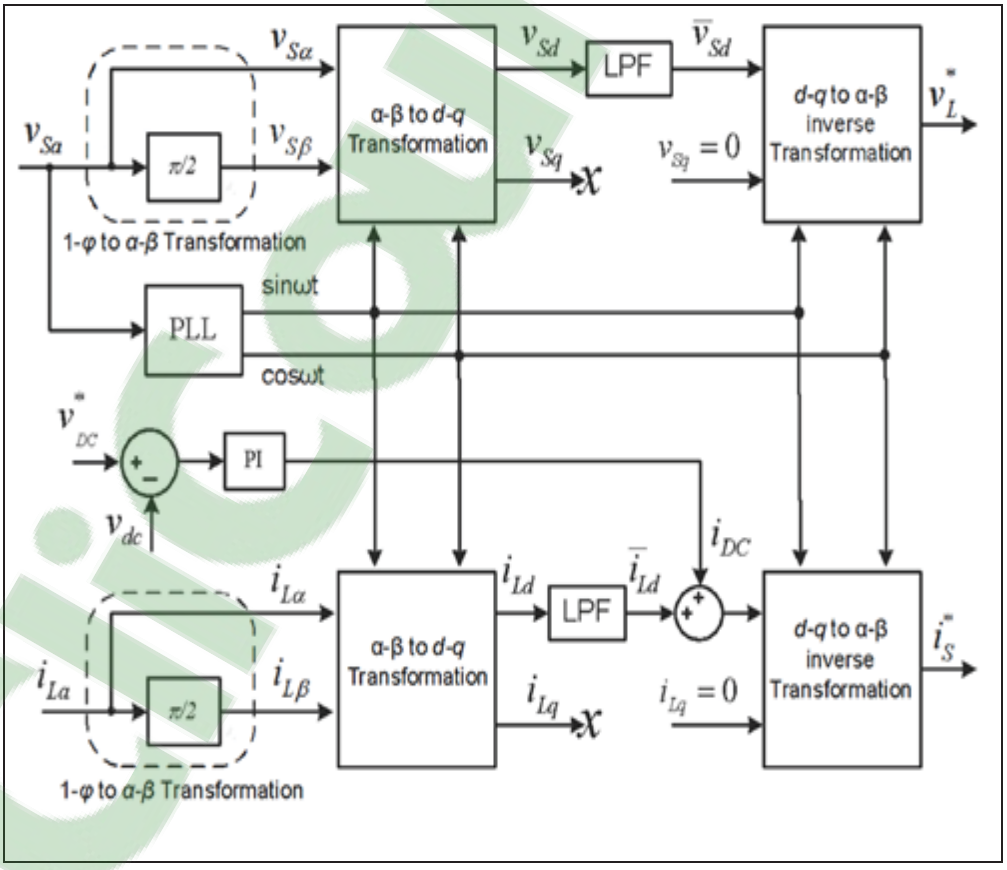

Figure 2.2 The control scheme for shunt and series inverters of single-phase UPQC in synchronous reference frame
Taken from (Khadkikar et Chandra, 2012)

2.4 Indirect current control

Figure (2.3) shows a block diagram of synchronous d-q reference frame using indirect current controller. As can be seen in the figure, the reference source current and supply voltage profile are not connected, indicating the applicability of single-phase d-q theory for supply voltage distortion.

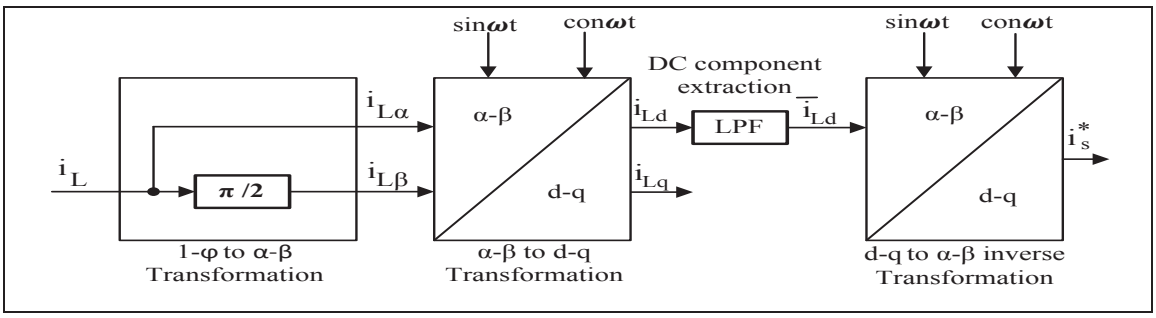

Figure 2.3 Single-phase indirect d-q current control
Taken from (Khadkikar et Chandra, 2012)

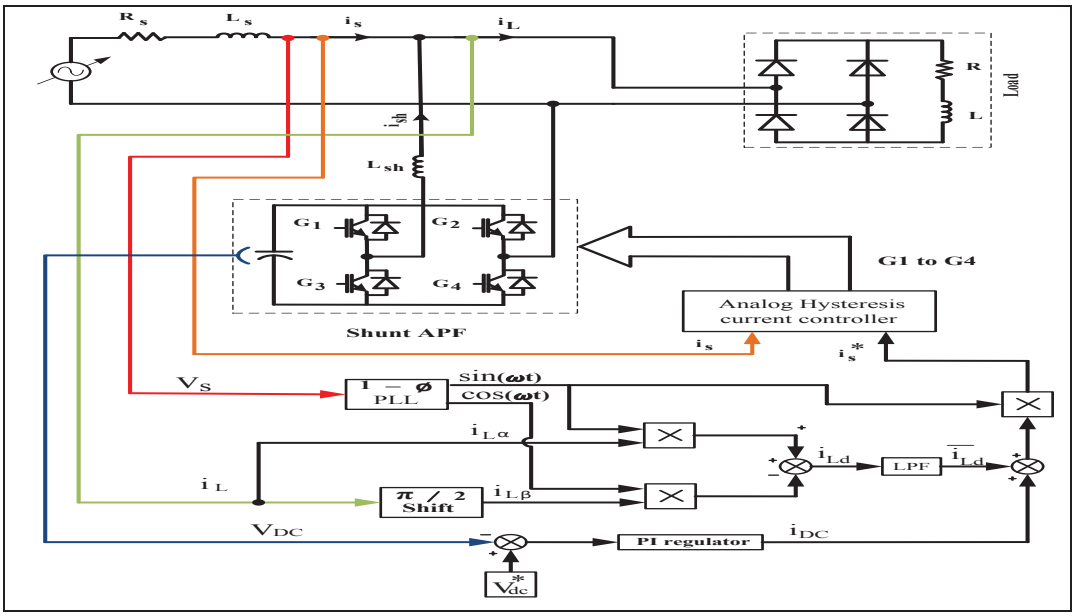

Figure 2.4 Single-phase d-q frame control based on shunt APF
Taken from (Khadkikar et Chandra, 2012)

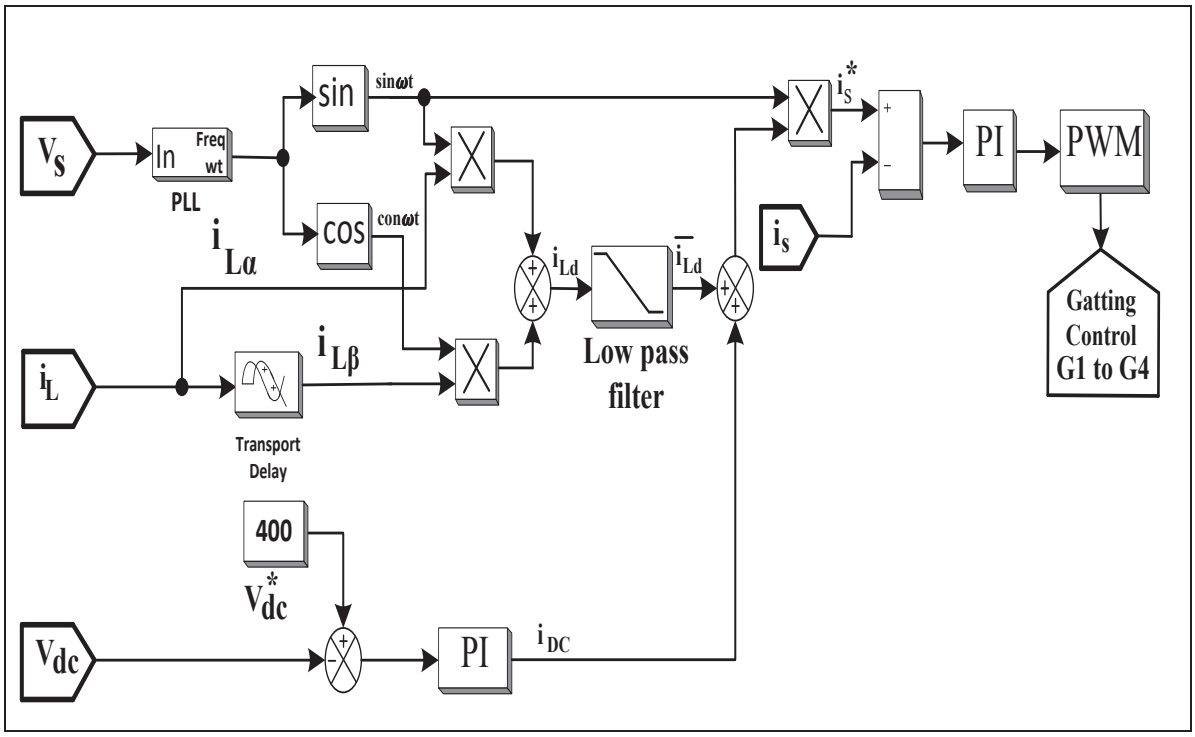

Figure 2.5 The d-q reference frame control diagram

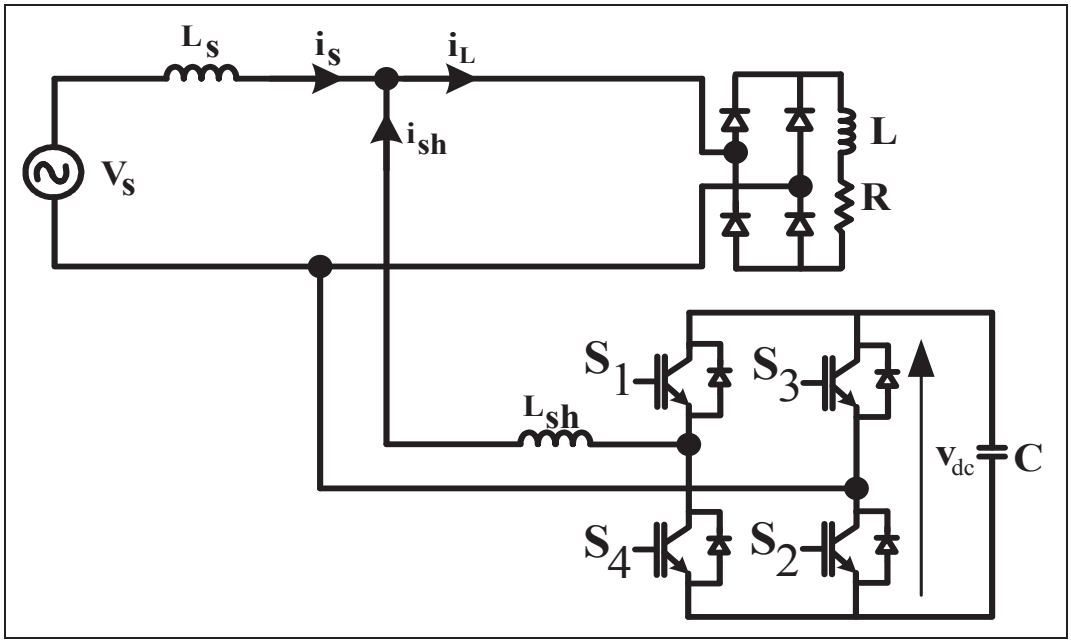

Figure 2.6 Single-line diagram of shunt active power filter
Taken from (Khadkikar et Chandra, 2012)

2.4.1 Modeling and control for d-q theory

First, in the case of a three-phase system, the three currents or the three-voltage signals of (ABC) are converted into the orthogonal frame stationary of (α-β) using equation (2.1). Next, by applying equation (2.2), they are converted to (d-q), synchronous frame rotation. The necessary components are then taken by the d-q frame, considering the required control. Finally, the (d-q) to (α-β) frame conversion, followed by the (ABC) frame conversion is done by applying equations (2.3) and (2.4), respectively. The aim is to create reference signals before reverting them to the initial frame, such that.

(ABC) to (α-β) conversion:

$$\begin{bmatrix} x_\alpha \\ x_\beta \end{bmatrix} = \sqrt{\frac{2}{3}} \cdot \begin{bmatrix} 1 & -1/2 & 1/2 \\ 0 & \sqrt{3/2} & -\sqrt{3/2} \end{bmatrix} \cdot \begin{bmatrix} x_a \\ x_b \\ x_c \end{bmatrix} \tag{2.1}$$

where (x) is the variable under consideration which is either current or voltage.

(α-β) to (d-q) conversion:

$$\begin{bmatrix} x_d \\ x_q \end{bmatrix} = \begin{bmatrix} sin\,\omega t & -cos\,\omega t \\ cos\,\omega t & sin\,\omega t \end{bmatrix} \cdot \begin{bmatrix} x_\alpha \\ x_\beta \end{bmatrix} \tag{2.2}$$

(d-q) to (α-β) the inverse conversion:

$$\begin{bmatrix} x_\alpha^* \\ x_\beta^* \end{bmatrix} = \begin{bmatrix} \sin\omega t & \cos\omega t \\ -\cos\omega t & \sin\omega t \end{bmatrix} \cdot \begin{bmatrix} x_d^* \\ x_q^* \end{bmatrix} \tag{2.3}$$

In equations (2.3) and (2.4) the quantities with notation ("*") are the reference signals

The inverse conversion: (α-β) to (ABC)

$$\begin{bmatrix} x_a^* \\ x_b^* \\ x_c^* \end{bmatrix} = \sqrt{\frac{2}{3}} \cdot \begin{bmatrix} 1 & 0 \\ -1/2 & \sqrt{3/2} \\ 1/2 & -\sqrt{3/2} \end{bmatrix} \cdot \begin{bmatrix} x_\alpha^* \\ x_\beta^* \end{bmatrix} \tag{2.4}$$

At the same time, we can see that the park transformation shown in equation (2.1) is applicable for three-phase systems, but alterations to the analyses need to be made in order to apply it to single-phase d-q transformation (Jinjun, Jun et Zhaoan, 1999) presented a single-phase system from an (α-β) frame without resorting to matrix conversion. Instead, they applied a hypothetical second variable in their orthogonal (β) and (α). This was actually, a variable that was formed out of the voltage and current of the initial variable through using a 90° phase- shifting. Using this approach, both the hypothetical and the initial signals, are considered equal to single-phase systems presented in an orthogonal (α-β) frame (Khadkikar et al., 2010) later applied and verified this method for single-phase (p-q) theory (Khadkikar et al., 2010)

The load current present in an α-β frame is formulated, as per equation (2.5) below, by employing single-phase p-q theory

$$\begin{bmatrix} i_{L\alpha} \\ i_{L\beta} \end{bmatrix} = \begin{bmatrix} i_L(\omega t + \varphi) \\ i_L(\omega t + \varphi + \pi / 2) \end{bmatrix} \tag{2.5}$$

(Zhang et al., 2002), expressed this single-phase system for a d-q frame by further extending the approach which applies a hypothetical variable in the single-phase p-q method. When replaced with a variable in equation (2.5), the α-β frame variable present in equation (2.2) provides a similar d-q frame rendering for a single- phase system. This can be expressed by equations (2.6) and (2.7).

$$\begin{bmatrix} i_{Ld} \\ i_{Lq} \end{bmatrix} = \begin{bmatrix} \sin \omega t & -\cos \omega t \\ \cos \omega t & \sin \omega t \end{bmatrix} . \begin{bmatrix} i_{L\alpha} \\ i_{L\beta} \end{bmatrix} \tag{2.6}$$

$$\begin{bmatrix} i_{Ld} \\ i_{Lq} \end{bmatrix} = . \begin{bmatrix} \bar{i}_{ld} & + & \tilde{\imath}_{ld} \\ \bar{i}_{lq} & + & \tilde{\imath}_{lq} \end{bmatrix} = \begin{bmatrix} i_{L\alpha} . (\sin \omega t) & - & i_{L\beta} . (\cos \omega t) \\ i_{L\alpha} . (\cos \omega t) & + & i_{L\beta} . (\sin \omega t) \end{bmatrix} \tag{2.7}$$

The fundamental reactive and active current components for load i_L in equation (2.7) are the DC terms $\bar{i}_{ld}$ and $\bar{i}_{lq}$ In the same equation, the harmonic components are the AC terms $\tilde{\imath}_{lq}$ and $\tilde{\imath}_{ld}$ The AC and DC components can be easily taken from i_{Ld} and i_{Lq} using either way low pass filter (LPF) and high pass filter (HPF), respectively.

$$\begin{bmatrix} i^*_{Ld} \\ i^*_{Lq} \end{bmatrix} = . \begin{bmatrix} \bar{i}_{Ld} & + 0 \\ 0 & + 0 \end{bmatrix} \tag{2.8}$$

If we remove the quantities in (2.6) replace them with the quantities in (2.8), and take it in reverse, we can develop a reference source current signal for (α-β) frame, as follows ,

$$\begin{bmatrix} i^*_{S\alpha} \\ i^*_{S\beta} \end{bmatrix} = \begin{bmatrix} \sin \omega t & -\cos \omega t \\ \cos \omega t & \sin \omega t \end{bmatrix}^{-1} . \begin{bmatrix} i^*_{Ld} \\ i^*_{Lq} \end{bmatrix} \tag{2.9}$$

$$\begin{bmatrix} i^*_{S\alpha} \\ i^*_{S\beta} \end{bmatrix} = \begin{bmatrix} \sin \omega t & \cos \omega t \\ -\cos \omega t & \sin \omega t \end{bmatrix} . \begin{bmatrix} \overline{i_{Ld}} + i_{DC} \\ 0 \end{bmatrix} \tag{2.10}$$

The term of i_{DC} in equation (2.10) expresses the component required to keep a constant self-supporting the DC bus's voltage that is crossing the active filter. The term $i^*_{S\beta}$ is a hypothetical component of the initial system and thus can be ignored. Hence

$$i^*_S(\omega t) = i^*_{S\alpha}(\omega t) = \sin \omega t \,.\, (\overline{i_{Ld}} + i_{DC}) \tag{2.11}$$

2.4.1.1 Simulation results

Table 2.1Specification parameters used for dq control simulation

Description	Value
Phase voltage	V_s = 120 V (rms)
Frequency	F_s = 60 Hz
Line impedance	L_s = 0.5 mH
Voltage-source type nonlinear load	C_L = 500 μF , R_L = 25 Ω
current-source type nonlinear load	L_L = 50 mH , R_L = 10 Ω
Active filter parameters	L_c = 3.5 mH , R_c = 0.1 Ω C_{dc1} = C_{dc2} =2000 μF
DC-bus voltage	V_{dc}^* = 400 V
PI regulation parameters	K_p = 2 and K_i = 50

In this section, we discuss a single-phase synchronous d-q reference controller's performance and implementation for compensating harmonics that have been developed using non-linear loads in a real hardware system, as illustrated in Figure (2.7)

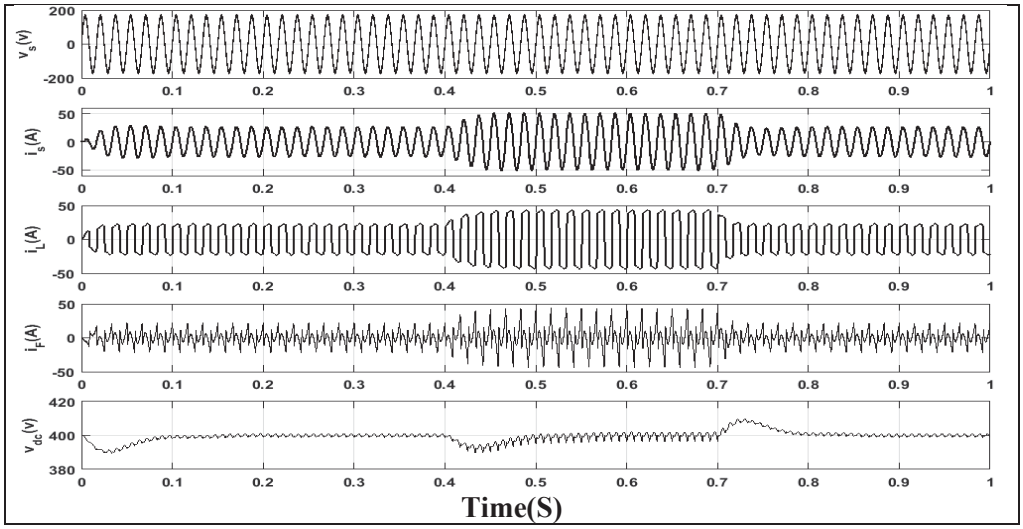

Figure 2.7 Single phase based on synchronous d-q control with load variation

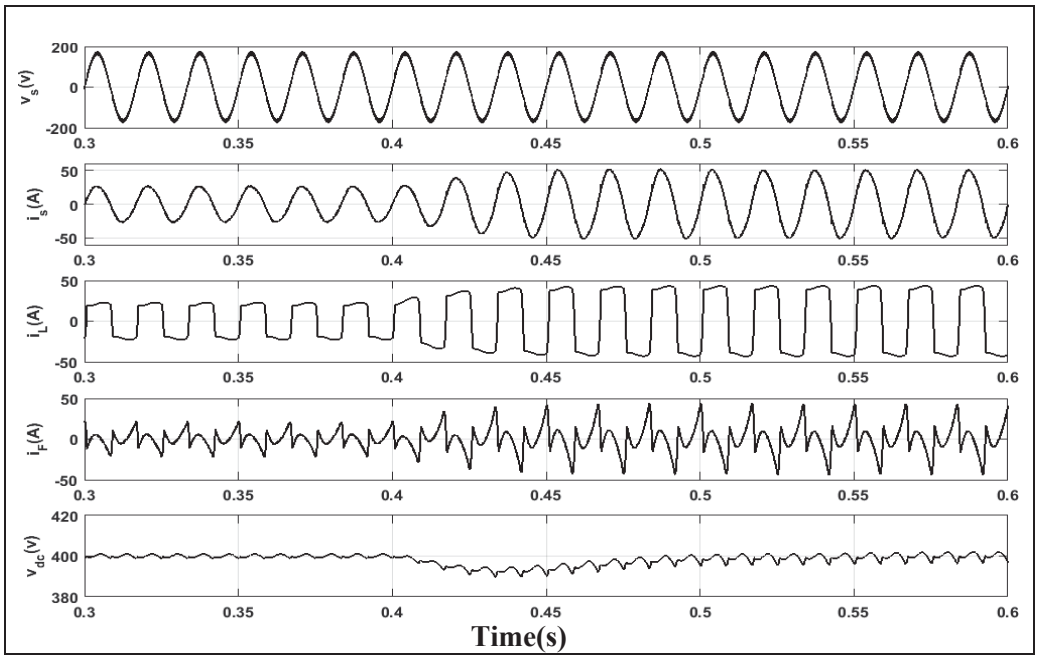

Figure 2.8 System response to load current increase

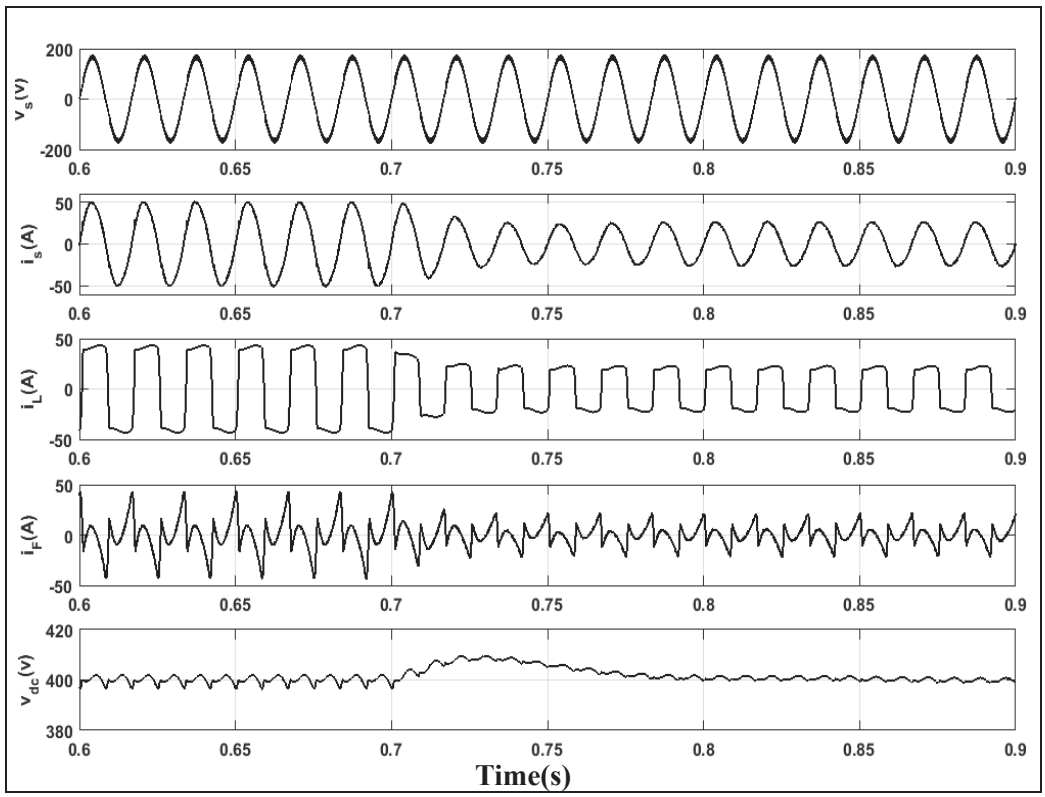

Figure 2.9 System response to a step decrease of load current

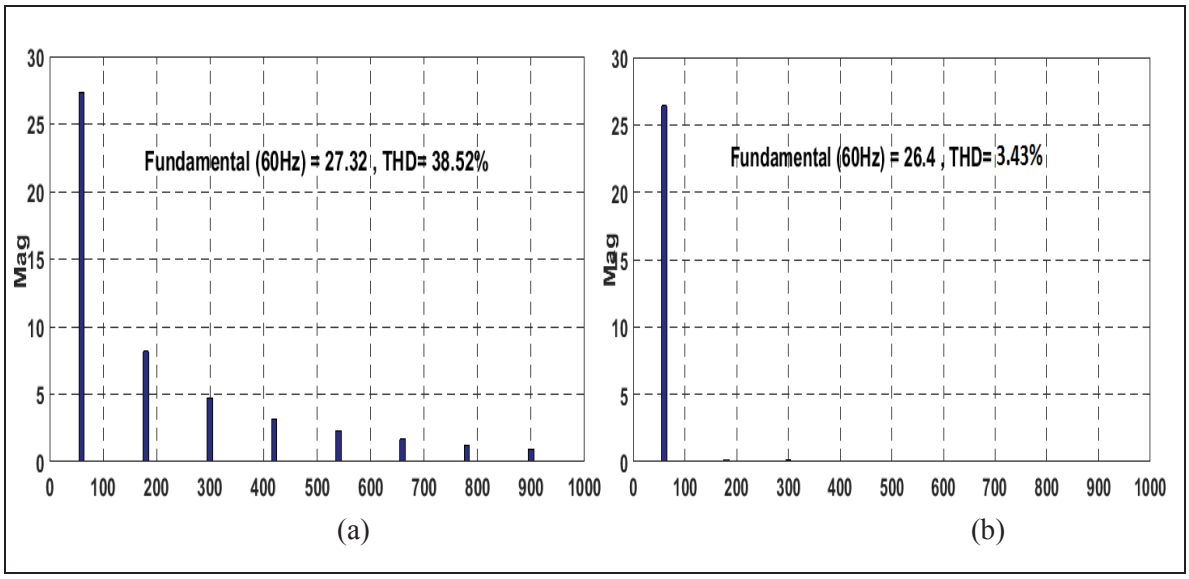

Figure 2.10 The total harmonic distortion a) load current, b) source current in study state operation mode

2.5 PQ control

2.5.1 Introduction

A general single-phase p-q method is developed in this section by using a p-q control approach applied to active power filters for single-phase systems. The control is then slightly changed so that it can be used during distorted utility voltage conditions. Direct as well as indirect current control strategies are realized and the prototype of the single-phase shunt active power filter (APF) applied under various loads and operating conditions in order to gauge the p-q method's applicability and practicality.(Khadkikar, Chandra et Singh, 2009).As mentioned in previous sections, three-phase three-wire and three-phase four-wire systems have been enabled by the PQ method and extensively applied for implementing power electronic circuits, such as active filters, static compensators, rectifiers, etc., relies on this theory. In order to widen the PQ theory's application in single-phase systems, many researchers have discussed and used the single-phase PQ theory to realize the control of the single-phase power electronic circuits. In the present study, we base the single-phase p-q

method on instantaneous π/2 lag and π/2 lead for current and voltage as a means to frame the initial system as pseudo two-phase

However, the synchronous reference frame approach has been unable to compensate reactive power, as instantaneous p-q theory in only able to measure components of harmonic current when they occur in conditions of balanced load. Consequently, the system is quite simply expressed using α-β coordinates. In this formulation, original load current and source voltage are viewed as α-axis quantities, while current and source voltage for π/2lag and π/2 lead are viewed as β-axis quantities. Our approach for PQ control uses both direct and indirect current control in the for shunt active power filter.

2.5.2 Modeling and control general PQ control

The equation below expresses single-phase source voltage using α-β coordinates at π/2 lead, as follows:

$$\begin{bmatrix} v_{S\alpha}(\omega t) \\ v_{S\beta}(\omega t) \end{bmatrix} = \begin{bmatrix} v_S(\omega t) \\ v_S(\omega t + (\pi/2)) \end{bmatrix} = \begin{bmatrix} V_m \sin(\omega t) \\ V_m \cos(\omega t) \end{bmatrix} \tag{2.12}$$

Equation (2.13) uses load current formulation as α – β coordinates at $\pi/2$ lead as shown below.

$$\begin{bmatrix} i_{L\alpha}(\omega t) \\ i_{L\beta}(\omega t) \end{bmatrix} = \begin{bmatrix} i_L(\omega t + \varphi_L) \\ i_L(\omega t + \varphi_L + (\pi/2)) \end{bmatrix} \tag{2.13}$$

So, as shown in Equation (2.14) and according to the initial 3-phase p-q method outlined previously, both instantaneous single-phase reactive power and active power can be expressed as;

$$\begin{bmatrix} p(\omega t) \\ q(\omega t) \end{bmatrix} = \begin{bmatrix} v_{S\alpha}(\omega t) & v_{S\beta}(\omega t) \\ -v_{S\beta}(\omega t) & v_{S\alpha}(\omega t) \end{bmatrix} \cdot \begin{bmatrix} i_{L\alpha}(\omega t) \\ i_{L\beta}(\omega t) \end{bmatrix} \tag{2.14}$$

The$p(\omega t)$) and $q(\omega t)$can be expressed as

$$p(\omega t) = \bar{p}(\omega t) + \tilde{p}(\omega t) \tag{2.15}$$

$$q(\omega t) = \bar{q}(\omega t) + \tilde{q}(\omega t) \tag{2.16}$$

where $\bar{p}(\omega t)$ $\bar{q}(\omega t)$ denote the DC components integral to instantaneous fundamental active & reactive power, and $\tilde{p}(\omega t)$ $\tilde{q}(\omega t)$ indicate AC components harmonic power. The inverse of equation (2.14) gives us the reference compensating current

$$\begin{bmatrix} i_{C\alpha}(\omega t) \\ i_{C\beta}(\omega t) \end{bmatrix} = \begin{bmatrix} v_{S\alpha}(\omega t) & v_{S\beta}(\omega t) \\ -v_{S\beta}(\omega t) & v_{S\alpha}(\omega t) \end{bmatrix}^{-1} \cdot \begin{bmatrix} -\tilde{p}(\omega t) \\ -q(\omega t) \end{bmatrix} \tag{2.17}$$

$$\begin{bmatrix} i_{C\alpha}(\omega t) \\ i_{C\beta}(\omega t) \end{bmatrix} = \frac{1}{v_{S\alpha}^2(\omega t) + v_{S\beta}^2(\omega t)} \times \begin{bmatrix} v_{S\alpha}(\omega t) & -v_{S\beta}(\omega t) \\ v_{S\beta}(\omega t) & v_{S\alpha}(\omega t) \end{bmatrix} \cdot \begin{bmatrix} -\tilde{p}(\omega t) \\ -q(\omega t) \end{bmatrix} \tag{2.18}$$

Equation (2.18) indicates that, the supply voltage profile derives from APF current signal extraction reference shunt. Thus supply voltage distortion is able to cause inaccurate evaluations for reference currents, which is a major limitation that needs to be, remediated by the distorted supply voltage.

$$\begin{bmatrix} p(\omega t) \\ q(\omega t) \end{bmatrix} = \begin{bmatrix} v_{S\alpha}^*(\omega t) & -v_{S\beta}^*(\omega t) \\ v_{S\beta}^*(\omega t) & v_{S\alpha}^*(\omega t) \end{bmatrix} \cdot \begin{bmatrix} i_{L\alpha}(\omega t) \\ i_{L\beta}(\omega t) \end{bmatrix} = \begin{bmatrix} \bar{p}(\omega t) + \tilde{p}(\omega t) \\ \bar{q}(\omega t) + \tilde{q}(\omega t) \end{bmatrix} \tag{2.19}$$

where $v_{S\alpha}^*(\omega t)$ constitutes the induced reference supply voltage signal. We can see in Equation (2.19) that the reference currents have, two possible extracting methods.

2.5.3 Direct PQ control

In this section, we apply compensating currents for shunt APF current. The shunt APF has to make up for it through introducing current that basically sums reactive and harmonic currents needed by the load in order to compensate for harmonics caused from single-phase load reactive power issues. Hence our reference compensating current derives from $\tilde{p}(\omega t)$ $\tilde{q}(\omega t)$ and $\bar{q}(\omega t)$ as presented in (Khadkikar, Chandra et Singh, 2009) Figure (2.11) below

illustrates a single-phase shunt APF system comprising a self-supporting DC bus and a four-switch bridge inverter. Several different control strategies are used, including the p-q theory, as a means to deal with any power quality problems that could arise in single-phase systems.

2.5.3.1 Modeling and control

Here, we will apply compensating currents for shunt APF currents as shown in figure (2.6). Hence, our reference compensating current derives from $\tilde{p}(\omega t)$ $\tilde{q}(\omega t)$ and $\bar{q}(\omega t)$ as presented in(Khadkikar, Chandra et Singh, 2009). In equation (2.19) $\tilde{p}(\omega t)$ is assumed as $p(\omega t)$) with (HPF) as follows

$$\begin{bmatrix} i_{C\alpha}(\omega t) \\ i_{C\beta}(\omega t) \end{bmatrix} = \frac{1}{Ax}.\begin{bmatrix} v^*_{S\alpha}(\omega t) & -v^*_{S\beta}(\omega t) \\ v^*_{S\beta}(\omega t) & v^*_{S\alpha}(\omega t) \end{bmatrix} \times \begin{bmatrix} -\tilde{p}(\omega t) + \overline{P}_{dc}(\omega t) \\ -q(\omega t) \end{bmatrix} \tag{2.20}$$

Therefore

$$\begin{aligned} i_{C\alpha}(\omega t) = i^*_{Comp,sh} \\ &= \frac{1}{Ax}\left[-v^*_{S\alpha}(\omega t).\tilde{p}(\omega t) + v^*_{S\alpha}(\omega t).\overline{P}_{dc}(\omega t)\right. \\ &\left. + v^*_{S\beta}(\omega t).q(\omega t)\right] \end{aligned} \tag{2.21}$$

where Ax = $[v^*_{S\beta}(\omega t)]^2$ + $[v^*_{S\beta}(\omega t)]^2$ and $\overline{P}_{dc}(\omega t)$ indicate the amount the shunt APF assumes in order to obtain a DC bus which is self-supporting. Because active power must be used to compensate losses caused by the shunt APF, DC bus voltage needs to be bigger than the peak amplitude of the input voltage, as shown in Figure (2.11)

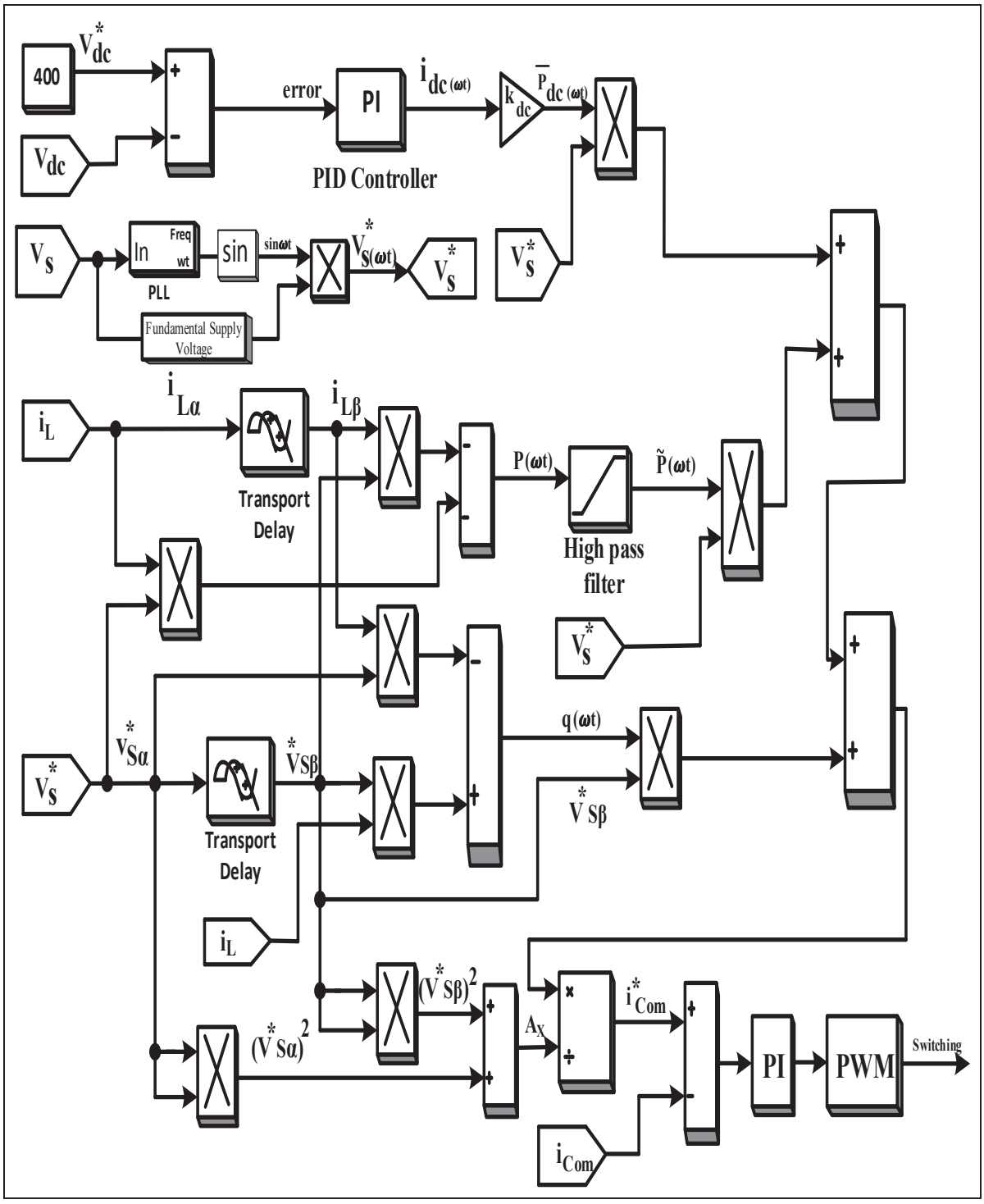

Figure 2.11 The diagram of direct current control technique for shunt APF

2.5.3.2 Simulation results

Table 2.2 The specification parameters used for pq direct control simulation

Description	Value
Phase voltage	V_s = 120 V (rms)
Frequency	F_s = 60 Hz
Line impedance	L_s = 0.5 mH
Voltage-source type nonlinear load	C_L = 500 µF , R_L = 25 Ω
current-source type nonlinear load	L_L = 50 mH , R_L = 10 Ω
Active filter parameters	L_c = 4 mH , R_c = 0.2 Ω C_{dc1} = C_{dc2} =2000 µF
DC-bus voltage	V_{dc}^* = 400 V
PI regulation parameters	K_p = 100 and K_i = 300

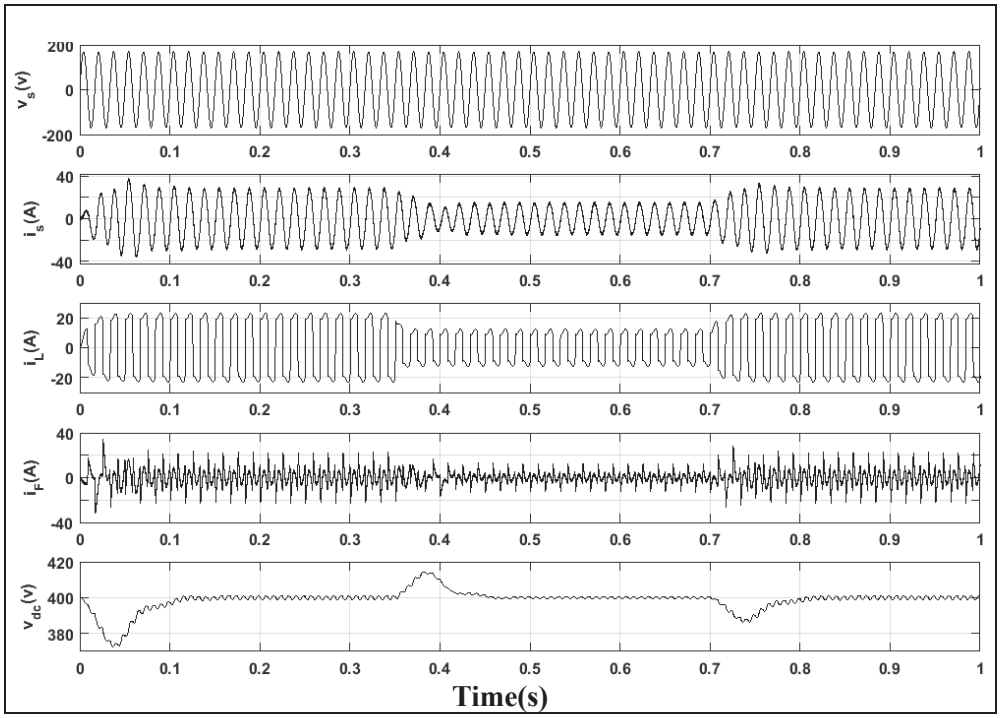

Figure 2.12 Simulation result during the direct control technique with load variation

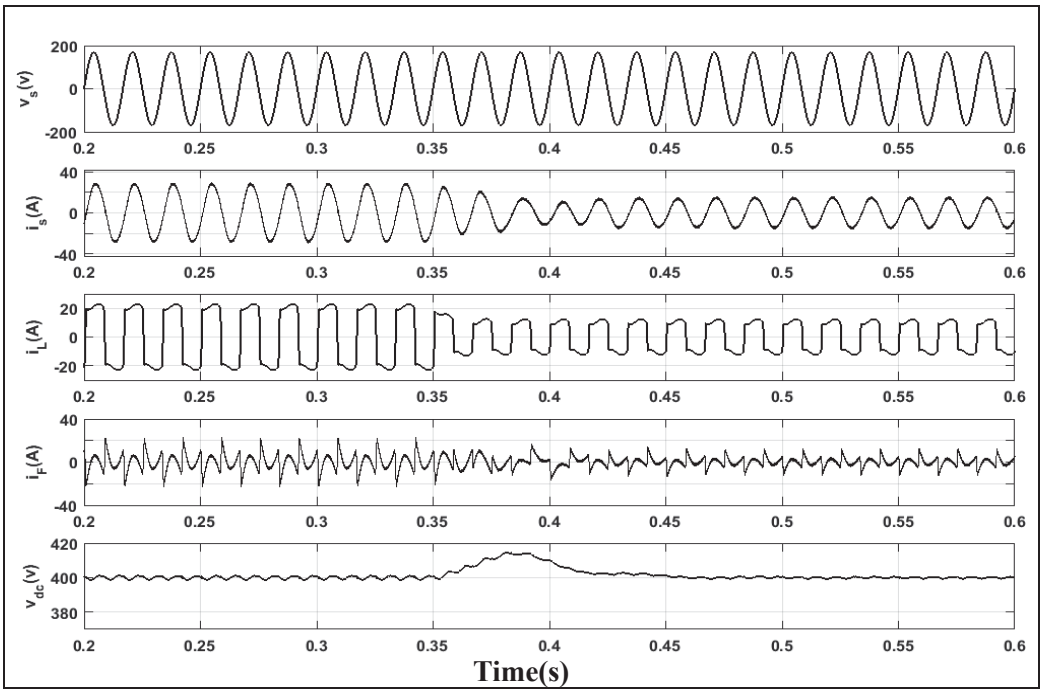

Figure 2.13 The Simulation result during step decrease of load current

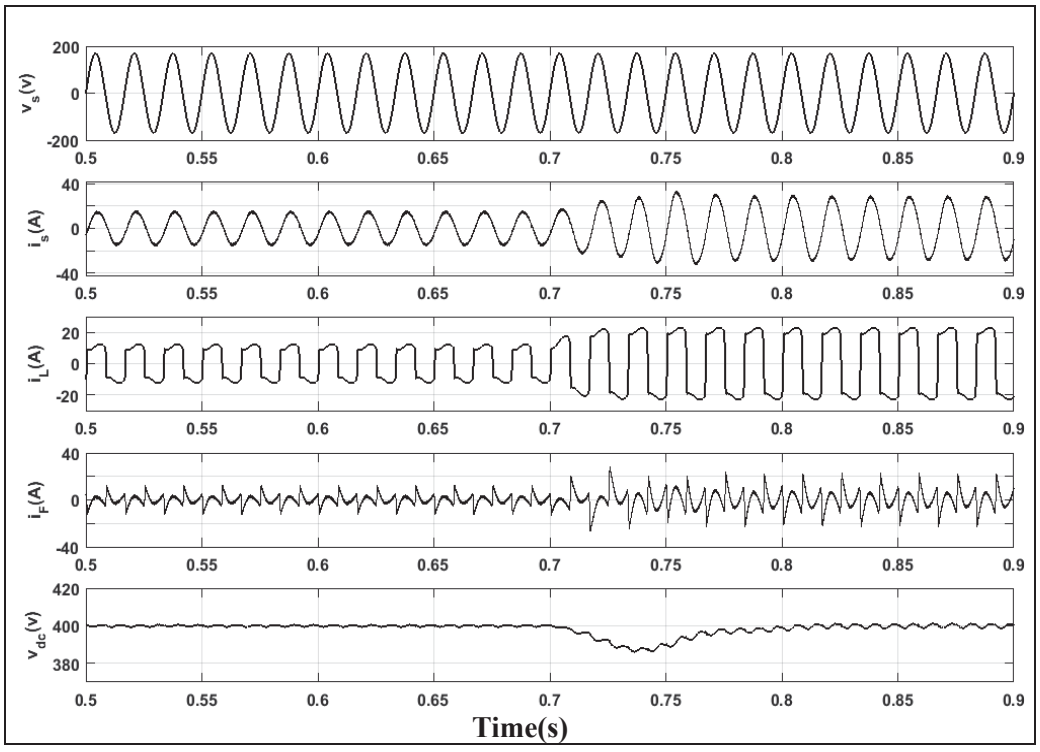

Figure 2.14 System response to a step increase load current

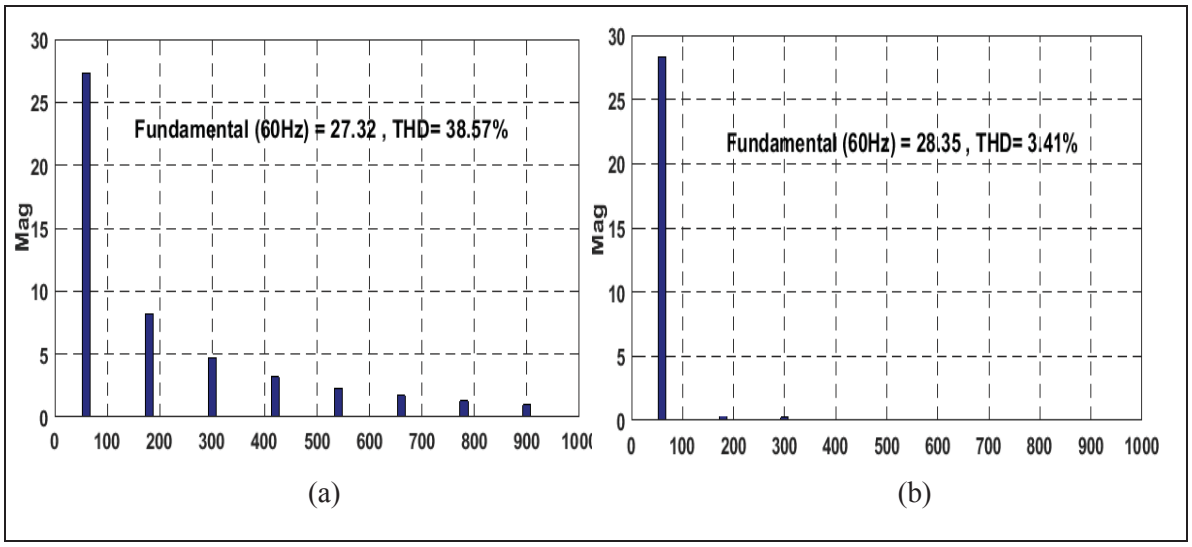

Figure 2.15 The total harmonic distortion a) load current b) source current in study state

2.5.4 Indirect PQ control

The immediate fundamental load active power can be written by the reference compensating current in the form of $\bar{p}(\omega t)$.Therefore, when extracting the reference compensating current for $\overline{p}(\omega t)$, fundamental active power only is obtained from the source indirectly, nullifying any harmonic or reactive power needs. (Khadkikar, Chandra et Singh, 2009)

As shown in equation (2.19), the source must supply the immediate fundamental load active power $\bar{p}(\omega t)$. In this case, $\bar{p}(\omega t)$ is looked at during extraction of the reference compensating current. Hence, the source can only give fundamental active power for the load and thus nullify the requirements of both the reactive and harmonic power. Also in equation (2.19), $\bar{p}(\omega t)$ is extracted from $p(\omega t)$ with an LPF:

$$\begin{bmatrix} i_{C\alpha}(\omega t) \\ i_{C\beta}(\omega t) \end{bmatrix} = \frac{1}{Ax} \cdot \begin{bmatrix} v_{S\alpha}^{*}(\omega t) & -v_{S\beta}^{*}(\omega t) \\ v_{S\beta}^{*}(\omega t) & v_{S\alpha}^{*}(\omega t) \end{bmatrix} \times \begin{bmatrix} \tilde{p}(\omega t) + \overline{P}_{dc}(\omega t) \\ 0 \end{bmatrix} \quad (2.22)$$

Therefore

$$i^*_{Comp,S} = \frac{1}{Ax}.\left[v^*_{S\alpha}(\omega t).\bar{p}(\omega t) + v^*_{S\alpha}(\omega t).\overline{P}_{dc}(\omega t)\right] \tag{2.23}$$

where $i^*_{Comp,S}$ denotes a reference source current. This current then needs to be looked at in relation to the real source current in order to obtain the expected switching pattern for VSI.

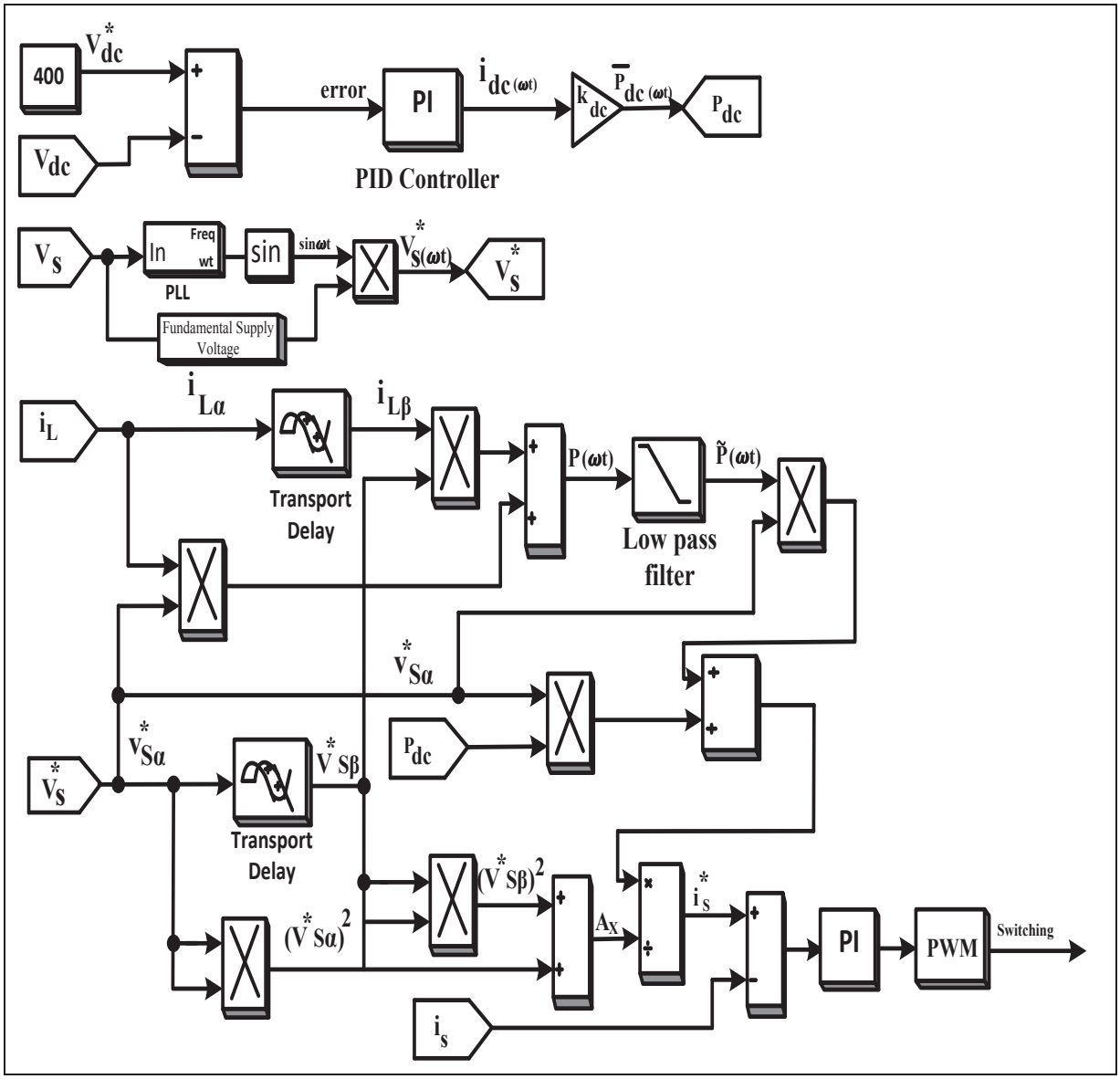

Figure 2.16 The block diagram of indirect current control technique for shunt APF

2.5.4.1 Simulation results

Table 2.3 The specification parameters used for pq indirect control simulation

Description	Value
Phase voltage	V_s = 120 V (rms)
Frequency	F_s = 60 Hz
Line impedance	L_s = 0.5 mH
Voltage-source type nonlinear load	C_L = 500 µF , R_L = 25 Ω
current-source type nonlinear load	L_L = 50 mH , R_L = 10 Ω
Active filter parameters	L_c = 3.5 mH , R_c = 0.1 Ω C_{dc1} = C_{dc2} =2000 µF
DC-bus voltage	V_{dc}^* = 400 V
PI regulation parameters	K_p = 0.6 and K_i = 10

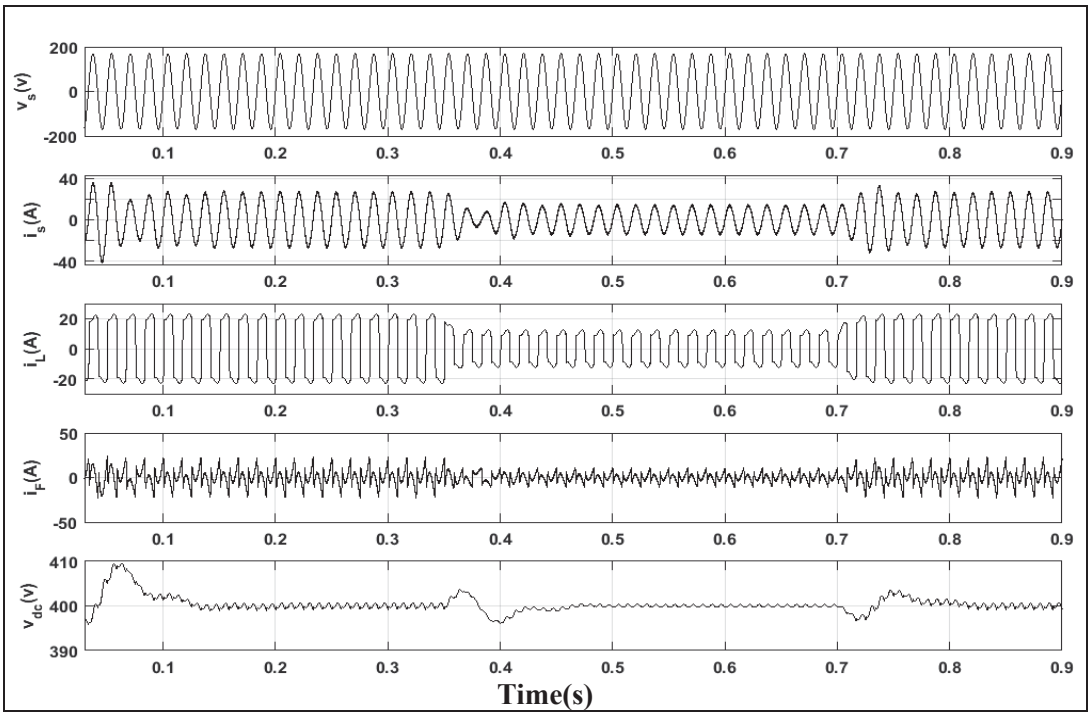

Figure 2.17 The Simulation result during indirect control technique with load variation

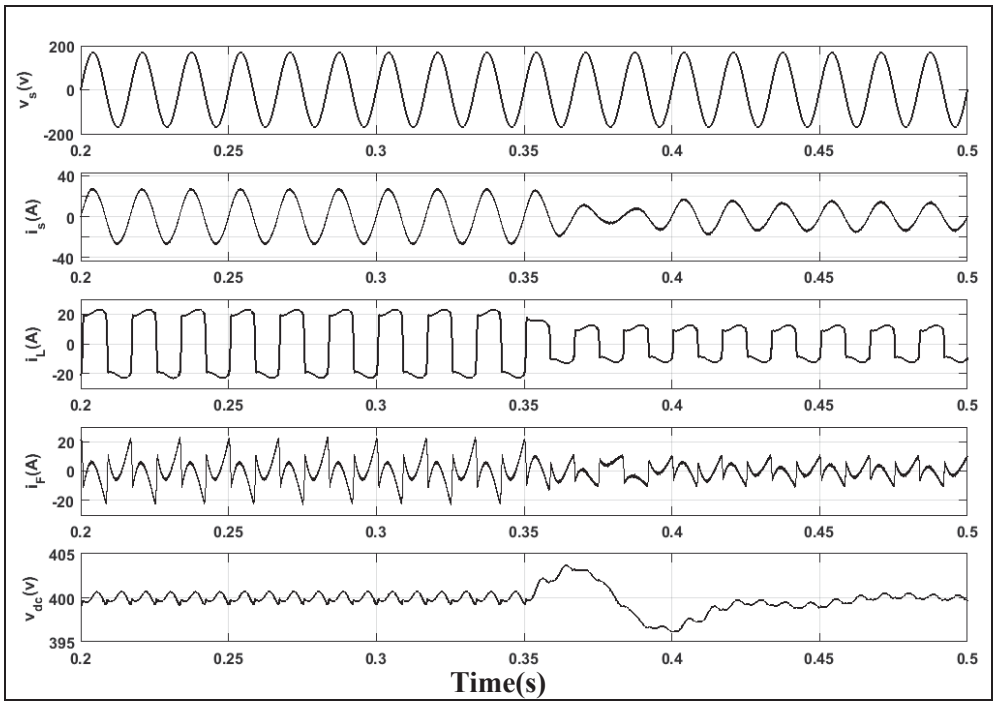

Figure 2.18 The Simulation result during load current decrease

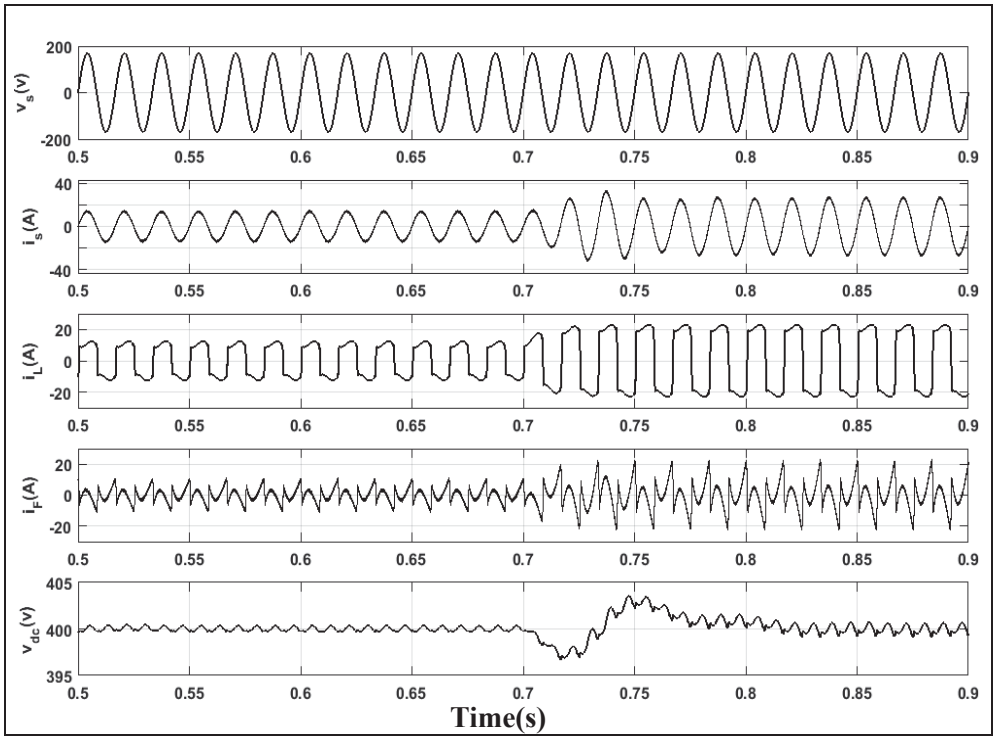

Figure 2.19 System response to a step increase of load current

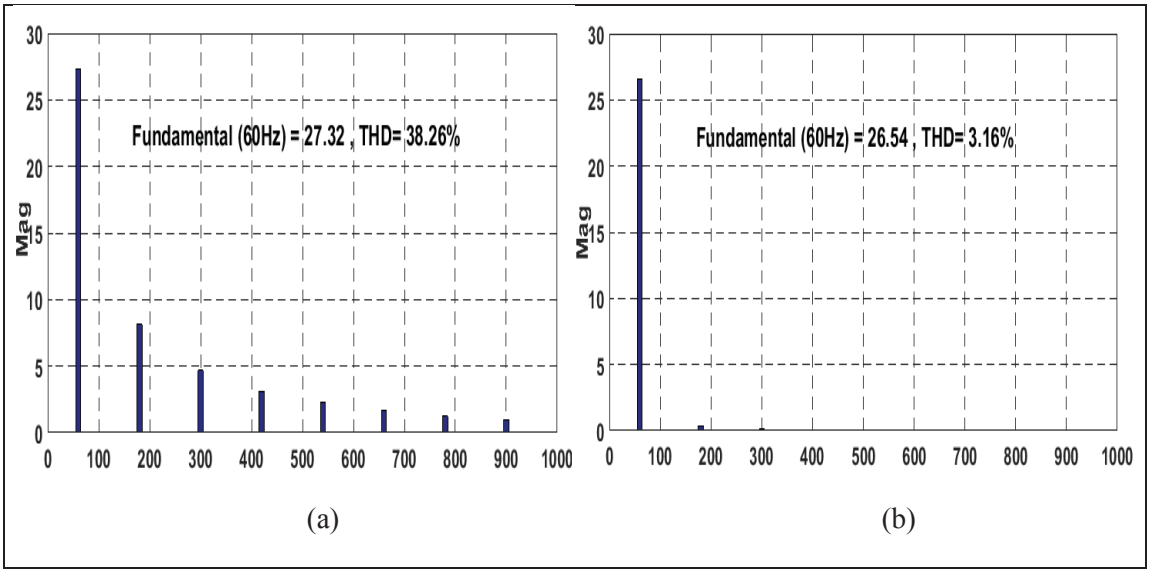

Figure 2.20 The total harmonic distortion a) load current b) source current in study state

2.6 Sliding mode control SMC

2.6.1 Introduction

Sliding mode control (SMC) is a nonlinear control technique characterized by outstanding properties, such as accuracy, robustness, easy tuning and easy implementation. Based on the SMC theory, it is possible to build robust controllers for high-order nonlinear plants functioning under diverse conditions of uncertainty. Nonetheless, their implementation may result in oscillations of finite amplitude and frequency in the control loop. The first main advantage of SMC is that the system's dynamic behavior may be tailored by the particular choice of sliding function. The second main advantage is that the closed loop response becomes totally unresponsive to some particular uncertainties. This principle extends to model parameter uncertainties, disturbance and non-linearity that are delimited. The current section presents an overview of the SMC theory and introduces the design tools used later in this thesis. It offers a comprehensive report of existing chattering reduction methods. The final methods evaluation and comparison offers a basis for implementation decisions of sliding mode controllers.

"The dynamic performance of the (SAPF) modeled in the synchronous orthogonal "dq" frame is enhanced by the nonlinear control technique. The exact feedback linearization theory was applied in the controller's design, which made it possible to decouple the currents, enhance their tracking behavior and improve the DC voltage regulation. The reference signals were obtained by taking the harmonic currents from the measured load currents. In the orthogonal frame, the fundamental current component can be considered as a DC component, and consequently, the harmonic load currents can be taken with high-pass filters (HPFs) which were based on fourth order Butterworth low-pass filters. This method's drawback is in the delay that takes place when the control system is digitally implemented. Even if the HPF works perfectly, not all the harmonic load currents can be filtered. Moreover, the system is not capable to entirely compensate load current unbalance due to the phase shift that is induced by the filter" (Rahmani, Mendalek et Al-Haddad, 2010)

2.6.2 Modeling and control

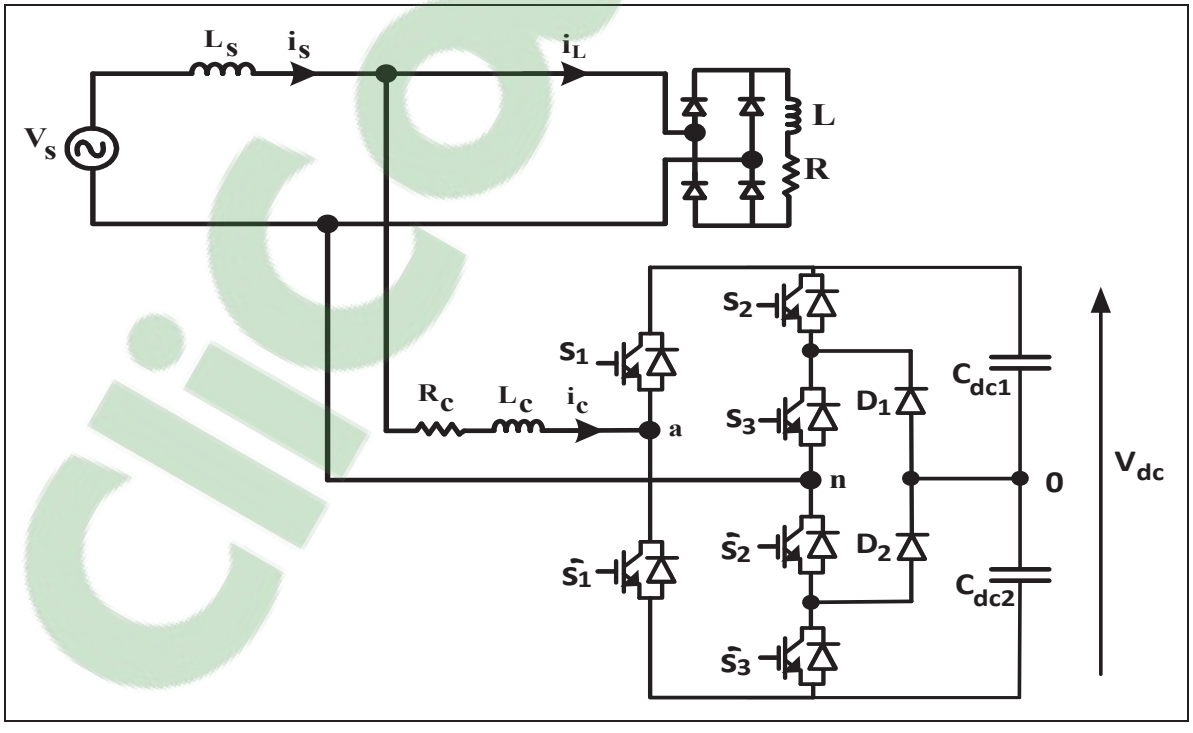

Figure 2.21 Single-phase shunt 5 level active power system
Taken from (Haddad et al., 2015)

We can express the system as follows by applying the Kirchhoff rules used in SPMAPF:

$$L_C \frac{di_c}{dt} = -R_c i_c - qV_{dc} + v_S \tag{2.24}$$

$$C_{dC} \frac{dV_{dc}}{dt} = q i_c \tag{2.25}$$

where $V_{dc} = V_{dc1} + V_{dc2}$

Then, using sliding mode law, we can express the sliding surface as:

$$\sigma = K(i_C - i_C^*) \tag{2.26}$$

Here, we can formulate the reference current i_C^* as:

$$i_C^* = i_{LH} + i_{dc} \tag{2.27}$$

In writing the equivalent control law, we can express the sliding surface derivate as follows :

$$\dot{\sigma} = K\left(\frac{-R_C i_C - q_{eq} V_{dC} + v_s}{L_C} - \frac{di_C^*}{dt}\right) = 0 \tag{2.28}$$

Then the equivalent control law will be:

$$q_{eq} = \frac{-R_C i_C + v_s - L_C . \frac{di_C^*}{dt}}{V_{dC}} \tag{2.29}$$

$$q = q_{eq} - K\, sgn(\sigma) \tag{2.30}$$

Our aim is that we maintain a constant DC bus voltage throughout all conditions. Hence, V_{dc} must follow reference V_{dc}^*, and the error $\tilde{V}_{dc} = V_{dc}^* - V_{dc}$ must be introduced via a Proportional Integral regulator::

$$I_{dc} = K_p\,\tilde{V}_{dc} + K_i \int \tilde{V}_{dc}\,dt \tag{2.31}$$

The resulting closed-loop transfer function of the DC voltage is:

$$\frac{V_{dc}(s)}{V_{dc}^{*}(s)} = \frac{K_p}{C_{dc}} \frac{s + \frac{K_i}{K_p}}{s^2 + \frac{K_p}{C_{dc}} s + \frac{K_i}{C_{dc}}} = 2\xi\omega_v \frac{s + \frac{\omega_v}{2\xi}}{s^2 + 2\xi\omega_v s + \omega_v^2} \tag{2.32}$$

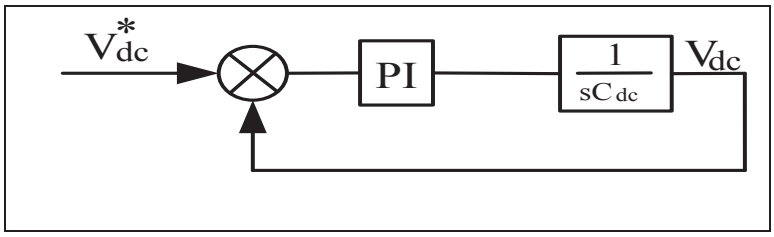

Figure 2.22 Control law of closed-loop transfer function of the DC voltage block diagram

By identification, the proportional and integral gains are given by:

$$K_p = 2\xi\omega_v C_{dc} \text{ and } K_i = \omega_v^2 C_{dc}$$

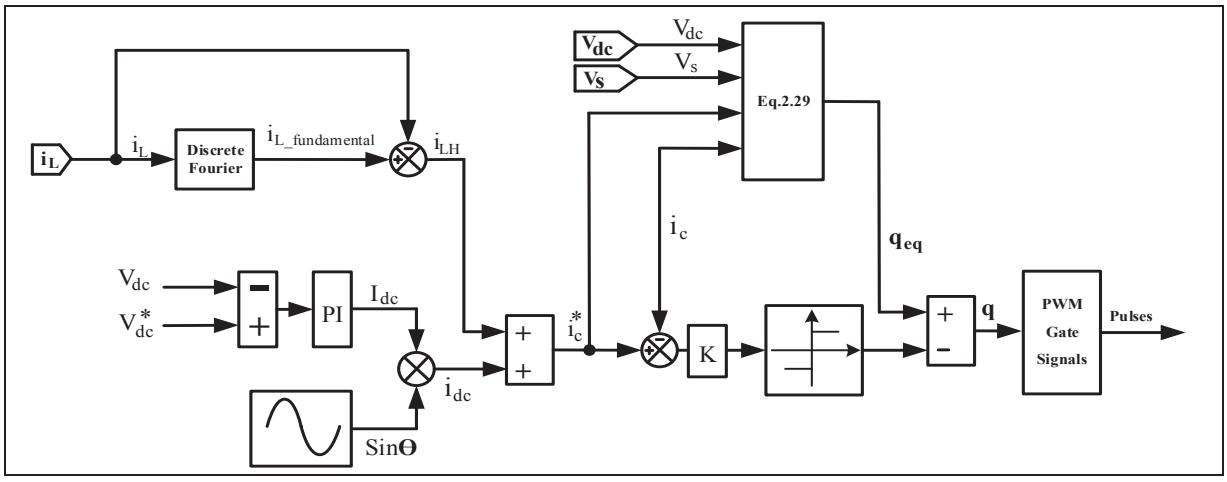

Figure 2.23 Sliding mode control law implementation

2.6.3 Simulation results

Table 2.4 Specification parameters used for sliding mode control simulation

Description	Value
Phase voltage	V_s = 120 V (rms)
Frequency	F_s = 60 Hz
Line impedance	L_s = 0.5 mH
current-source type nonlinear load	L_L = 50 mH , R_L = 10 Ω
Active filter parameters	L_c = 3.5 mH , R_c = 0.1 Ω C_{dc1} = C_{dc2} =2000 μF
DC-bus voltage	V_{dc}^* = 250 V
PI regulation parameters	K_p = 1 and K_i = 5

Table 2.5 Switching true table used for configuration state

State	V_{an}	S_1	S_2	S_3
1	V_{dc}	1	1	0
2	V_{dc} /2	0	1	0
3	0	0	0	0
4	-V_{dc}/2	0	1	1
5	-V_{dc}	0	0	1

S1, S2 and S3 are complementary respectively to S1′, S2′ and S3′.

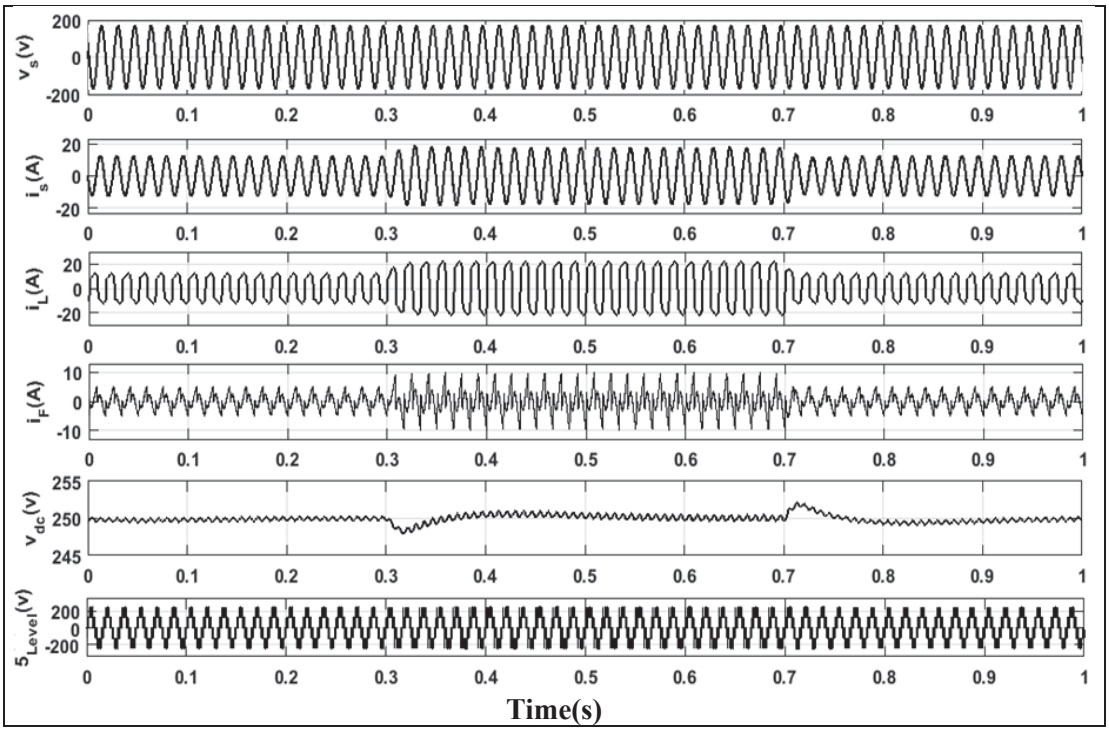

Figure 2.24 Simulation result during sliding mode control technique with load variation

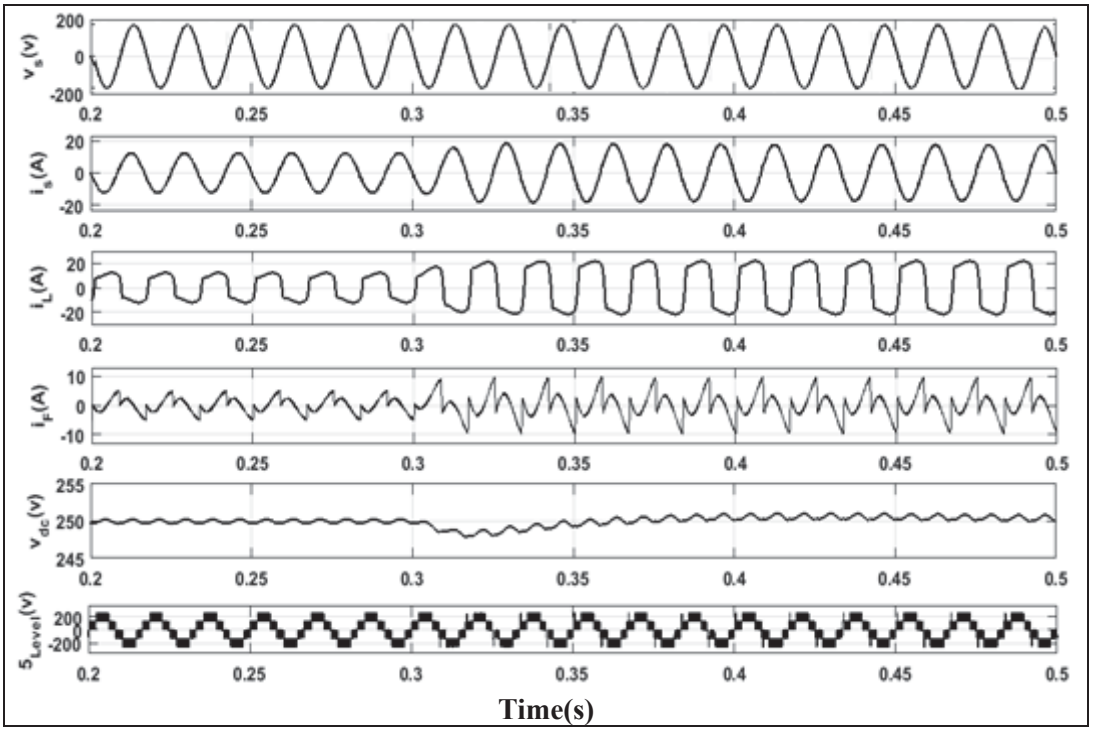

Figure 2.25 Simulation result during step increase of load current

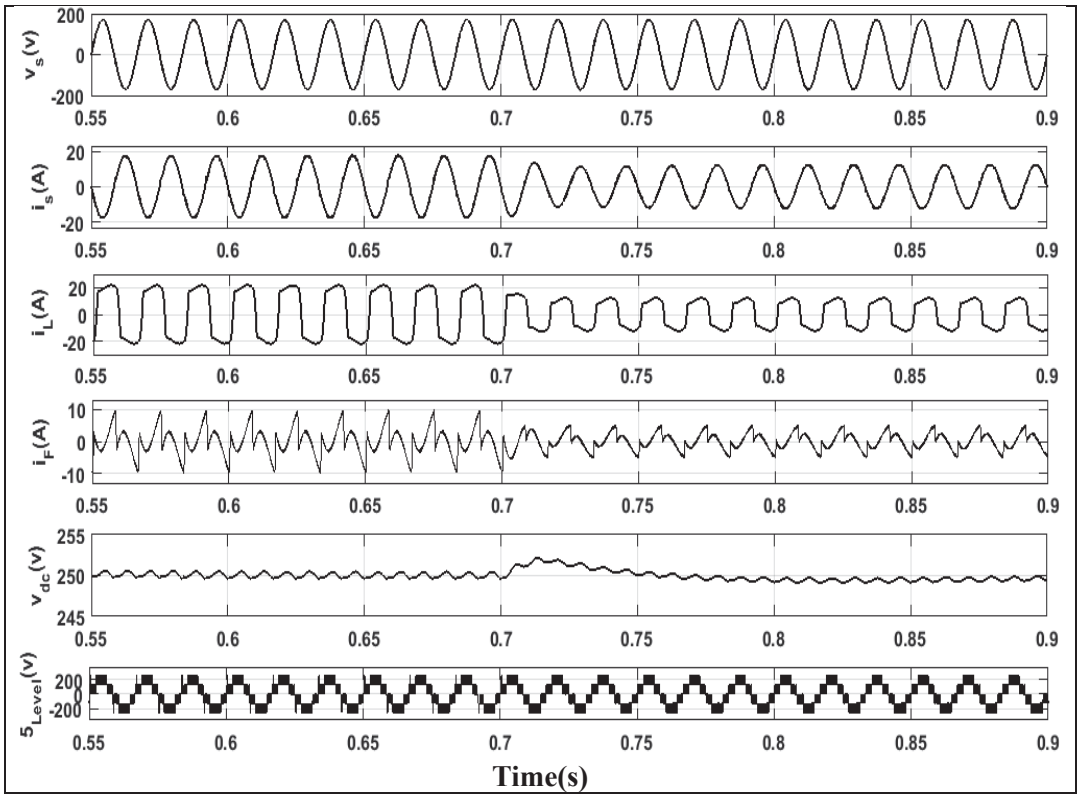

Figure 2.26 Simulation result during step decrease of load current

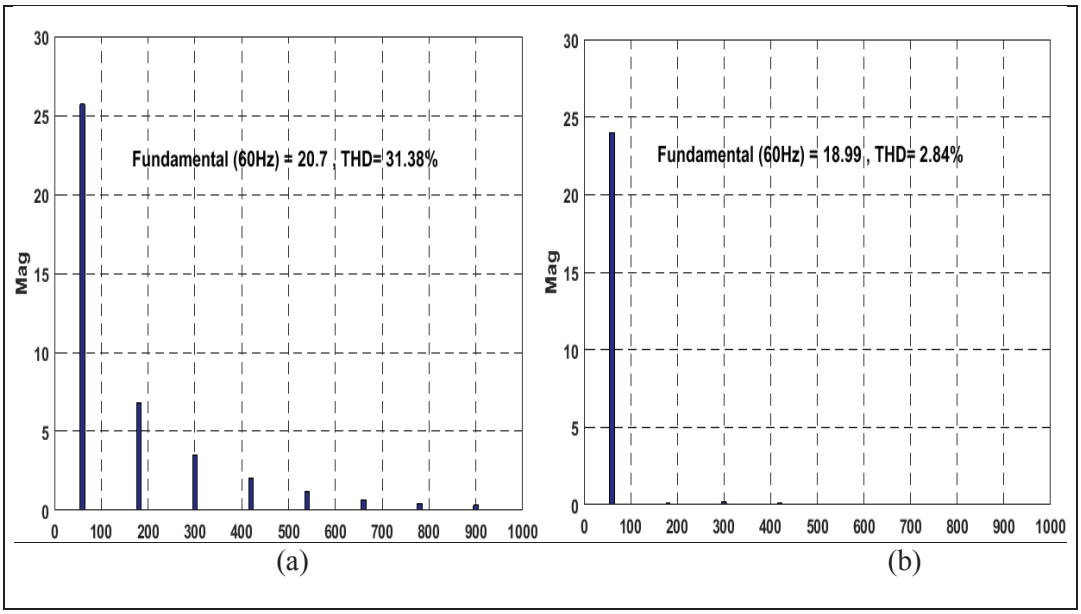

Figure 2.27 The total harmonic distortion a) load current b) source current at study state

2.6.4 Nonlinear control

(Mahmud, Pota et Hossain, 2014), a novel nonlinear current control scheme is presented in a single-phase grid-connected PV system. The controller is built using partial feedback linearization, and reference current calculations are performed using the maximum power point tracking system. This method.

highlights the internal dynamics of the system, showing stability as being central to implementing the controller. The controller is evaluated by tracking both the reference and the grid currents. The system is simulated to determine how it might perform in a variety of operating scenarios (e.g., system errors) and conditions (atmospheric changes) in comparison to traditional controllers.

The nonlinear system dynamics are converted mathematically using partial feedback linearization. The outcome is a partly linear or reduced-order linear system that functions without operating points, given that nonlinearities can be nullified by the application of non-linearity. It also brings an autonomous system whose dynamics are called internal dynamics that need to be stable. One of the primary benefits of this controller is its ability to function outside the full model's dynamics. Hence, a new current controller with partial feedback linearization needs to be designed as a means of controlling any current being pushed towards the grid.(Mahmud, Pota et Hossain, 2014)

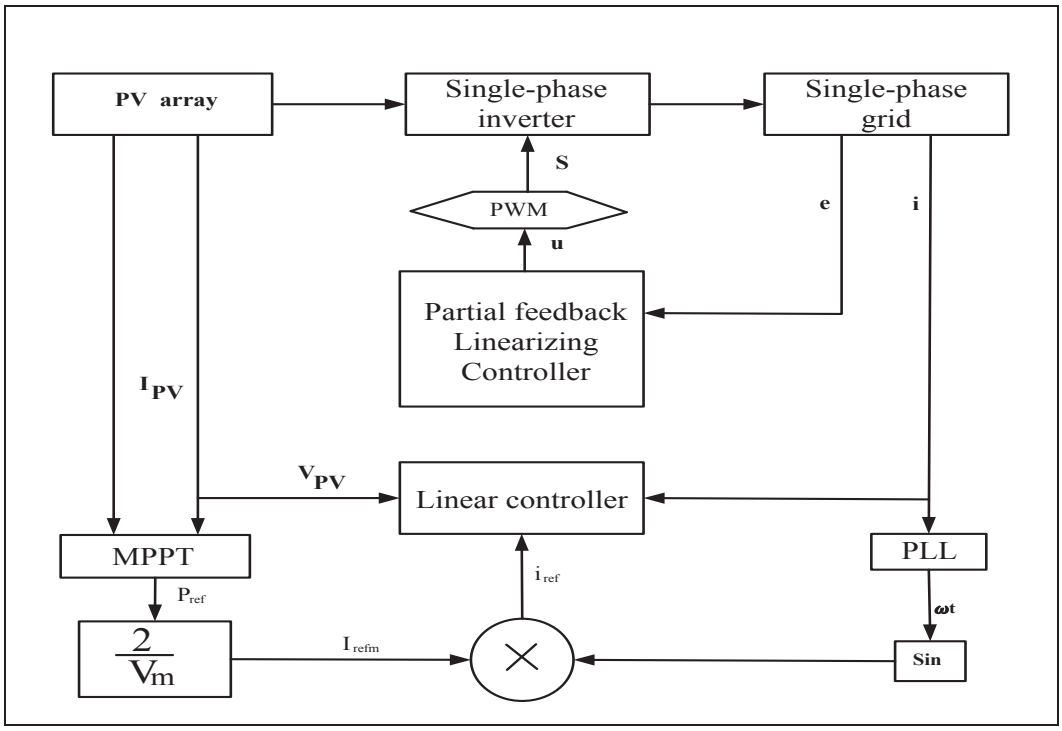

Figure 2.28 Implementation block diagram of partial feedback linearizing controller
Taken from (Mahmud, Pota et Hossain, 2014)

2.6.5 Nonlinear control based Lyapunov direct method

(Komurcugil, 2009) proposed using Lyapunov's direct method as the basis for his novel nonlinear control strategy designed for single-phase PWM current-source inverters. The approach focuses on energy creation inverter system states, framed as a Lyapunov function, and figuring out which control strategy can render the time derivative in the Lyapunov function perpetually negative in all values. The research indicates the plausibility of designing having a control which is universally stable, but which sacrifices the inductor current's time-varying reference function. Despite the challenge presented in evaluating the inductor current's ripple component, the researcher succeeds in devising a control method which is essentially based on the Lyapunov model and includes an inductor current constant reference. The performance and practicality of the suggested control strategy are shown through computer simulations and experiments (Komurcugil, 2009)

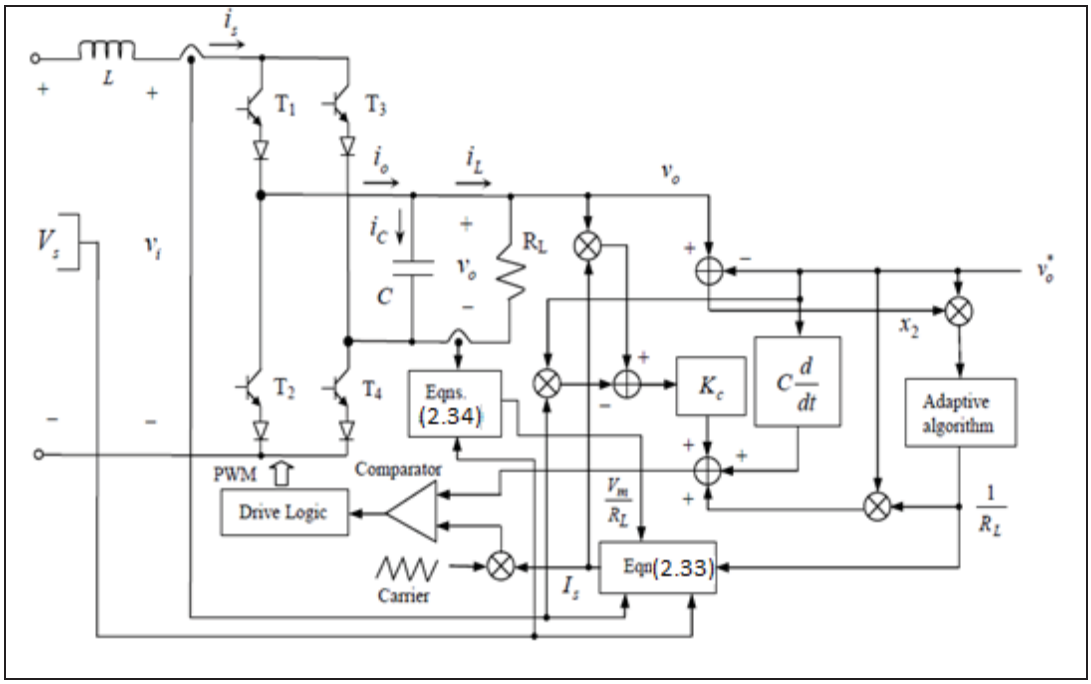

Figure 2.29 The block diagram of the control strategy system
provided by the article for a single-phase
Taken from(Komurcugil, 2009)

((Komurcugil, 2009) control strategy's performance was verified by several different simulations and experiments under a resistive load operation (Komurcugil, 2009).

. (Komurcugil, 2009)

$$\mathrm{I}_s = 0.5[(V_s/\mathrm{r}) \pm \sqrt{(V_s/r)^2 - (2V_m^2/\mathrm{r}R_L)}] \tag{2.33}$$

$$i_L^{\alpha} = (V_s/R_L)\sin(\omega t) \tag{2.34}$$

2.6.6 Nonlinear feed-forward controller

"A nonlinear feed-forward controller applied to a single-phase uninterruptible power supplies (UPS) is presented in this article. The controller was designed using a one cycle based PWM generator and an output-current feedforward, in order to cancel input-voltage disturbances and nonlinear load currents, respectively. It also comprises an external control loop to

guarantee good output-voltage tracking. The controller's design is based on a large-signal approach, made to achieve good transient response and stability within a wide range of parameter variations. Moreover, despite the nonlinear nature of the controller, a linear average output-voltage dynamic response is obtained. The proposed control has the following characteristics: fast transient response, low THD sine-wave output-voltage, fixed switching frequency and high resistance against load and line step changes. Simulation results demonstrate that this control technique is effective for inverters in UPS applications, especially in the case when nonlinear loads must be provided and UPS DC-link has large undesirable ripple"(Guerrero et al., 2002)

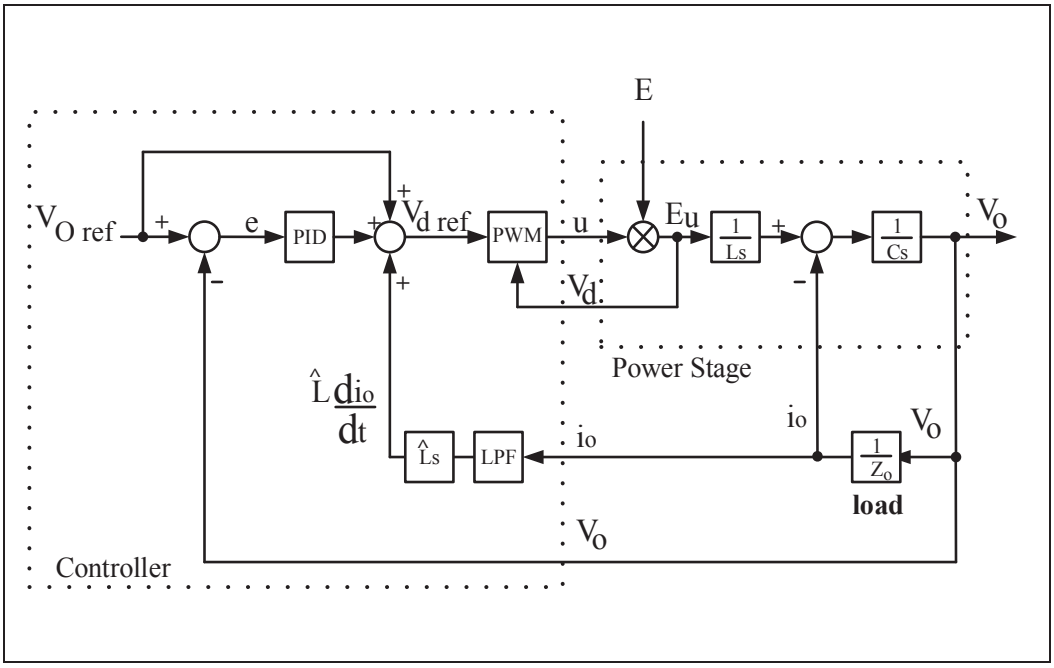

Figure 2.30 Block diagram scheme of the closed-loop system
Taken from (Guerrero et al., 2002)

2.7 Conclusion

Four different controls strategies have been simulated in different scenarios resulting pretty much the same in case of two level type of converter. Whereas, the big difference was observed in case of five level, where the result in terms of compensation quality of signal and THD are much better compared to the two level. The reason of choosing five level

instead of two level is that Low dc bus voltage can be used, better quality of output voltage waveform (use low filter) and consequently lower voltage rating devices can be used. However, there are drawbacks such as higher component count and extra and more complex control for six switches converter compared to the well-known four devices one.

CHAPTER 3

SCOTT AND LEBLANC TRANSFORMERS DESSIGN AND SIMULATION FOR POWER QUALITY IMPROVEMENT

3.1 Introduction

In general, energy companies that have public ownership power the majority of current electrical railway systems around the world. However, because of the train's high speed and the extensive distances they travel, the trains' energy is mostly derived from single-phase systems that feed off their respective three-phase public systems. Because of this, the running of the world's train systems have caused voltage unbalances to a significant degree, which in turn has caused issues related to the quality of energy allocated to other areas of publicly-owned power systems. This problem has also impacted various types of equipment used in the system.

Specifically, power unbalances can lead to both minor and major issues, such as malfunctioning of protective relays, overheating of motors, and communication interference. Individually, and when dealt with as they occur, these issues have only minor impacts, but collectively, and if not resolved in the short term, the problems can ultimately lead to system shut-down. For example, if induction motors are malfunctioning due to energy imbalances, they will be less efficient and could severely overheat, causing power loss. These issues can also cause a shorter life-cycle of the equipment or component. China is going full-speed ahead with implementation of the latest in high-speed train technology, mainly to augment and expand the country's current rail transport system. Unfortunately, the expansion is causing major issues related to power quality, such as harmonic currents, unbalance, and negative sequence currents.(Chen, 1994)

In general, issues around power can be in intimately related to the type of transformer that exists in a traction system. The most popular transformers for industrial and commercial applications are the Scott transformers and Leblanc transformers, although the Woodbridge

transformers and three-phase V/V transformers are also relatively widely used. Scott connections change three-phase into two-phase, or into two single-phases. Such changes serve to decrease the voltage imbalances that can arise in the operation of massive rail systems.

Given this advantage of the Scott approach, this system is particularly attractive to operators of rail lines that feature only moderate short-circuit capacity. However, a major drawback of the Scott transformer is its high cost, which can be nearly double that of single-phase systems. A secondary drawback is its relatively low efficiency levels, making single-phase transformers a better alternative in both of these regards. Yet despite their high cost and low efficiency, Scott transformers operate as highly balanced transformers, making feeder sections power-balanced without the presence of harmonics. Likewise, with the Scott system, any current which enters the utility grid is also balanced and without the presence of harmonics.

Nowadays, Scott transformers are typically employed in traction systems. At the same time, the Leblanc system, which has been around for over a century, is also able to change three-phase supplies into two-phase ones, so it offers an alternative to the Scott system. The present work looks at both Scott and Leblanc transformers in detail in relation to the application in modern rail systems.

3.2 Modeling of Scott transformer

Issues related to unbalance issues of traction stations can be easily resolved through the use of Scott transformers. Scott systems can be used to shift a balanced two-phase system to a balanced three-phase AC network. Figure 3.1 depicts some connection diagrams in a Scott-connected scheme, showing the transformation of a three-phase supply into a two-phase/two single-phase one. As shown in the diagram, the two single-phase loads on the secondary load obtain three-phase power from the primary side, causing the voltage imbalance to reduce.
(Chen, 1994)

3.2.1 Current and voltage relationships for Scott transformer

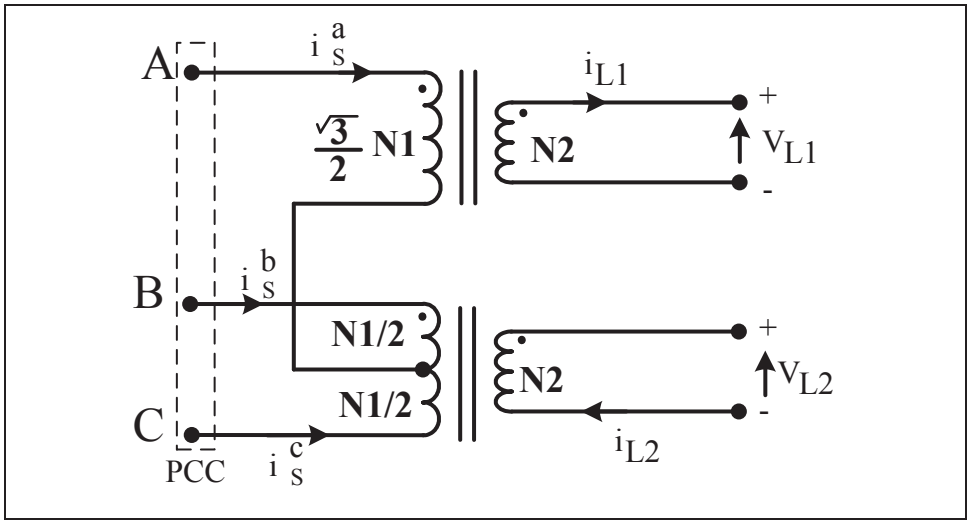

Figure 3.1 Phasor and connection diagrams of a Scott connected transformer
Taken from (Chen, 1994)

As shown in Figure 3.1, secondary or primary voltage/current relationships in Scott transformers can be expressed as:

$$I_S^a = \frac{2}{\sqrt{3}} \frac{N_2}{N_1} i_{L1} \tag{3.1}$$

$$I_S^b = \frac{I_L^a}{2} - \frac{N_2}{N_1} i_{L2} = \frac{N_2}{N_1} \left(-\frac{1}{\sqrt{3}}\ i_{L1} + i_{L2}\right) \tag{3.2}$$

$$i_S^b = \frac{N_2}{N_1} \left(i_{L2} - \frac{1}{\sqrt{3}}\ i_{L1}\right) \tag{3.3}$$

$$I_S^c = \frac{I_L^a}{2} + \frac{N_2}{N_1} i_{L2} = -\frac{N_2}{N_1} \left(\frac{1}{\sqrt{3}}\ i_{L1} + i_{L2}\right) \tag{3.4}$$

$$I_S^c = -\frac{N_2}{N_1}\left(i_{L2} + \frac{1}{\sqrt{3}}\, i_{L1}\right) \tag{3.5}$$

$$V_{AB} = \frac{N_1}{2N_2}\,(\sqrt{3}V_{L1} - V_{L2}) \tag{3.6}$$

And

$$V_{BC} = \frac{N_1}{N_2}\, V_{L2} \tag{3.7}$$

$$V_{CA} = -\frac{N_1}{2N_2}\,(\sqrt{3}V_{L1} + V_{L2}) \tag{3.8}$$

3.2.2 Equivalent loads for Scott transformer

To make the derivations less complex, we assume the transformers as being ideal, meaning that they feature zero impedance and zero voltage drop, and thus zero loss. With this scenario, both the transformers and traction load for the rail substation are given as equivalent loads. Such that the transformer's primary-side voltage imbalances at the point of common coupling (PCC) can be quickly and simply formulated. For the secondary side, the relationships between voltages, currents and complex power can be given as follows:(Chen, 1994)

$$i_{l1}^* = \frac{S_{L1}}{V_{L1}} = \frac{-S_{L1}}{\sqrt{3}\,(\frac{N_2}{N_1})\, V_{pcc}^a} \tag{3.9}$$

$$i_{L2}^{*} = \frac{S_{L2}}{V_{L2}} = \frac{-j\,S_{L2}}{\sqrt{3}\,(\frac{N_2}{N_1})\,V_{pcc}^{a}} \tag{3.10}$$

$$i_s^{a\,*} = \frac{2}{3}\frac{S_{L1}}{V_{pcc}^{a}} \tag{3.11}$$

$$i_s^{b\,*} = -\frac{1}{3}\frac{S_{L1}}{V_{pcc}^{a}} + j\frac{S_{L2}}{\sqrt{3}V_{pcc}^{a}} \tag{3.12}$$

$$i_s^{c\,*} = -\frac{1}{3}\frac{S_{L1}}{V_{pcc}^{a}} - j\frac{S_{L2}}{\sqrt{3}V_{pcc}^{a}} \tag{3.13}$$

Therefore,

$$S_s^{a} = V_{pcc}^{a}\, i_s^{a\,*} = \frac{2}{3}S_{L1} \tag{3.14}$$

$$S_s^{b} = V_{pcc}^{b}\, i_s^{b\,*} = -\frac{\alpha^2}{3}S_{L1} + j\frac{\alpha^2}{\sqrt{3}}\,S_{L2} \tag{3.15}$$

$$S_s^{c} = V_{pcc}^{c}\, i_s^{c\,*} = -\frac{\alpha}{3}S_{L1} - j\frac{\alpha}{\sqrt{3}}\,S_{L2} \tag{3.16}$$

where $\alpha\ is\ the\ unity\ complex\ vector = ej2\pi/3$

An equivalent three-phase load for two single-phase traction loads S_{L1} and S_{L2} is expressed in Equation (3.16), showing the Scott system changing two single-phase sources into a three phase one (Chen, 1994)

3.3 Modeling of Leblanc transformer

The Leblanc transformer provides an alternative to the Scott system for dealing with unbalance issues at traction substations. Leblanc transformers are able to transfer load-side balanced two-phase systems over to balanced three-phase AC networks. Figure 3.2 illustrates a Leblanc connected transformer. As can be seen in the phasor diagram, Leblanc transformers can change three-phase supplies into two-phase ones, thereby decreasing voltage imbalances that result from single-phase traction loads. Further, as depicted in Figure 3.2, the Leblanc primary windings have a three-phase delta interphase connection, which is typical for a step-down unit from a high voltage source. This winding is beneficial for suppressing third-harmonic voltages. As can be seen, there is a common core which features a three-phase, three-limb design

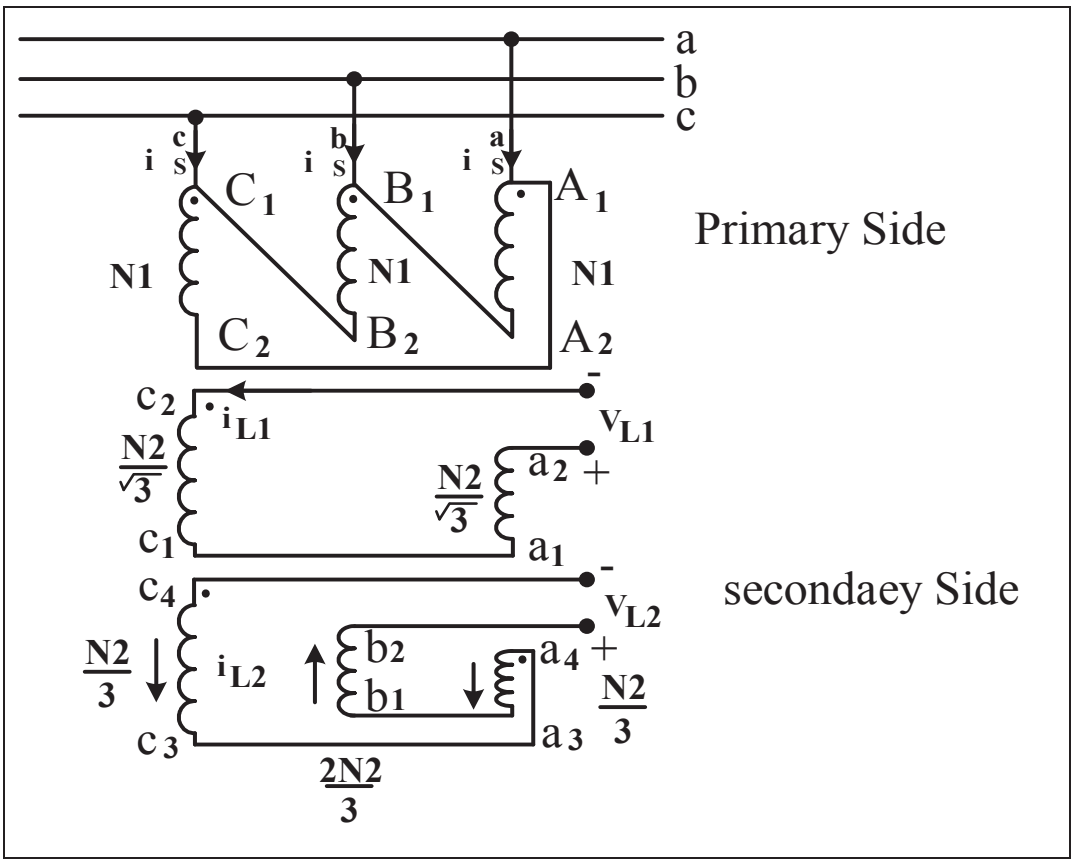

Figure 3.2 Phasor and connection diagrams of a Leblanc connected transformer
Taken from(Chen, 1994)

instead of the two single-phase core design found in Scott transformers. As well as having a less complex core set-up, Leblanc are cheaper to build as they require fewer active materials. They also require less floor space than a Scott connector.

3.3.1 Current and voltage relationships for Leblanc transformer

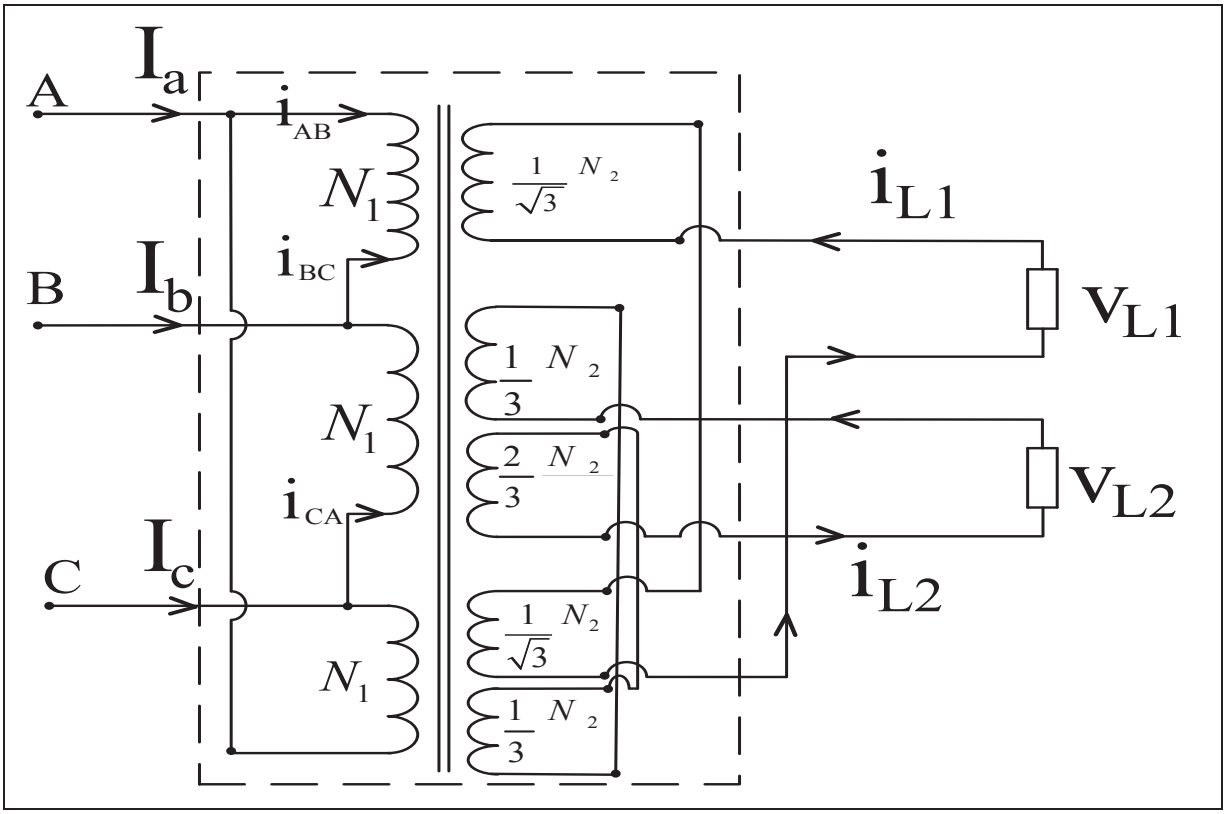

Figure 3.3 The connection diagrams of a Leblanc transformer

As shown in Figure 3.3, secondary or primary voltage/current relationships in Leblanc transformers can be expressed as:

$$I_S^a = \left(\frac{-1}{\sqrt{3}}\frac{N_2}{N_1}\, i_{L1} + \frac{1}{3}\frac{N_2}{N_1}\, i_{L2}\right) - \left(\frac{1}{\sqrt{3}}\frac{N_2}{N_1}\, i_{L1} + \frac{1}{3}\frac{N_2}{N_1}\, i_{L2}\right) \tag{3.17}$$

$$I_S^a = i_{L1}\left(\frac{-1}{\sqrt{3}}\frac{N_2}{N_1} - \frac{1}{\sqrt{3}}\frac{N_2}{N_1}\right) + i_{L2}\left(\frac{1}{3}\frac{N_2}{N_1} - \frac{1}{3}\frac{N_2}{N_1}\right) \tag{3.18}$$

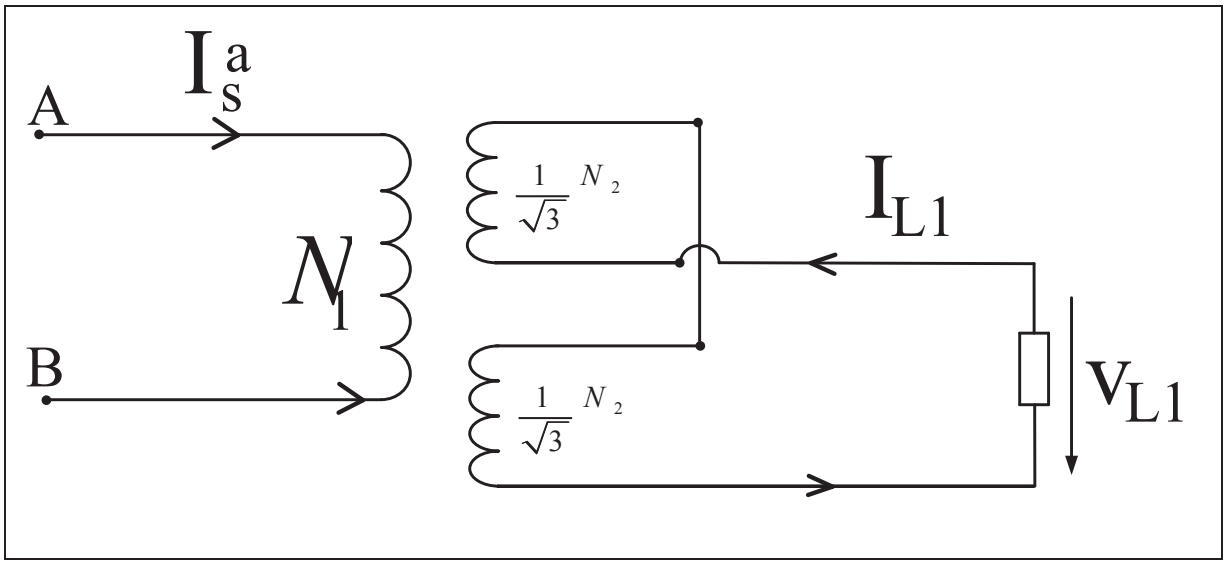

Figure 3.4 Part A and B of Leblanc connected transformer

$$I_s^a = -\frac{2}{\sqrt{3}}\frac{N_2}{N_1}\, i_{L1} \tag{3.19}$$

$$I_S^b = \left(-\frac{2}{3}\frac{N_2}{N_1}\, i_{L2}\right) - \left(-\frac{1}{\sqrt{3}}\frac{N_2}{N_1}\, i_{L1} + \frac{1}{3}\frac{N_2}{N_1}\, i_{L2}\right) \tag{3.20}$$

$$I_S^b = -\frac{N_2}{N_1}\, i_{L2}\left(-\frac{2}{3} - \frac{1}{3}\right) + \left(\frac{1}{\sqrt{3}}\frac{N_2}{N_1}\, i_{L1}\right) \tag{3.21}$$

$$I_S^b = \frac{N_2}{N_1}\left(\frac{1}{\sqrt{3}}\, i_{L1} + i_{L2}\right) \tag{3.22}$$

$$I_S^c = \left(\frac{1}{\sqrt{3}}\frac{N_2}{N_1}\, i_{L1} + \frac{1}{3}\frac{N_2}{N_1}\, i_{L2}\right) + \left(\frac{2}{3}\frac{N_2}{N_1}\, i_{L2}\right) \tag{3.23}$$

$$I_S^c = \frac{N_2}{N_1}\, i_{L2}\left(\frac{1}{3}+\frac{2}{3}\right)+\left(\frac{1}{\sqrt{3}}\,\frac{N_2}{N_1}\, i_{L1}\right) \tag{3.24}$$

$$I_S^c = \frac{N_2}{N_1}\left(\frac{1}{\sqrt{3}}\;\; i_{L1} - \;\; i_{L2}\;\right) \tag{3.25}$$

From figure 3.3

$$V_{L1} = \; -\frac{N_2}{\sqrt{3}N_1} V_{pcc}^{ab}(1-\alpha) = -\frac{N_2}{N_1}\, V_{pcc}^{ab}\angle -30° \tag{3.26}$$

$$V_{L2} = \; -\frac{1}{3}\,\frac{N_2}{N_1} V_{pcc}^{ab}(-1+2\alpha^2-\alpha) = -\frac{N_2}{N_1}\, V_{pcc}^{ab}\angle 60° \tag{3.27}$$

In which

$$V_{pcc}^{a} = \; \frac{V_{pcc}^{ab}\angle -30°}{\sqrt{3}} \tag{3.28}$$

$$V_{pcc}^{b} = \; \frac{V_{pcc}^{ab}\angle -30°}{\sqrt{3}}\,\alpha^2 \tag{3.29}$$

$$V_{pcc}^{c} = \; \frac{V_{pcc}^{ab}\angle -30°}{\sqrt{3}}\,\alpha \tag{3.30}$$

3.3.2 Equivalent loads for Leblanc transformer

Similar to the assumption made in relation to the Scott transformer, equivalent loads can be used to represent Leblanc transformers and traction load for rail substations, in which case, Relationships among voltages, currents and complex powers for secondary can be expressed as:

$$i_{L1}^{*} = \frac{S_{L1}}{V_{L1}} = \frac{-S_{L1}}{\sqrt{3}\ {}^{N_2}/_{N_1}\ V_{pcc}^{a}} \tag{3.31}$$

$$i_{L2}^{*} = \frac{S_{L2}}{V_{L2}} = \frac{-j\ S_{L2}}{\sqrt{3}({}^{N_2}/_{N_1})V_{pcc}^{a}} \tag{3.32}$$

$$i_{L}^{a\,*} = \frac{2}{3}\frac{S_{L1}}{V_{pcc}^{a}} \tag{3.33}$$

$$I_{s}^{b\,*} = -\frac{1}{3}\frac{S_{L1}}{V_{pcc}^{a}} + j\frac{S_{L2}}{\sqrt{3}V_{pcc}^{a}} \tag{3.34}$$

$$I_{s}^{c\,*} = -\frac{1}{3}\frac{S_{L1}}{V_{pcc}^{a}} - j\frac{S_{L2}}{\sqrt{3}V_{pcc}^{a}} \tag{3.35}$$

Therefore

$$S_{s}^{a} = V_{pcc}^{a}\ i_{s}^{a\,*} = \frac{2}{3}S_{L1} \tag{3.36}$$

$$S_{s}^{b} = V_{pcc}^{a}\ i_{s}^{b\,*} = -\frac{\alpha^2}{3}S_{L1} + j\frac{\alpha^2}{\sqrt{3}}S_{L2} \tag{3.37}$$

$$S_{s}^{c} = V_{pcc}^{c}\ i_{s}^{c\,*} = -\frac{\alpha}{3}S_{L1} - j\frac{\alpha}{\sqrt{3}}S_{L2} \tag{3.38}$$

Equation (3.38) expresses how Leblanc transformers change two single-phase traction loads S_{L1} and S_{L2} into equivalent three-phase loads like for Scott transformers. Consequently, any voltage unbalances due to single-phase traction loads coming from both transformers will be similar.(Chen, 1994)

3.4 Comparison of Scott and Leblanc transformer

From the perspective of imbalance issues, Leblanc transformers perform at the same level as Scott transformers, but the Leblanc one is much cheaper than the Scott one. Imbalances can be decreased by making the two transformer loads closer, but this might not be possible as the traction loads must adhere to scheduling and the trains must also maintain a certain distance. As a result, employing either the Scott or Leblanc systems means that an appropriate operating schedule shall enable the operators to gain the benefits of the systems.(Chen, 1994)

3.4.1 Validation of Leblanc transformer

The functionality of the Leblanc transformer is tested with balance and unbalanced load. In Figure 3.5 and 3.6, the connection of Leblanc transformer with the Three-phase source.

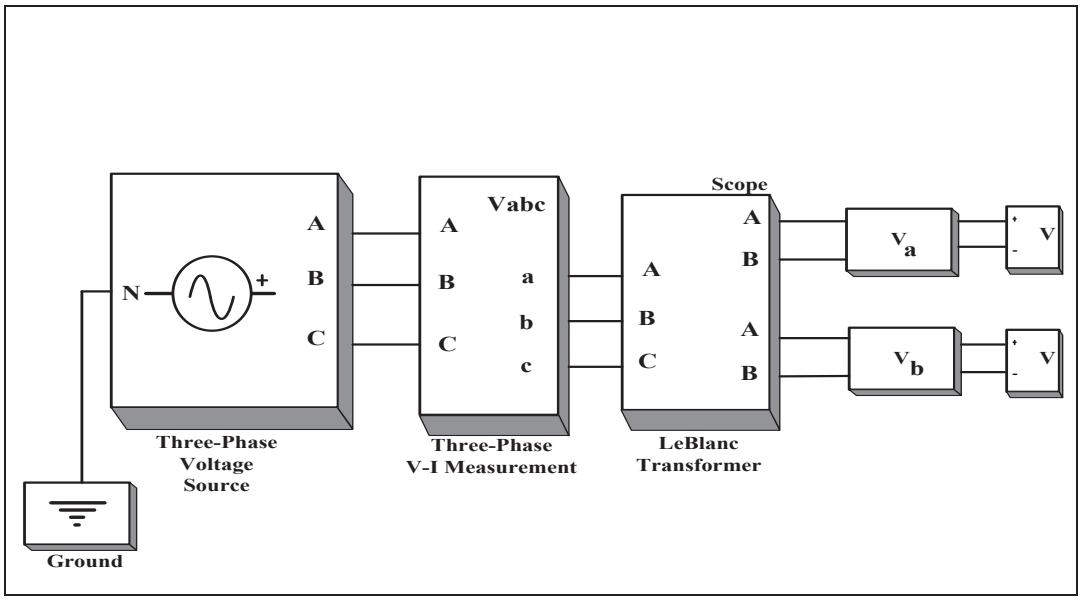

Figure 3.5The Leblanc transformer diagram by Matlab simulation

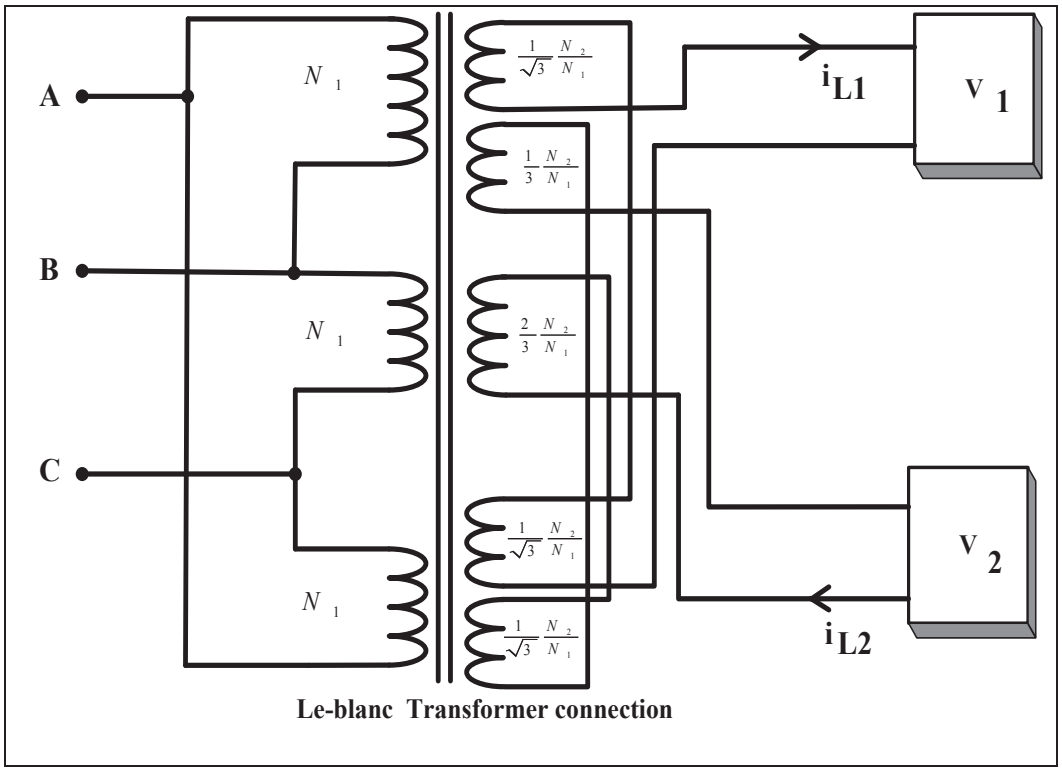

Figure 3.6 The special connection of Leblanc transformer by Matlab simulation

Table 3.1 The specification parameters used for LeBlanc simulation

Description	Value
Primary voltage	V_p = 600 V (rms)
Secondary voltage	V_s = 208 V (rms)
linear load RL 1&2	L_L = 50 mH , R_L = 10 Ω
Nonlinear load RL 1&2	L_L = 50 mH , R_L = 10 Ω
Frequency	F_s = 60 Hz
Line impedance	L_s = 0.5 mH , Rs = 0.1 Ω

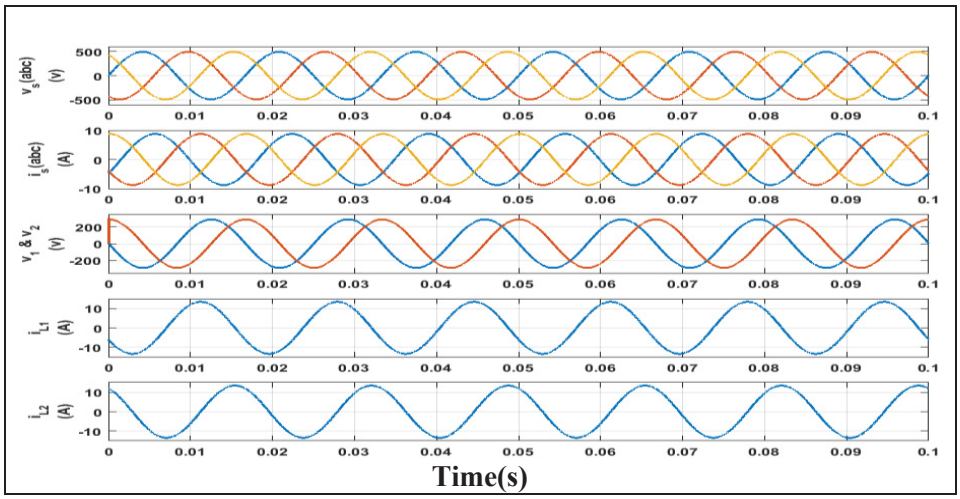

Figure 3.7 Input and output of voltage &current for Leblance transformer

The simulation results of figure (3.7) shows, the balancing of linear equal loads connected to two single phase voltage with 90 º phase shift, that the grid currents (i_{sabc}) are will balanced. The same simulation was also run with unequal different linear loads connected to the two single-phase 90 º phase shifted supply. Secondary voltage as depicted in figure (3.8) shows that grid current is unbalanced but remain sinusoidal since the load side currents are sinusoidal as well. This unbalances may cause voltage drop depends on the cable and facility impedances and cause voltage distortion as well

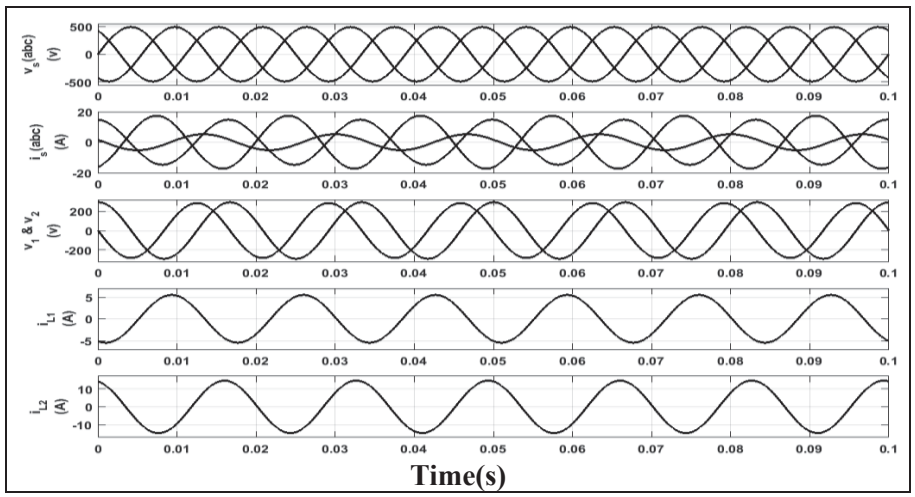

Figure 3.8 Voltage &Current for Leblance transformer in case of unbalanced load

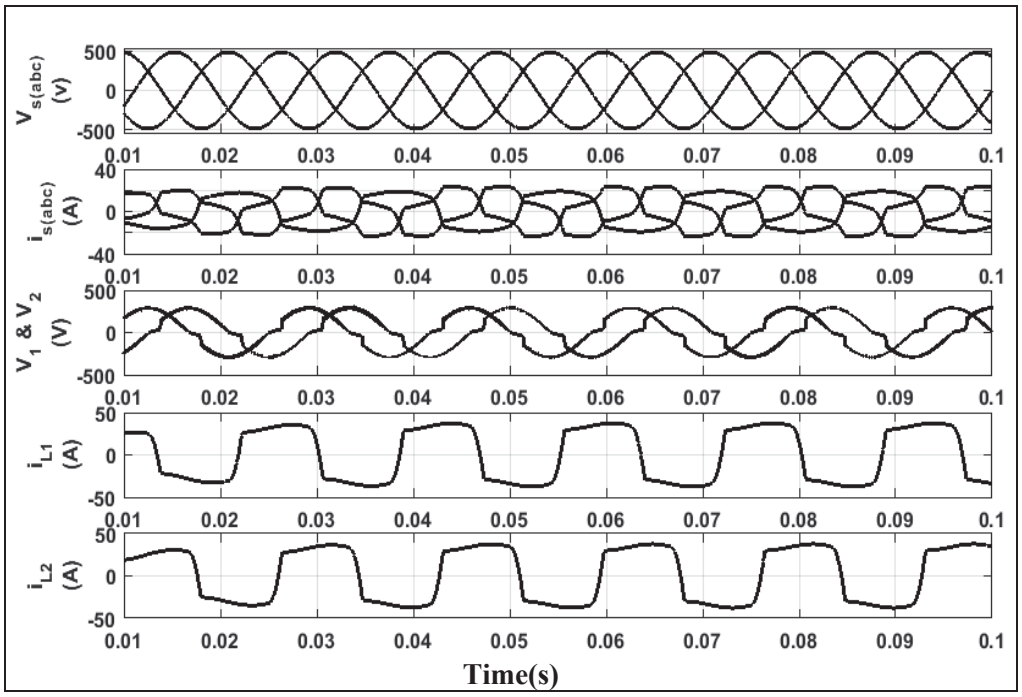

Figure 3.9 Voltage &Current of Leblanc transformer in case of balanced nonlinear load

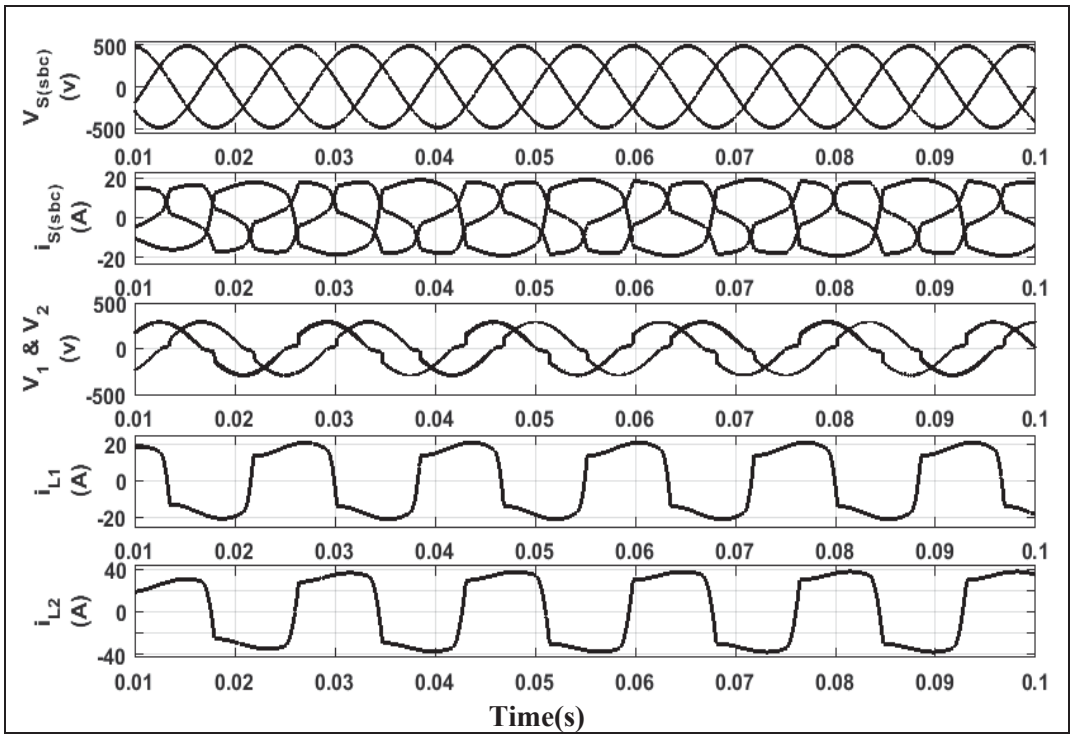

Figure 3.10 Voltage &Current of Leblanc transformer in case of unbalanced nonlinear load

The simulation results in figure 3.9 shows the conversion of the three-phase source voltage and two single phase voltage with 90º phase shift in case of nonlinear load. As we can see the grid currents are unbalanced and have to mush distortion which will affect the grid voltage. The grid current has to be balanced for power quality Performance. As shown in Figure 3.10, the load is unbalanced, which may cause an unbalanced grid current that on the impedance of cable and the impedance of the grid. We can see the different between linear and nonlinear load by calculating the Total Harmonic distortion as showing in the Figure 3.11

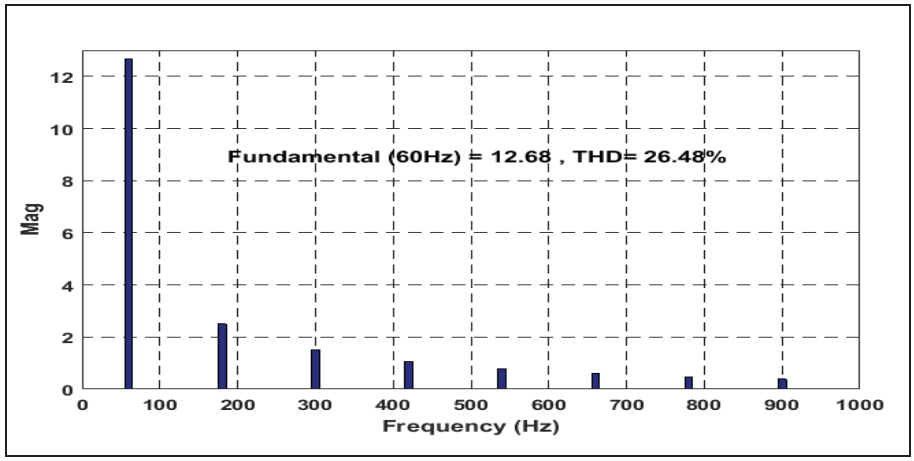

Figure 3.11 Harmonic spectrum of the source current in study state

3.4.2 Conclusion

This chapter has investigated power quality issues affecting the Leblanc and Scott connections. The solutions are suitable for vehicle systems that run on high-voltage electricity as well as for railway traction. The system is modeled and the technique is applied and evaluated to eliminate power quality problem. The results of the tests have shown that both the Scott and the Leblanc systems have similar unbalance impacts on power systems. Furthermore, PQ problems and other approaches can be used to deal appropriately with reactive power issues as well as unbalance and harmonics. The test results show improved performances by suppressing unbalance and reactive power.

CHAPTER 4

INTERFACING OF LEBLANC TRANSFORMER TO SUPPLY DIFFERENT UTILITIES

4.1 Introduction

The current chapter assesses Power-quality (PQ) of the traction power-supply system (TPSS) in trains. The proposed study concerns the design and control of PV solar and two single-phase five-level inverters connected to Leblanc transformer in order to feed two single phases' loads and produce 750 V for train utilities. Due to the electrified railway system being a nonlinear model of time varying natures of modern trains, the calculation and assessment of such power quality (PQ) problems is somewhat complex to establish. The suggested configuration guarantees complete compensation of unbalanced loads, the reactive power, and the current harmonics in three phase grid systems. Both inverters' controllers use a sliding mode type with indirect control. The first one regulates the dc bus voltage, the counterbalancing of the reactive and the current harmonics for the corresponding phase. The second indirect control, applied to the second inverter, counterbalances the reactive and the current harmonics for the corresponding phase b, balances the current between the two single-phase source current in order to guarantee balanced three phases current within the grid system. The suggested system is designed and simulated using Matlab Simulink/Simpower, and its performance is examined and discussed in the chapter. This chapter technically represents an important contribution to the integration of renewable energy and distributed generation to railway trains supply systems.

The PQ drawbacks encountered in this kind of power supply systems, such as harmonic, unbalance, and low-frequency voltage variation, have attracted growing awareness because of their unfavourable outcomes on both traction electrical devices and utility power systems. The PQ issues may have a negative impact on the rail signalling and critical communication systems, as well as the control system of the HST (high-speed train). Thus, it is imperative not only to balance the load but also to enhance the PQ as a means to ensure the reliability

and the stability of both the Traction Power Supply System (TPSS) and the Utility Power System.

A great number of researchers have looked at the harmonic modeling, harmonic analysis techniques, and the impacts of the harmonics on the TPSS. Another major issue in the HSR system is the natural instability of the traction loads. In cases of three-phase to single-phase or two-phase traction transformer, the instability of traction current creates a negative-sequence element that is equal or close to the positive-sequence element.

In this work, a developed configuration meant to improve the power quality of the entire system is presented. The latter includes a compensation of the current harmonics, power factor correction and current unbalances in the grid side. Moreover, multi-level inverters, sliding mode control and indirect control have been used to validate the compensation of the proposed configuration. It was found that from three-phases to two phases transformation, the Leblanc approach is particularly attractive to operators of rail lines.

4.2 Power quality issues

4.2.1 Harmonic and resonance

Fourier theory holds that periodic electrical quantities which are non-sinusoidal are represented by an infinite sum derived from the sine/cosine functions. From these, a series of harmonic components emerges, and the frequencies of these series can be formulated as integral multiples from the fundamental frequency. Therefore, in order to formulate a network currents' and voltages' harmonic content, the total harmonic distortion (THD) must first be stated.

Energy systems are able to exhibit harmonic resonance frequency due to interactions which can occur between distributed capacitance and transmission lines. In HSR systems, resonance results if harmonic currents which have been added from HSTs are identical to the natural frequencies of the system. However, this resonance could also lead to instability in HST

tractive drive systems, disrupting electrical devices such as communication tools and railroad signals and causing voltage distortions leading to power grid loss. Over-voltage of the resonance can hit various pieces of equipment and components, including the circuit breaker and arrester, destroying the protective insulation, while the over-current can lead to the magnetic field distortions. Such distortions can cause massive outbursts of electromagnetic radiation, which in turn can lead to communication system interference. Resonance can also saturate the core of the transformer, which affects the accuracy of the measurements.(He, Zheng et Hu, 2016)

4.2.2 System Unbalance

A balanced power system will have three-phase currents/voltages showing identical amplitudes, while phase differences are 120°. In an unbalanced system, however, the currents/voltages are not equal; the unbalance is measured with reference to the nominal quantities (voltage/current). If the unbalanced currents are sufficiently large, the resultant negative currents might have an effect on a power system's electrical devices, even to the point of disabling the protection device. This is because the negative sequence current that enters a generator's stator winding can spark a second harmonic current at the rotor's winding. Such a current might lead to temperature increases that will negatively impact the generator's functioning and lifespan. Furthermore, there could be malfunctioning of the relay protection components as a result of the surge in negative sequence current flow. This kind of malfunction can also lead to a less reliable power system.(He, Zheng et Hu, 2016)

4.2.3 Reactive power

Reactive power can be defined as energy exchange between a load's reactive portion and the energy source. Using the power factor, the presence of reactive power can be gaged, with a low power factor representing a large proportion of reactive power, while a high power factor represents a small proportion of it. The power factor in the traction power supply system (TPSS) is gaged as low, indicating equipment underuse, which can lead to problems in the upstream power system.(He, Zheng et Hu, 2016)

4.2.4 Rail potential and communication impacts

In the proper functioning of HSTs, there is more and more rail potential. This potential is derived from the leakage current caused by the rail hitting the ballast bed as insulation. As a consequence, there is a leaking of the traction current onto the ground caused by transverse impedance from the rail and train's point of contact. The leakage current then goes to the nearest substation. This ground/rail resistance provides rail potential. Additionally, the current caused by mutual inductance of rail and catenary flows further increases the potential. However, if this rail potential becomes too strong, it becomes hazardous and can disrupt communications.(He, Zheng et Hu, 2016)

4.2.5 Low-frequency voltage fluctuation

Amplitude fluctuation in superimposed voltage which has a frequency less than 10 Hz (with 50 Hz being the rated power frequency) is known as low-frequency voltage fluctuation (LVF). Locomotives' traction ability is reduced when voltage fluctuation amplitudes are so large that they lead to rectifier protection action. Because LVF can happen even during standard conditions and have major impacts, it is important to understand the LVF mechanism.(He, Zheng et Hu, 2016)

4.2.6 Electrical Plug vehicle using Leblanc connection

The driving habits of an electrical vehicle (EV) driver includes the driver's use of grid electricity to power his/her EV. There is a need to know this particular habit, as it affects the ability of the power system to provide sufficient service. Thus, co-ordinating electrical loads for a given time period (e.g., day/week/month/year) must take into account the charging habits of EV users.

A recently published report (Dallinger, Krampe et Wietschel, 2011) looks at the habits of EV users across Denmark, using the National Travel Survey data2 and data from 350 EVs as well as AKTA data3 from 2002 and 2003. The standard adopted for analysis of the EV data

is a battery capacity of 24 kWh and a 150 km average range. The data indicated that most of the charging took place at the homes of the EV drivers and that they used single-phase grid connections. A full recharge of the vehicles took approximately eight hours. The drivers also recharged in public venues that offered the service, such as parking lots and shopping malls. In these instances, the charging was accomplished with 16 A or 32 A(Dallinger, Krampe et Wietschel, 2011)

The report (Dallinger, Krampe et Wietschel, 2011) also revealed that 26% of the EVs did not operate during weekdays, while 36% did not operate on weekends. In these instances, the EVs remained at home. Furthermore, the preferred charging time was at night. This data provide a window into potential adjustment of services according to user habits, as well as forecasting of EV loads (Dallinger, Krampe et Wietschel, 2011)

The main electrical aim of using the Le-Blanc transformer connection supply the single-phase power to electrical vehicles plug in from the general grid of three-phase system to keep the main grid currents is balanced. Nowadays, current and voltage unbalance is one of the major problems in railway traction systems regarding power quality for networks. A variety of approaches can be applied to decrease these issues. One approach is the use of specially connected transformers like the Le-Blanc, which is a winding connection transformer used for single-phase power in electric rail systems.

The next section presents a Leblanc transformer, modeled in a MATLAB simulation, to demonstrate the efficiency of the approach. The following figures contains the simulation of the electrical vehicle plug in feed from three-phase system connecting with LeBlanc transformer to change it from three-phase system to two phase system with good quality in case of (AC) main and the (DC) side have the five-level inverter to performance the power quality as shown in the Figure (4.1). This simulation was done using PI controllers in the control system of the five-level inverter and the filter current. The simulation was under the balance and unbalance load variations to verify the compensation performance of the filter and the five-level inverter. The simulation results are presented in the Figures 4.19 and 4.20.

Table 4.1The most common EV charging options and power levels
Taken from (Marra, Larsen et Træholt, 2013)

AC current	**AC voltage**	**Grid connection**	**Power**
10 A	230 V	single phase	3.2 KW
16 A	230 V	single phase	3.7 KW
32 A	230 V	single phase	7.4 KW
16 A	400 V	three-phase	11 KW
32 A	400 V	three-phase	22 KW
63 A	400 V	three-phase	43 KW
DC current	**DC voltage**	**Grid connection**	**Power**
125 A	400 V	three-phase	50 KW

Figure (4.1) shows the application of the proposed system to power single-phase auxiliary loads and charging electrical vehicles while injecting energy from the solar panel; a second application is to power electrical railway traction with single-phase voltage while supplying the auxiliary loads as shown in figure (4.24)

The proposed configuration and control has investigated the power quality issues of the traction power-supply system, which may be suitable to be applied to single supply railway systems. The system is modeled; and control techniques are applied. Evaluation of the performances for different scenarios as shown in figures (4.19) are reported. The results show the performances the grid side full compensations are accomplished (current harmonics, reactive power and unbalance load). Moreover, the proposed technique to balance the current in the grid side gives complete satisfactory showing the controller forcing the current to be balanced in both inverters. Finally, this work introduces as well interesting integrated technological approaches to deal with the developments of integrated renewable energy systems applied to the railway's power systems. One can find in this section simulation result of the integration of renewable energies in the electrical vehicle and railway traction to reduce the burden on the utility during peak demand.

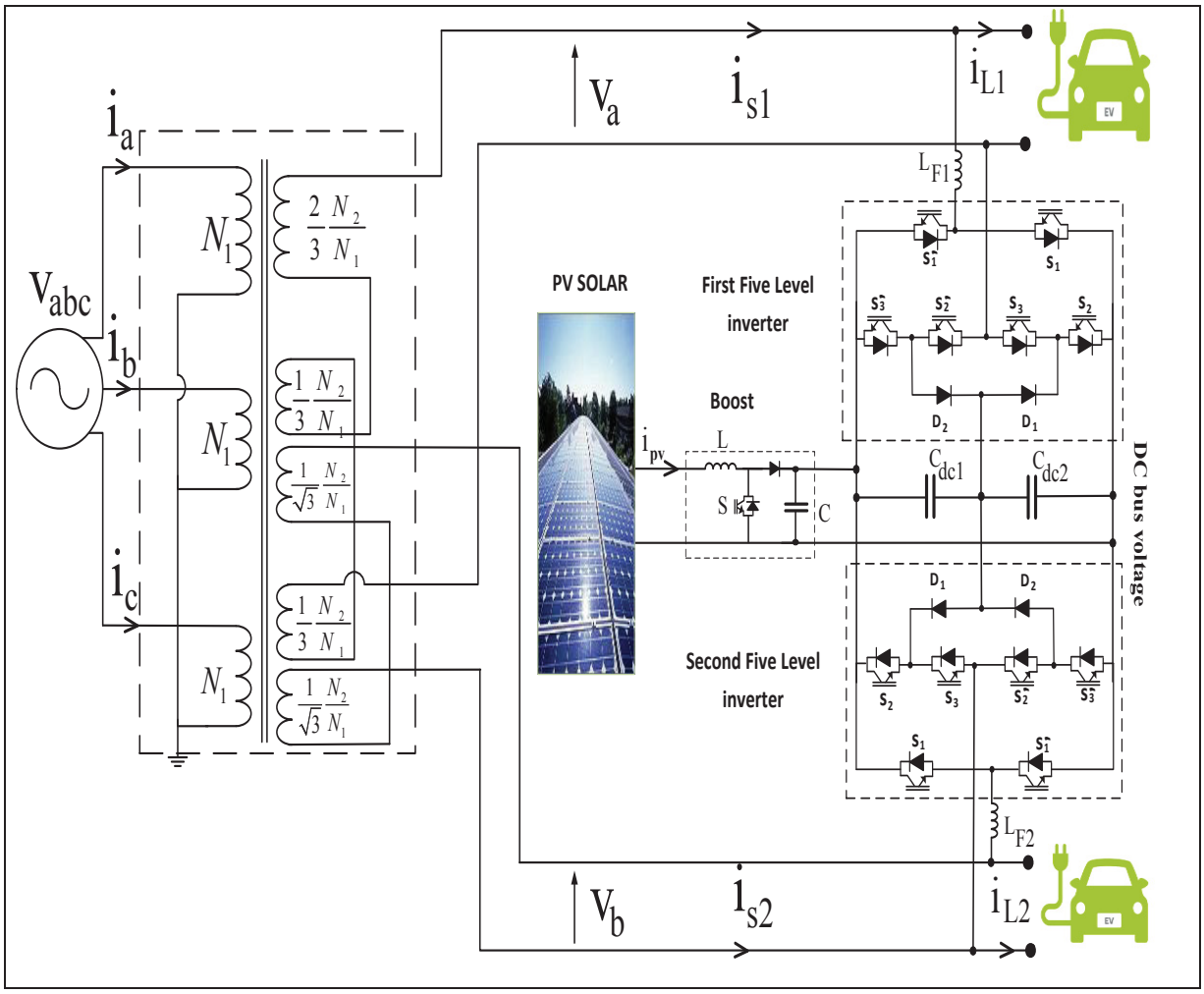

Figure 4.1 Circuit topologie of the plug in system

4.3 Modeling and control of the proposed configuration

4.3.1 Indirect control of the first inverter

The indirect control is applied to the first five level active filter. It ensures compensation for unbalanced load and current harmonic for the right side as well as dc bus voltage regulation. At the same time, it must balance the three-phase grid current the control scheme is given in Figure 4.2,

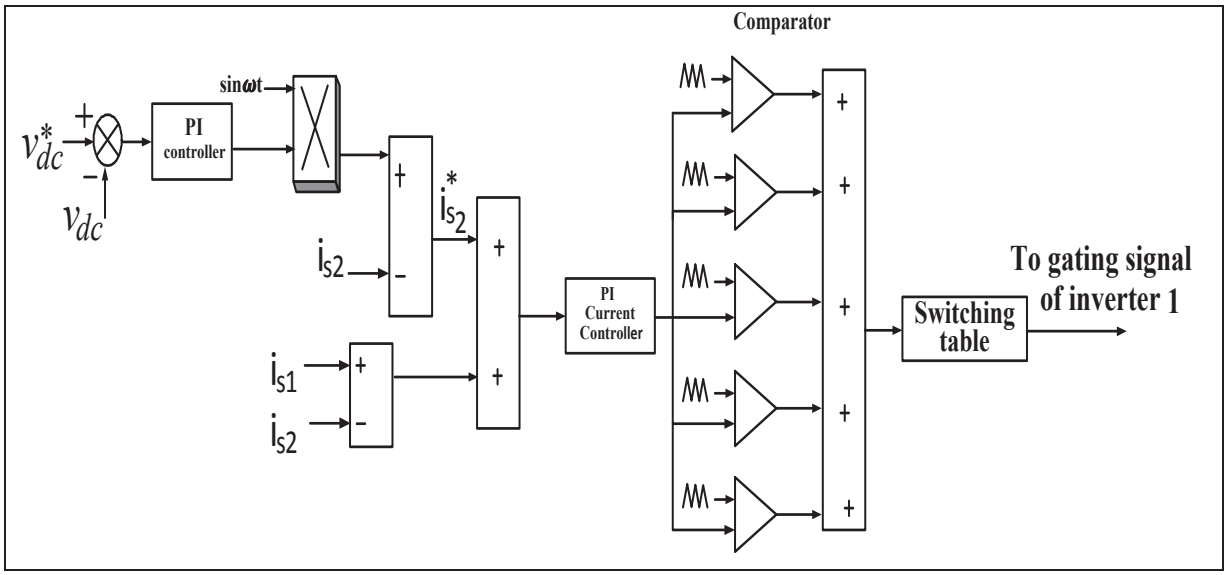

Figure 4.2 Control scheme for the Inverter1

4.3.2 Sliding mode Control of the Second Active inverter

Applied Kirchhoff's voltage and current laws to the single phase active filter we will get

$$L_F \frac{di_F}{dt} = \mathrm{v_s} - d\mathrm{v_{dc}} \tag{4.1}$$

$$C_{dc} \frac{dv_{dc}}{dt} = di_F \tag{4.2}$$

If we then use the sliding mode approach, we will get the sliding surface:,

$$\sigma = k_2(i_F - i_F^*) \tag{4.3}$$

First the generation the current reference of the active filter

$$C_{dc}\frac{dV_{dc}}{dv} = i_{F0} = \frac{dV_{dc}}{V_{dc}} = \frac{\hat{v}_s}{V_{dc}}\, i_{F0} \tag{4.4}$$

$$C_{dc}\frac{dV_{dc}}{dv} = di_{F1} = \frac{dV_{dc}}{V_{dc}} i_{F1} = \frac{\hat{v}_s}{V_{dc}} = i_{F0} \tag{4.5}$$

$$C_{dc}\frac{dV_{dc}}{dt} = i_{F10} = u_v \frac{V_{dc}}{\hat{v}_s} \tag{4.6}$$

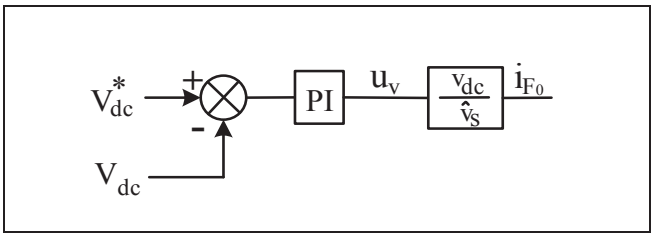

Figure 4.3 Control scheme for dc bus voltage active current regulation

The derivative is,

$$\dot{\sigma} = k_2\left(\frac{v_s - d_{eq}\, V_{dc}}{L_F} - \frac{di_F^*}{dt}\right) = \frac{v_s - d_{eq}\, V_{dc}}{L_F} - \frac{di_F^*}{dt} = 0 \tag{4.7}$$

The equivalent control law is:

$$d_{eq} = \frac{-v_s + L_F \frac{di_F^*}{dt}}{V_{dc}} \tag{4.8}$$

The control law is defined as follows,

$$d = d_{eq} - k_1\, sgn(\sigma) \tag{4.9}$$

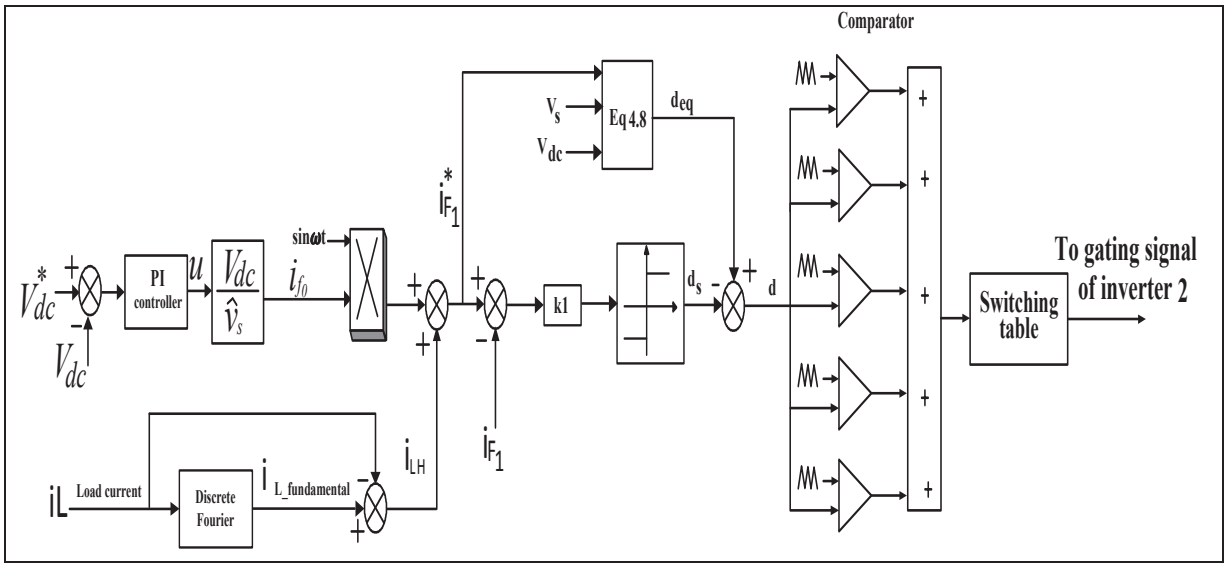

Figure 4.4 Control scheme for the Inverter2

4.3.3 Stability analysis

In order to guarantee the sliding mode's stability across the whole system, we can use the Lyapunov function:

$$V = \frac{1}{2}\sigma\sigma^T \tag{4.10}$$

Keeping in mind that the Lyapunov function must be a positive definite when the derivative presents as a negative definite.

$$\dot{V} = \sigma\dot{\sigma} = \sigma\left(k_2\left(\frac{-d_{eq}V_{dc} + v_s}{L_{F1}} - \frac{di_{F1}^*}{dt} - \frac{k_1\, sign(\sigma)}{L_{F1}}\right)\right) = \tag{4.11}$$

$$-\frac{k_1 k_2}{L_{F1}}\sigma.sign(\sigma)$$

Using the inequality: $\sigma.sign(\sigma) <= |\sigma|$

$$\dot{V} = -\frac{k_1 k_2}{L_{F1}} \sigma . sign(\sigma) \leq -\frac{k_1 k_2 |\sigma|}{L_{F1}} \tag{4.12}$$

This inequality (4.12) will be satisfied through choosing the best sliding mode parameters as $k_2 > 0$ and $k_1 > 0$. Choosing the right parameters is important, as these parameters will then determine the state variables' convergence rate and whether or not the stability condition is satisfied.

4.3.4 PV solar modeling

A main type of sustainable power source used today is the photovoltaic (PV) solar system. The PV system is made up of solar panels which make electricity through the rays of the sun, using the sun as a renewable energy source. The three main kinds of PV panels are thin film, more crystalline, and polycrystalline..

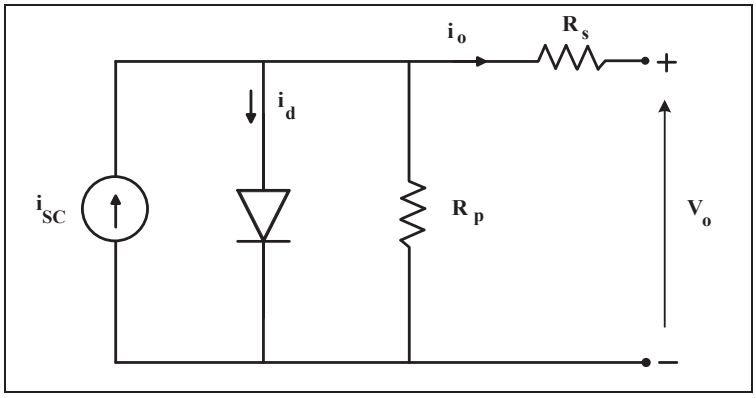

Figure 4.5 The equivalent circuit of a solar PV cell

$$I_d = I_s(e^{\frac{q*V_d}{K*T}} - 1) \tag{4.13}$$

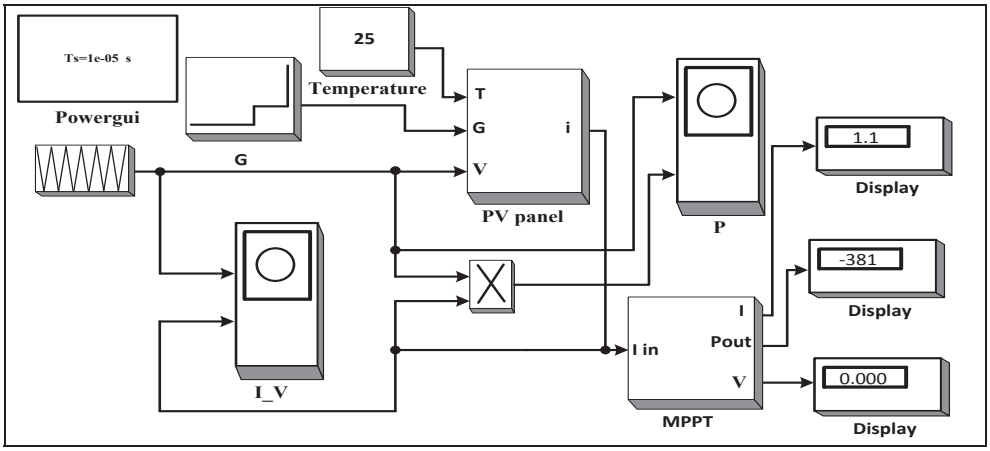

Figure 4.6 The system of solar cell diagram

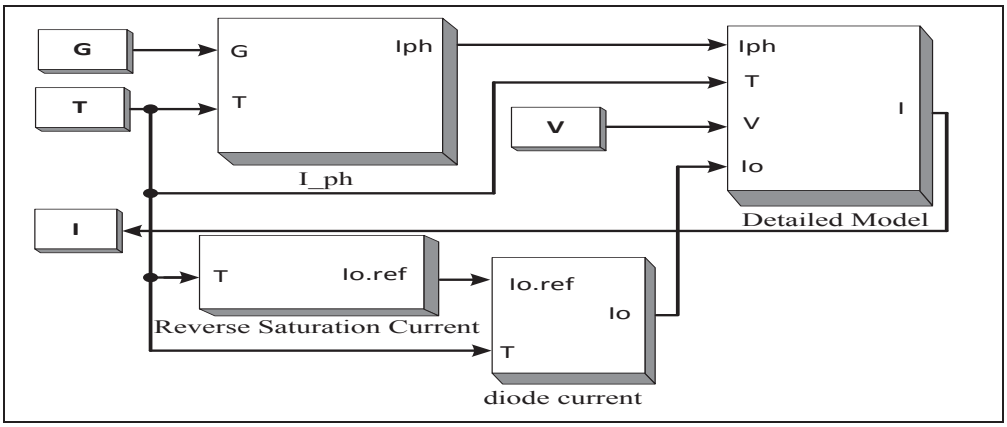

Figure 4.7 The Pv panel configuration

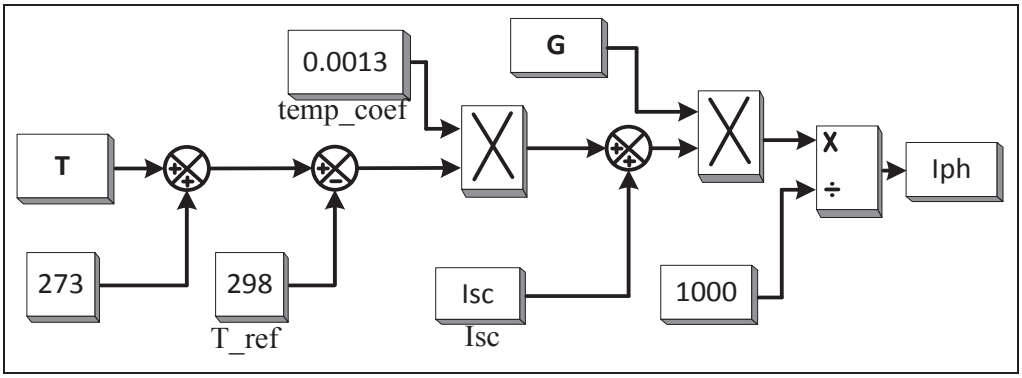

Figure 4.8 The I_ph configuration

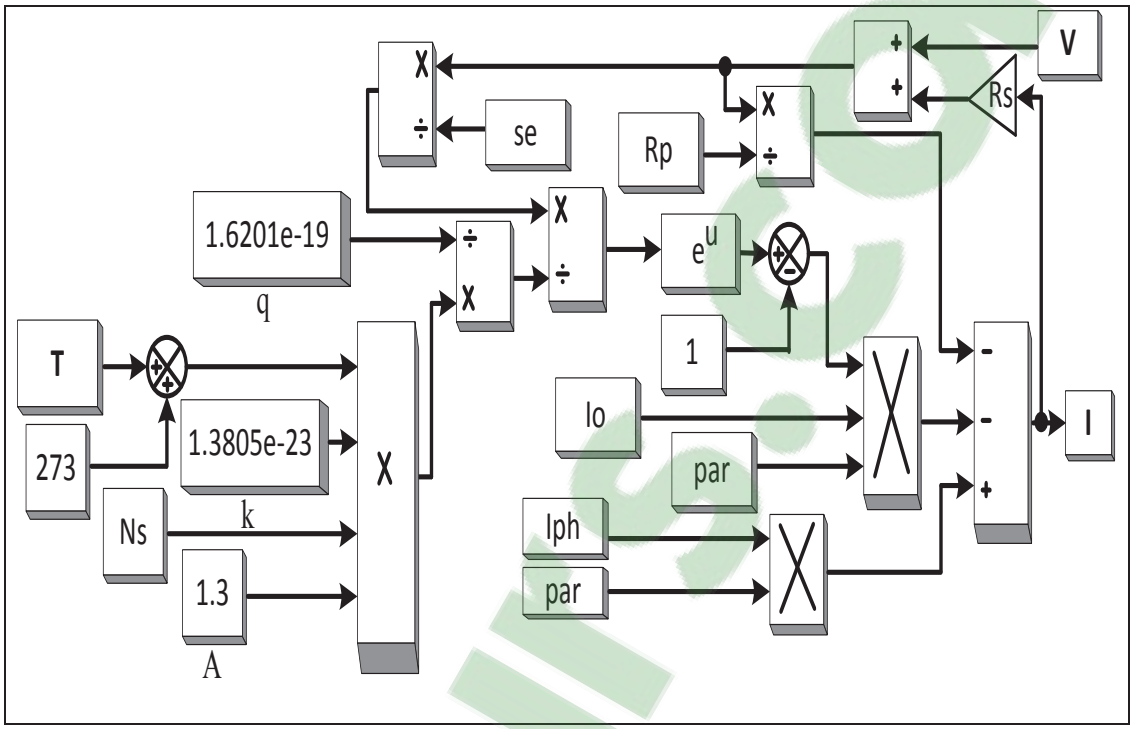

Figure 4.9 The Detailed Model configuration

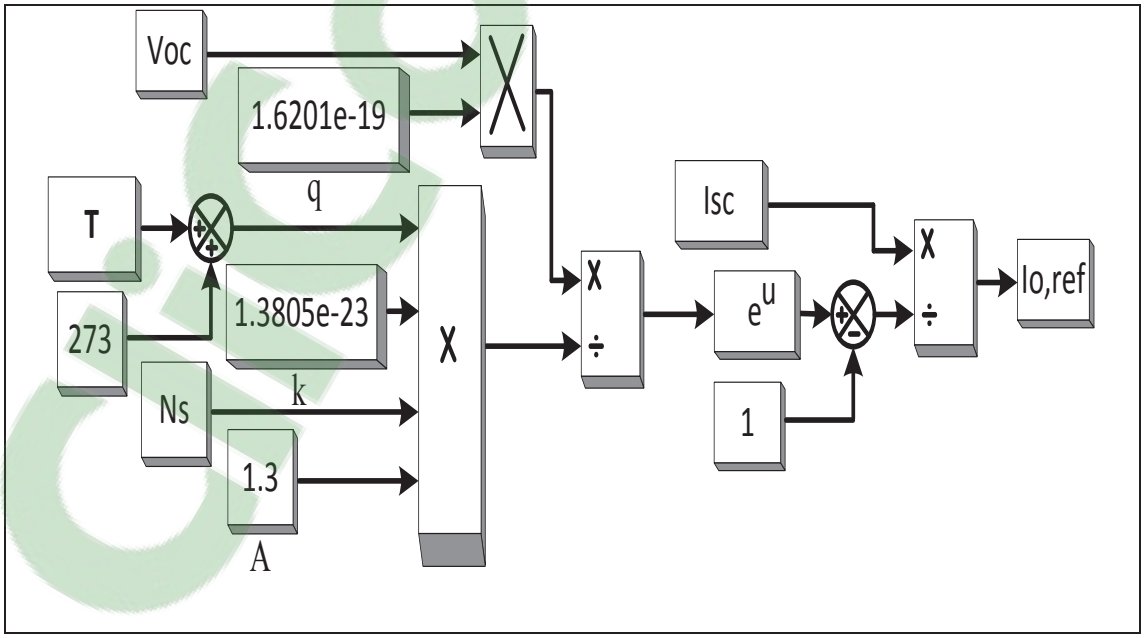

Figure 4.10 The Reverse Saturation Current configuration

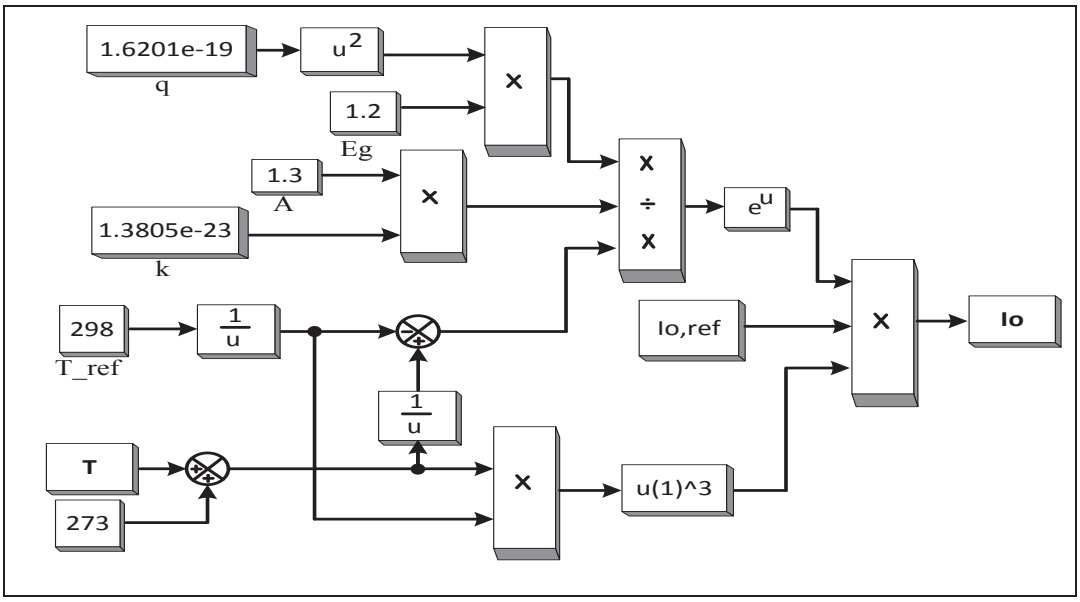

Figure 4.11 The diode current configuration

4.3.4.1 MPPT algorithm using perturbation and observation

Of the many possible methods, the Perturb and Observe approach has been broadly applied in MPPT.

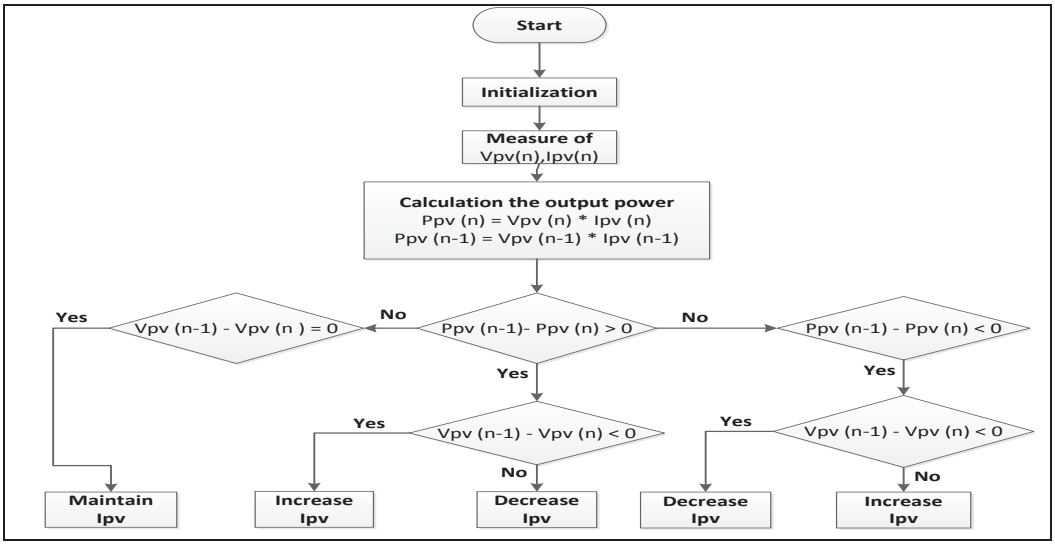

Figure 4.12 Perturb and observe MPPT algorithm flowchart.

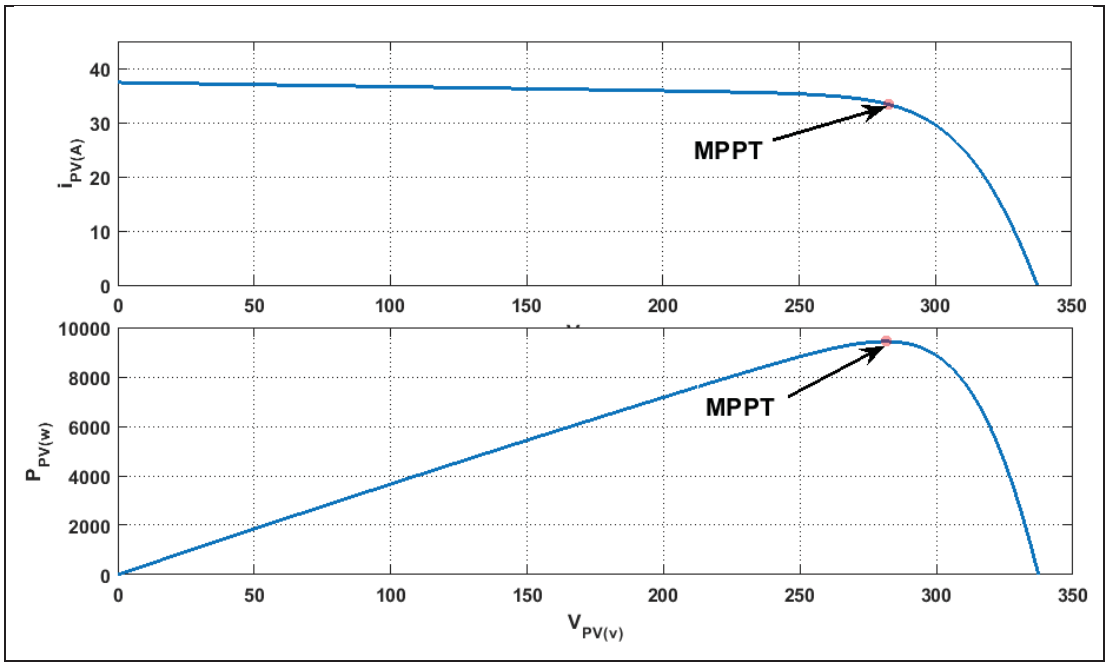

Figure 4.13 Deviation of MPPT with I and V method under rapid PV irradiance changes

The MPPT algorithm is depending on the several of calculations based on the actual and the previous values of PV output power (dP). At each repetition, the MPPT algorithm computes the (dP). The processes of the methods will end as soon as the difference (dP) is switching between positive and negative values, as designated in Figure. 4.12

4.3.4.2 Modeling and control of boost converter

The main job of a boost converter is to increase the magnitude of the input voltage up to the necessary magnitude for output voltage without employing a transformer. Boost converter components include a high frequency switch, diode and an inductor. All of these parts work together to provide an energy supply by using loads with larger voltage compared to input voltage magnitude. They do this by controlling the switch's duty cycle to change voltages. The topology for a typical boost converter is illustrated in Figure.(4.14) As can be seen, there are two main operational modes in this modeling approach: one is the charging mode (i.e., S switch is ON), and the other is the discharging more (i.e., S switch is OFF).

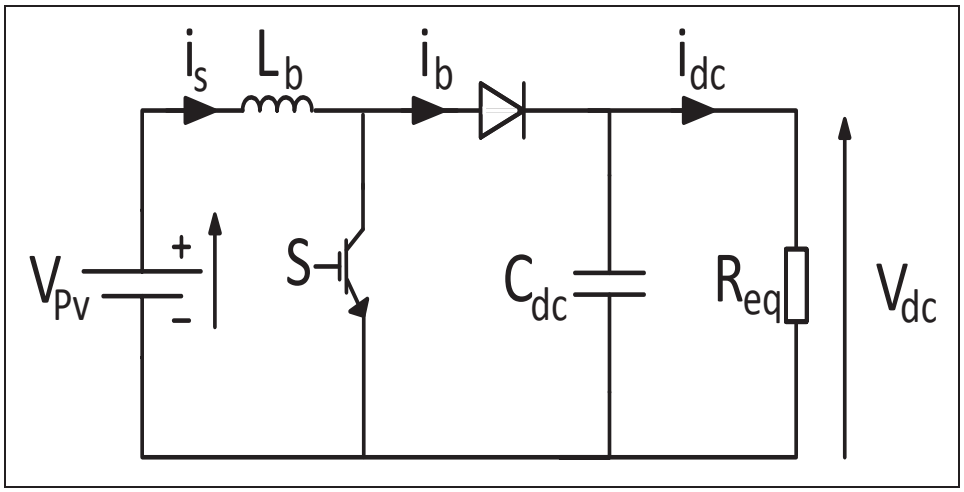

Figure 4.14 Post regulator boost converter

$$\dot{X} = A_1 X + B_1 v_i \tag{4.14}$$

$$\begin{bmatrix} \frac{di_s}{dt} \\ \frac{dv_{dc}}{dt} \end{bmatrix} = \begin{bmatrix} 0 & 0 \\ 0 & -\frac{1}{R_{eq}C_{dc}} \end{bmatrix} \begin{bmatrix} i_s \\ V_{dc} \end{bmatrix} + \begin{bmatrix} \frac{1}{L_b} \\ 0 \end{bmatrix} V_s \tag{4.15}$$

4.3.4.3 Charging Mode

In the charging mode, the switch is closed and the inductor is charged by the source via the switch, as per Figure 4.15. The charging current is exponential in nature but, to simplify, is considered to be fluctuating linearly. The diode limits the flow of current from the source to the load and the load's need is met by the discharging of the capacitor.

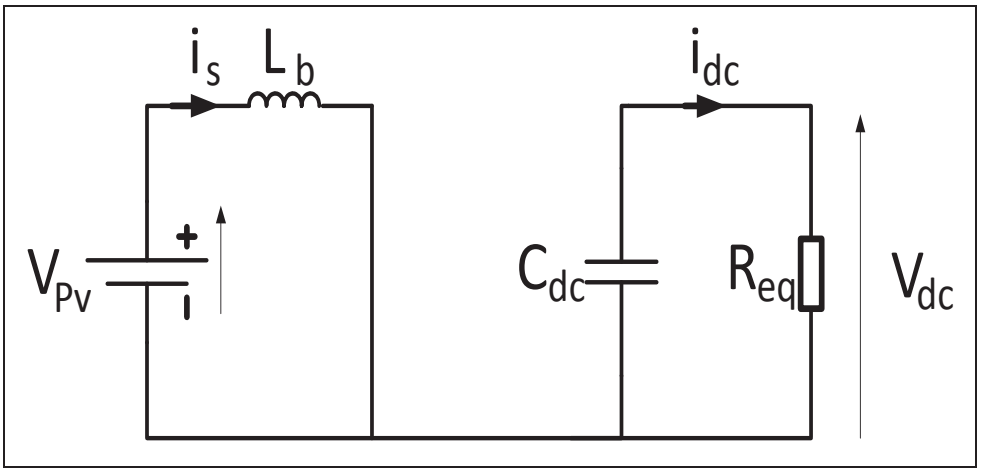

Figure 4.15 The boost converter When Switch **S** is ON

$$\dot{\mathbf{X}} = \mathrm{A}_2\,\mathrm{X} + \mathrm{B}_2\,\mathrm{v_i} \tag{4.16}$$

$$\begin{bmatrix} \frac{\mathrm{di_s}}{\mathrm{dt}} \\ \frac{\mathrm{dv_{dc}}}{\mathrm{dt}} \end{bmatrix} = \begin{bmatrix} 0 & -\frac{1}{L_b} \\ \frac{1}{C_{dc}} & -\frac{1}{R_{eq}C_{dc}} \end{bmatrix} \begin{bmatrix} \mathrm{i_s} \\ V_{dc} \end{bmatrix} + \begin{bmatrix} \frac{1}{L_b} \\ 0 \end{bmatrix} V_s \tag{4.17}$$

4.3.4.4 Discharging Mode

As can be seen in Figure 4.16, with the diode forward-biased and the switch S, the inductor is able to discharge. Thus, the capacitor, along with the source charges, can satisfy load requirements. As variations in the load current are negligible, the current can be assumed to remain constant during the entire operation..

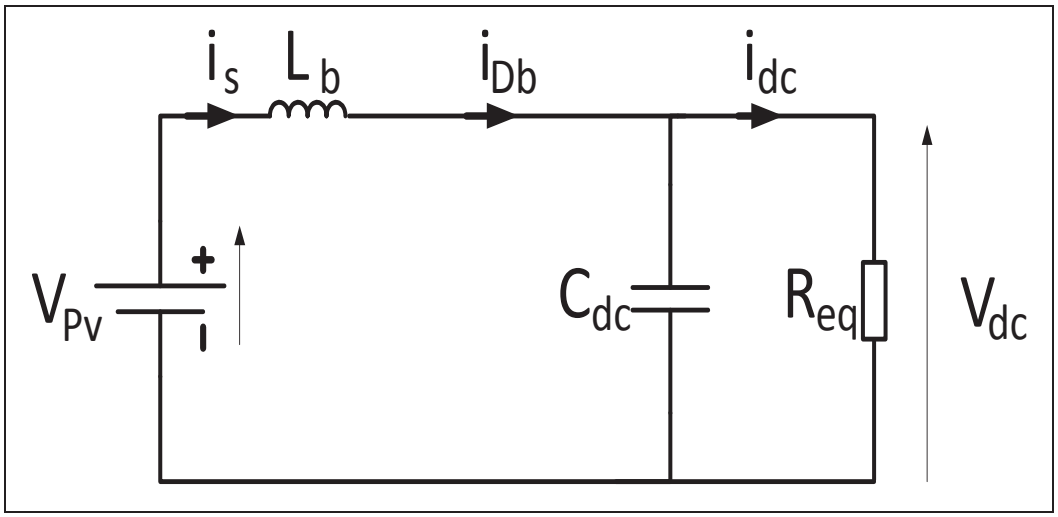

Figure 4.16 The boost converter When Switch **S** is OFF

$$\mathrm{A} = \mathrm{A}_1\,\mathrm{d} + \mathrm{A}_2\,(1-d) \tag{4.18}$$

$$\mathrm{B} = \mathrm{B}_1\,\mathrm{d} + \mathrm{B}_2\,(1-d) \tag{4.19}$$

$$\begin{bmatrix} \frac{\mathrm{di_s}}{\mathrm{dt}} \\ \frac{\mathrm{dv_{dc}}}{\mathrm{dt}} \end{bmatrix} = \begin{bmatrix} 0 & -\frac{(1-d)}{L_b} \\ \frac{(1-d)}{C_{dc}} & -\frac{1}{R_{eq}C_{dc}} \end{bmatrix} \begin{bmatrix} \mathrm{i_s} \\ V_{dc} \end{bmatrix} + \begin{bmatrix} \frac{1}{L_b} \\ 0 \end{bmatrix} V_s \tag{4.20}$$

$$\mathrm{A} = \begin{bmatrix} 0 & -\frac{(1-d)}{L_b} \\ \frac{(1-d)}{C_{dc}} & -\frac{1}{R_{eq}C_{dc}} \end{bmatrix} \tag{4.21}$$

4.3.4.5 Sliding Mode Control of DC-DC converter

In applying the sliding mode control on the DC-DC converter, maximum power can be extracted from PVs. At the same time, perturbation and observation can be used in order to determine the most appropriate current for the PV's maximum power.

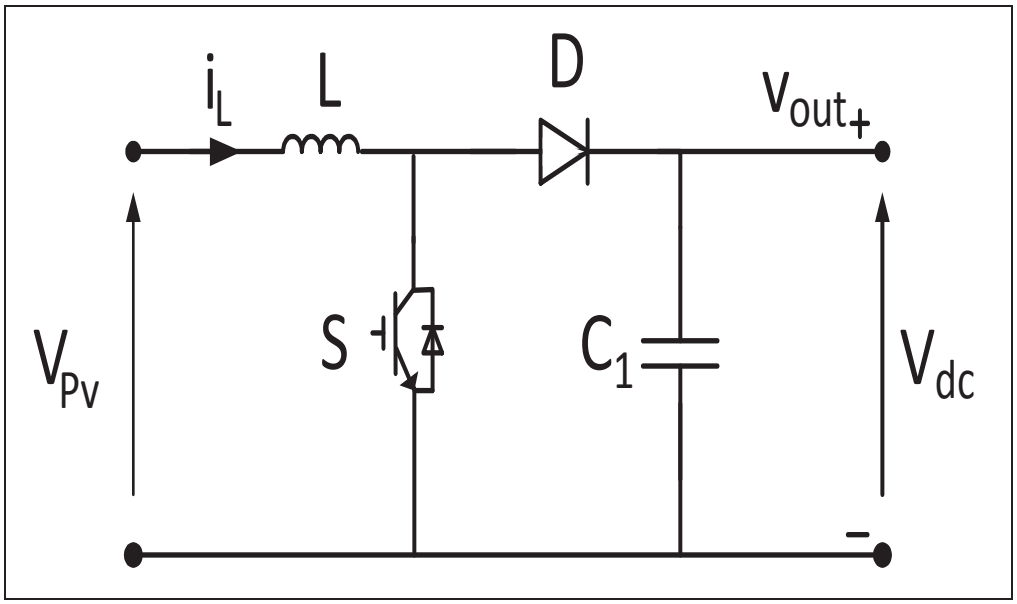

Figure 4.17 Boost Converter Configuration

The dynamic modeling of the boost is given by

$$L\frac{di_L}{dt} = V_{dc} - (1 - \mathrm{d})v_{pv} \tag{4.22}$$

Then, by employing sliding mode, we obtain the following formulation for the sliding surface:

$$\sigma = k_1\left(i_l - i_{pv}^*\right) \tag{4.23}$$

The derivative is,

$$\dot{\sigma} = K_1\left(\frac{V_s - d_{eq}V_{dc}}{L_f} - \frac{di_{pv}^*}{dt}\right) = 0 \tag{4.24}$$

The equivalent control law is:

$$\mathrm{d}_{eq} = \frac{-L\frac{di_{pv}^{*}}{dt} + v_s}{V_{dc}} \tag{4.25}$$

The control law is defined as follows,

$$\mathrm{d} = \mathrm{d}_{eq} - k_1 sgn(\sigma) \tag{4.26}$$

The MPPT (Maximum Power Point Tracking) uses a perturbation and observes algorithm which requires only the parameters to be sensed, PV voltage and current.

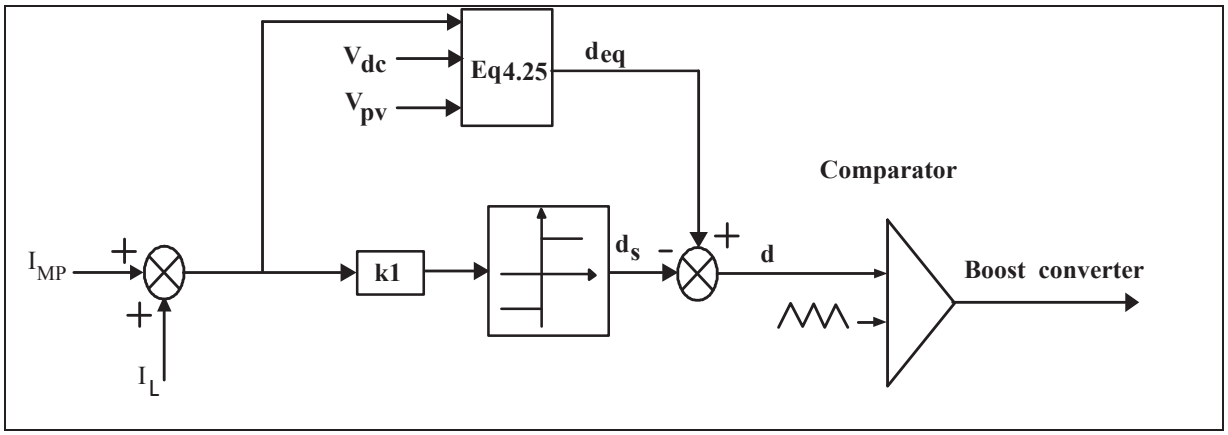

Figure 4.18 Scheme of sliding mode control law of the boost converter.

4.3.5 SIMULATION RESULTS

The validation by simulation of different scenarios:

- Study state;
- Unbalance load;
- Load variation;
- PV solar variation.

Table 4.2 The specification parameters used for Electrical Vehicle simulation

Description	|Value
Primary line voltage	V_p = 208 V (rms)
Secondary voltage	V_s = 208 V (rms)
Nonlinear load R_{L2}	L_L = 50 mH , R_L = 10 Ω
Line voltage	V_s = 170 V (rms)
Frequency	F_s = 60 Hz
Line impedance	L_s = 0.5 mH , Rs = 10 Ω , C_s =20 µF
Active filter parameters	L_c = 5 mH , R_c = 0.1 Ω ,C_{dc} =5000 µF
DC-bus voltage	V_{dc}^* = 400 V
PI regulation parameters	K_p = 0.6 and K_i = 10

4.3.5.1 Simulation results throughout the study state of the system

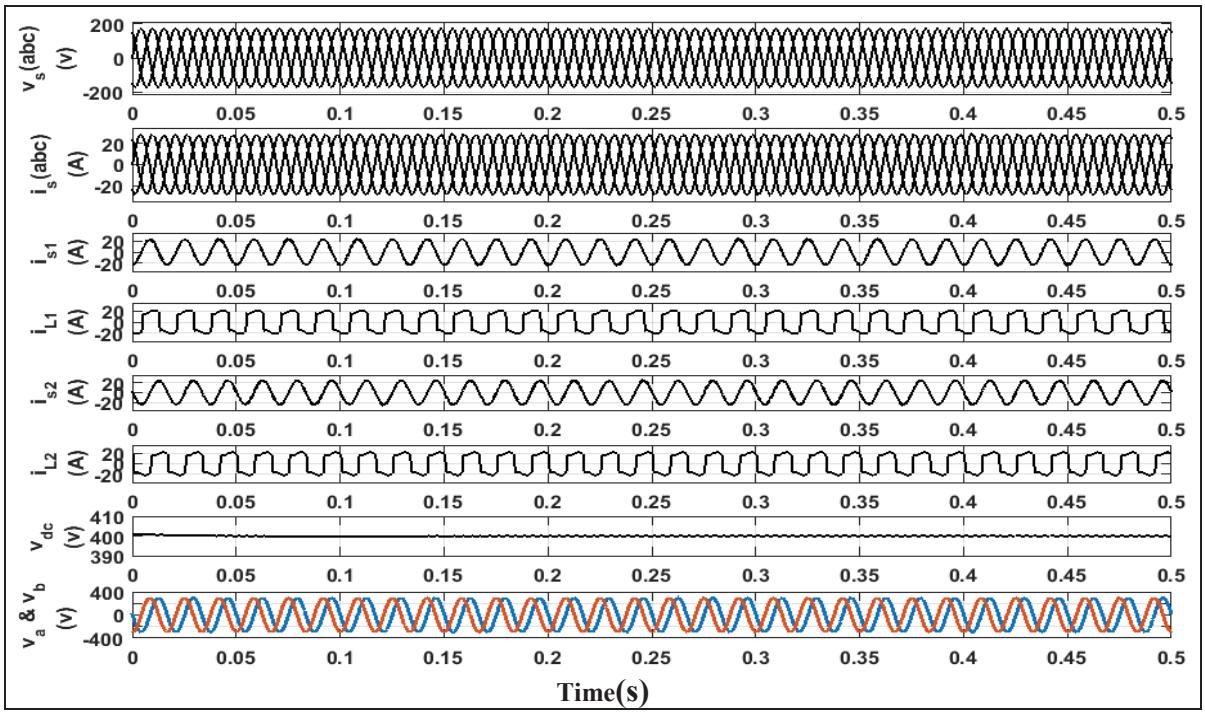

Figure 4.19 Simulation of steady state response

The Figure 4.19 shows the three-phase source currents (I_s abc) are balanced and approximately sinusoidal in case Of the study state. The obtained results also show the two single phase current (i_S) and load (i_L), and the output of Leblanc transformer, the two phases (V_a & V_b) are in a good performance and shifted by 90º degree with the same amplitudes. We can also see the output of the multilevel inverter the signal of five levels is clear and in good performance. Therefore, the proposed model offers a good compensation performance at the steady state and adapting the dc bus voltage, reactive power compensation and the THD for less than 5% as shown in the figure 4.23

4.3.5.2 Simulation results throughout unbalanced load

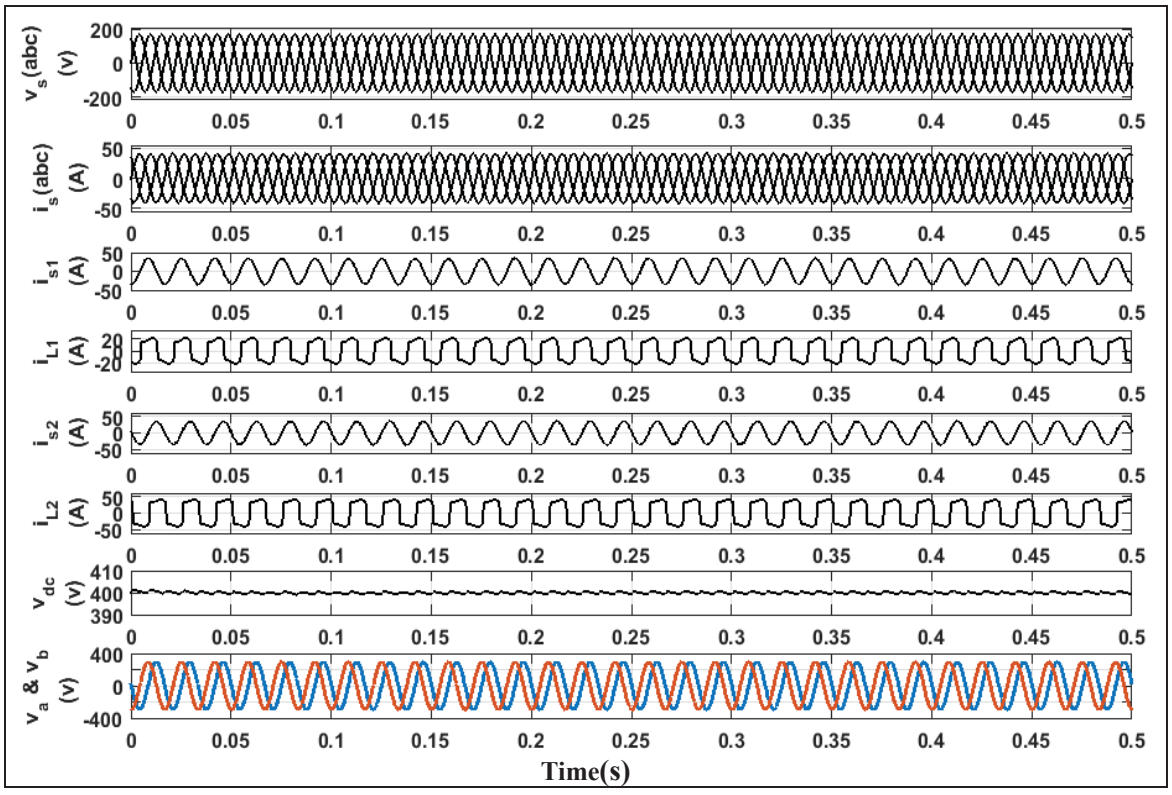

Figure 4.20 The dynamic response during unbalanced load

The figure 4.20 shows the three-phase source currents (I_s abc) are balanced and almost sinusoidal in case Of the unbalanced load. The obtained results also show the two single phase current source (i_S) and load (i_L), and the output of Leblanc transformer the two phases

(V_a & V_b) are in a good performance and shifted by 90º degree with the same amplitudes. We can also see the output of the multilevel inverter the signal is five levels is clear and in good performance. Consequently, the proposed model offers a good compensation performance at whatever time the unbalanced load and while load current changes adapting and regulating the dc bus voltage.

4.3.5.3 Simulation results throughout load variation

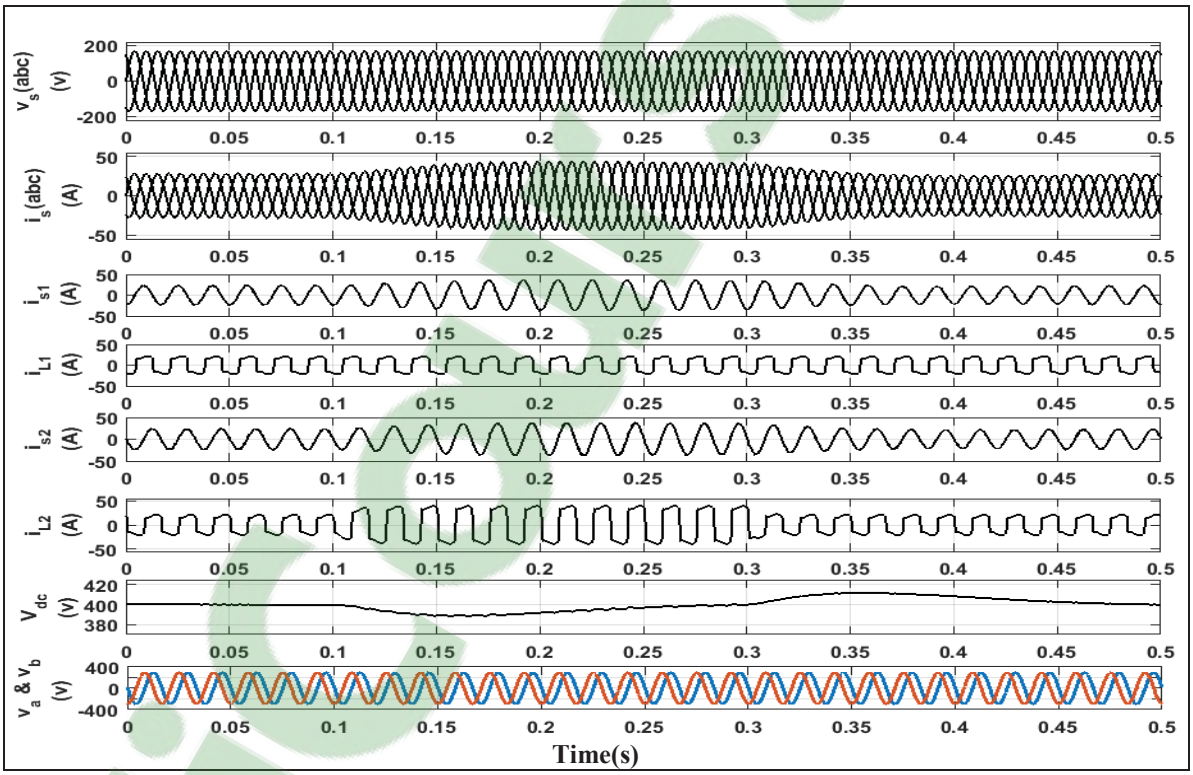

Figure 4.21 The dynamic response during load variation

The Figure 4.21 shows the three-phase source currents (I_s abc) are balanced and approximately sinusoidal in case of the current load variation. The obtained results also show the two single phase current source (i_S) and load (i_L), and the output of Leblanc transformers the two phases (V_a & V_b) are in a good performance and shifted by 90º degree with the same amplitudes. We can also see the output of the multilevel inverter the signal of five levels is clear and in good performance.

4.3.5.4 Simulation results throughout PV Solar variation

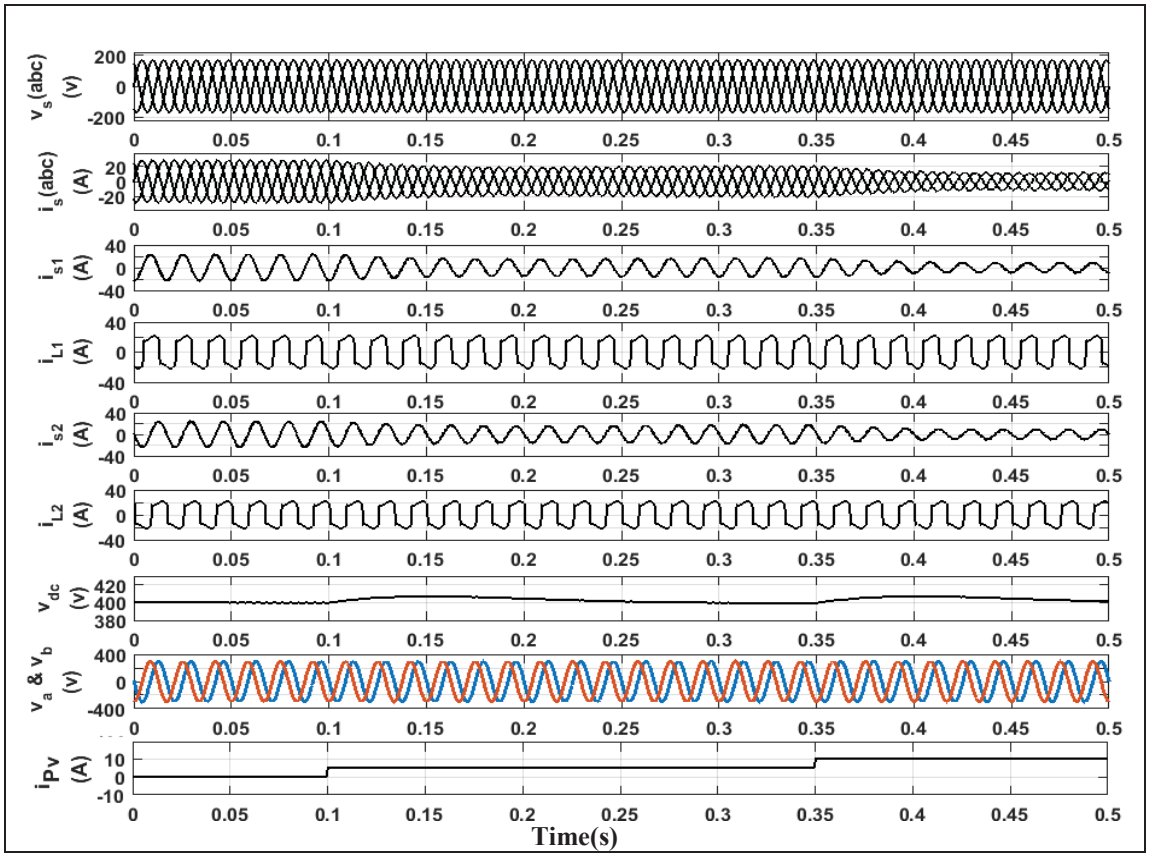

Figure 4.22 The dynamic response during the PV solar variation

The Figure 4.22 shows the three-phase source currents (I_s abc) are balanced and decreased as the PV solar power increased in case. The obtained results also show the two single phase current source (i_S) and load (i_L), and the output of Leblanc transformer the two phases (V_a & V_b) are in a good performance and shifted by 90º degree with the same amplitudes. We can also see the output of the multilevel inverter the signal of five levels is clear and in good performance. As a result the proposed model offers a good compensation performance at whatever the PV solar changes and while load current changes adapting and regulating the dc bus voltage, reactive power compensation and the THD for less than 5% as has been shown in the figure 4.23

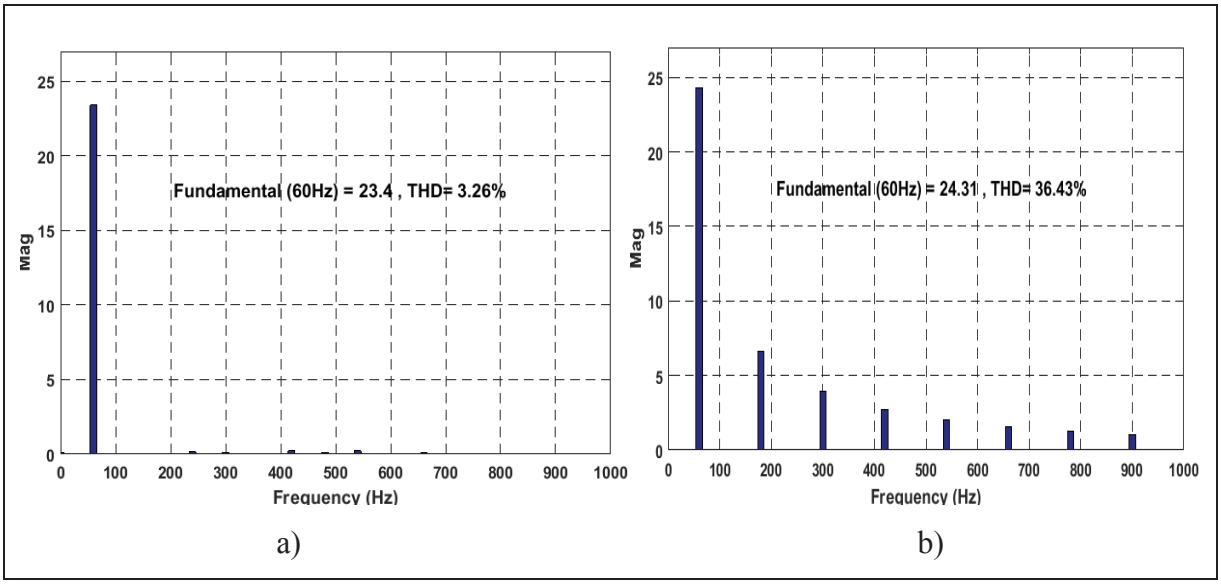

Figure 4.23 Harmonic spectrum a) Source current b) Load current

4.4 Montreal railway traction supply with added PV solar capacity using Leblanc transformer load balanced

The main grid comprises a three-phase system connected to a Le Blanc transformer through primary side windings. It features a two-phase system transfer from the special winding connection of the Leblanc transformer through secondary side windings, as depicted in Figure 4.24. Therefore, the PV solar cell is interfacing with the Leblanc transformer as an external power source to enable it to feed both the load and the grid, as required. Further, solar cells connected in series/shunt create a photovoltaic module. By using a single-phase solar cell, a single diode solar cell model can be developed employing one diode, two resistors, and a current source.

In a five-level inverter with DC bus regulator, an asymmetric neutral point clamped converter is used in order to boost the power quality from the non-linearity of the load. A nonlinear controller-based sliding mode is employed for reducing the negative effects of harmonics as well as load unbalance and reactive power according to load and grid conditions. The switching features of the inverter's proposed control law serves as a means to incline the

trajectory of the system in relation to the sliding surface. The results demonstrate the sliding mode control's usefulness in decreasing harmonic distortion in source current harmonics, especially those created in nonlinear loads. The sliding mode control strategy can also decrease dc bus voltage values near to those of network voltage. MATLAB/Simpower were used to provide simulation results.

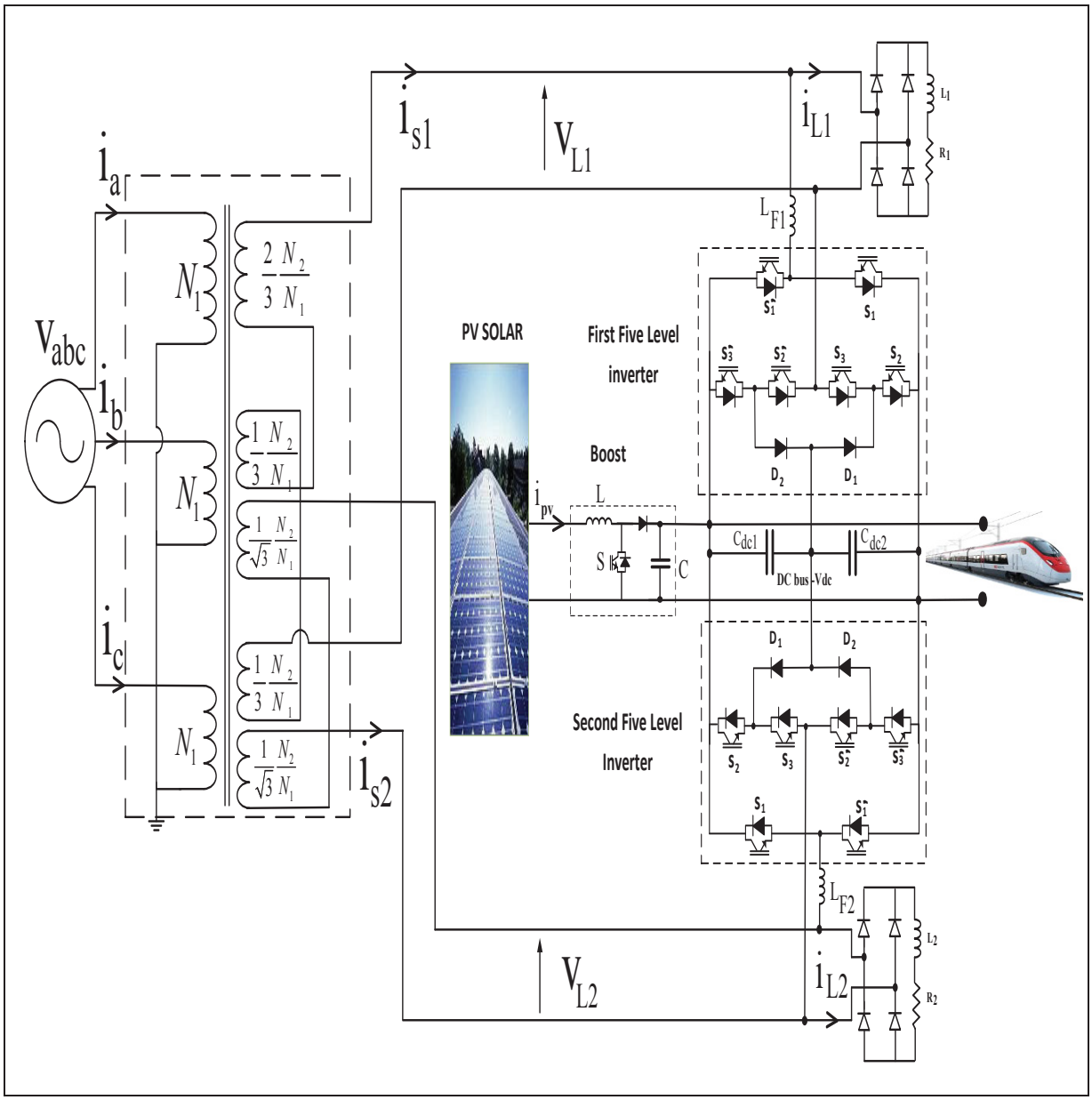

Figure 4.24 Circuit topologie of the system

4.4.1 SIMULATION RESULTS

The validation by simulation of different scenario:

- Load variation;
- Unbalance load;
- Reactive power compensation;
- PV solar variation.

Table 4.3 The specification parameters used for railway traction simulation

Description	Value
Primary line voltage	V_p = 600 V (rms)
Secondary voltage	V_s = 370 V (rms)
Nonlinear load R_{L1}	L_L = 50 mH , R_L = 10 Ω
Nonlinear load R_{L2}	L_L = 50 mH , R_L = 10 Ω
Line voltage	V_s = 490 V (rms)
Frequency	F_s = 60 Hz
Line impedance	L_s = 0.5 mH , Rs = 10 Ω , C_s =20 μF
Active filter parameters	L_c = 5 mH , R_c = 0.1 Ω ,C_{dc} =5000 μF
DC-bus voltage	V_{dc}^* = 750 V
PI regulation parameters	K_p = 1 and K_i = 10

4.4.1.1 Simulation results throughout the study state of the system

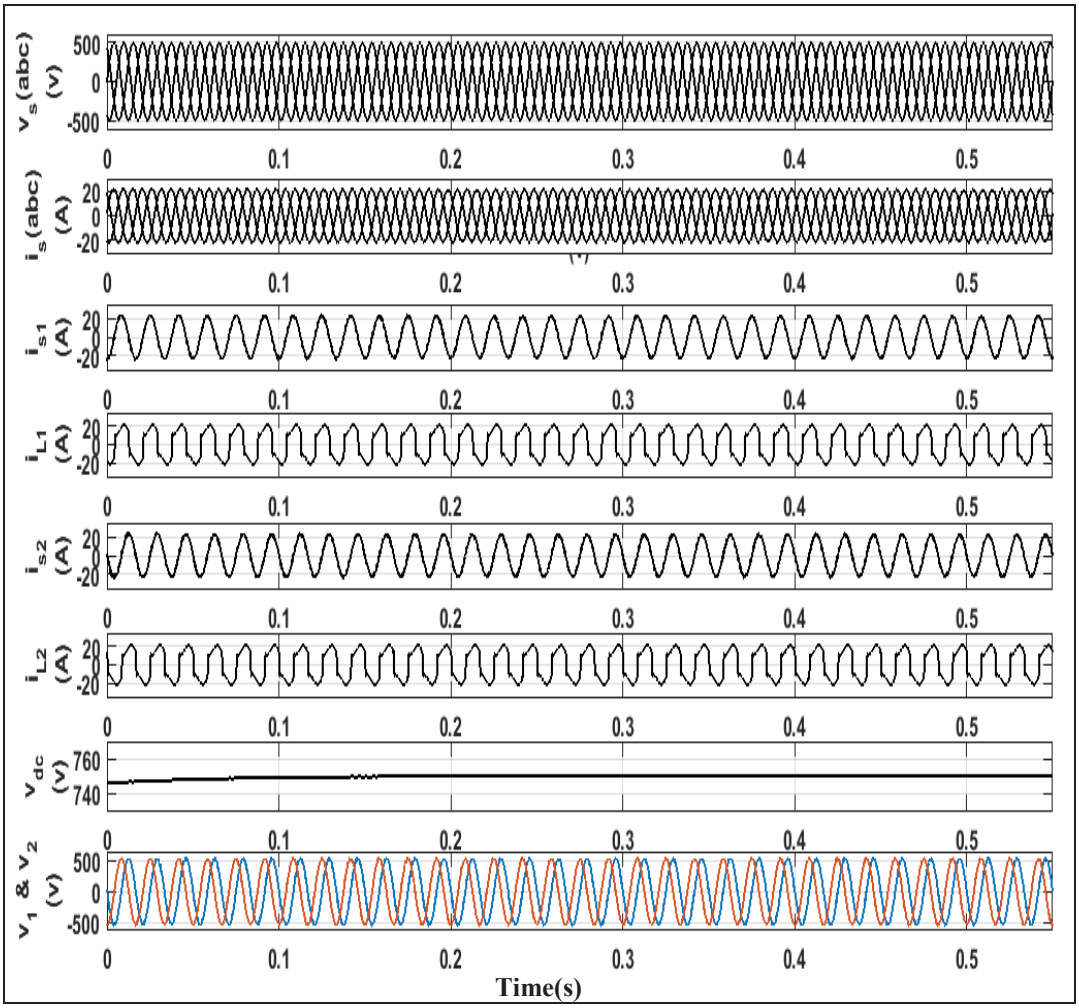

Figure 4.25 Simulation results showing steady state response of the system

The Figure 4.25 shows the three-phase source currents (Is abc) are balanced and approximately sinusoidal in case of the steady state. The obtained results also show the two single phase current (iS) and load (iL), and the output of Leblanc transformer, the two phases (V1 & V2) are in a good performance and shifted by 90º degree with the same amplitudes. We can also see the output of the multilevel inverter the signal of five levels is clear and in good performance.

4.4.1.2 Simulation results throughout load variation

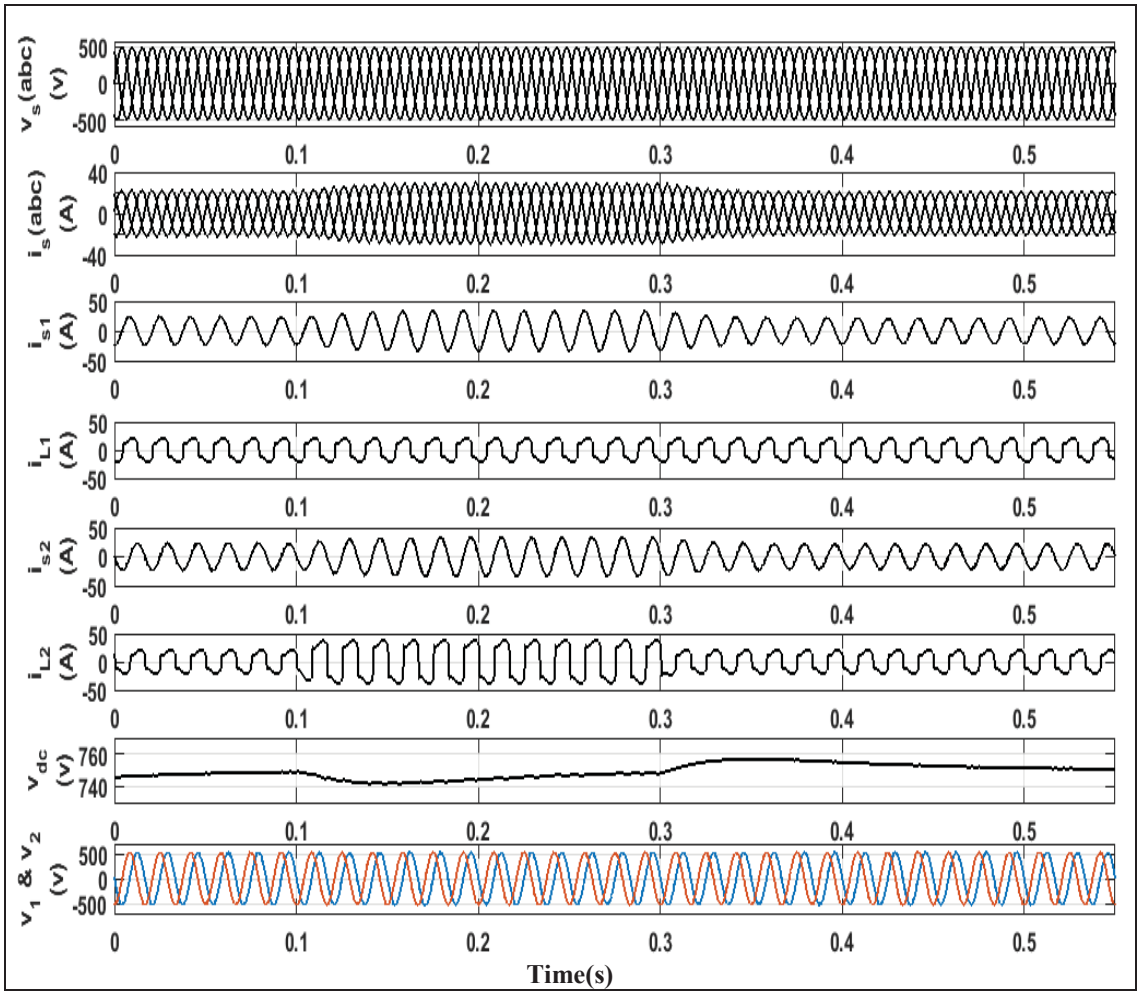

Figure 4.26 System response during load step up and step down variations

The Figure 4.26 shows the three-phase source currents (I_s abc) are balanced and approximately sinusoidal in case of the current load variation. The obtained results also show the two single phase current source (i_S) and load (i_L), and the output of Leblanc transformer the two phases (V_1 & V_2) are in a good performance and shifted by 90º degree with the same amplitudes. We can also see the output of the multilevel inverter the signal of five levels is clear and in good performance. As a result the proposed model offers a good compensation performance at whatever the load changes and while load current changes adapting and regulating the dc bus voltage and reactive power compensation

4.4.1.3 Simulation result throughout unbalanced load

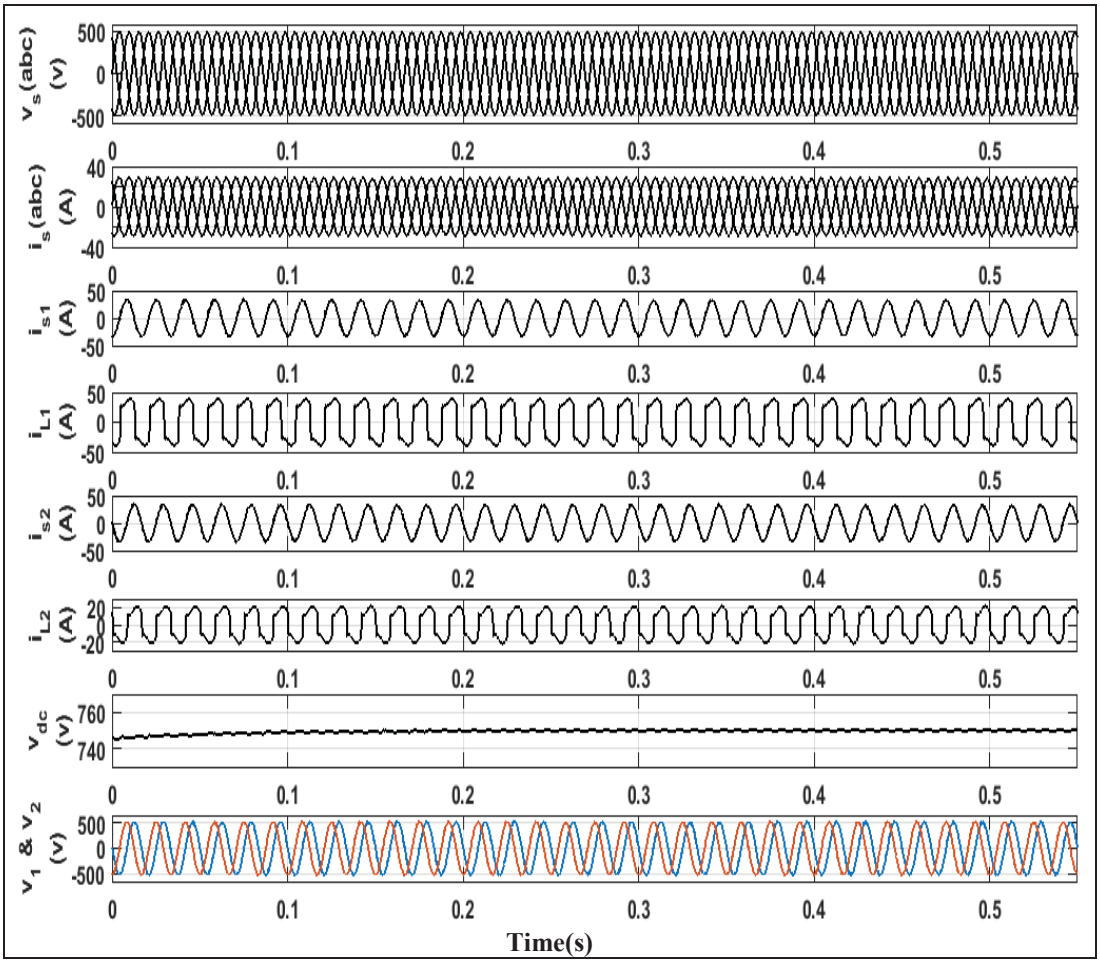

Figure 4.27 System response during unbalanced nonlinear load supply condition

The figure 4.27 shows the three-phase source currents (Is abc) are balanced and almost sinusoidal in case of the unbalanced load. The obtained results also show the two single phase current source (iS) and load (iL), and the output of Leblanc transformer the two phases (V1 & V2) are in a good performance and shifted by 90º degree with the same amplitudes. We can also see the output of the multilevel inverter the signal is five levels is clear and in good performance. As a consequence the proposed model offers a good compensation performance at whatever time the unbalanced load and while load current changes adapting and regulating the dc bus voltage,

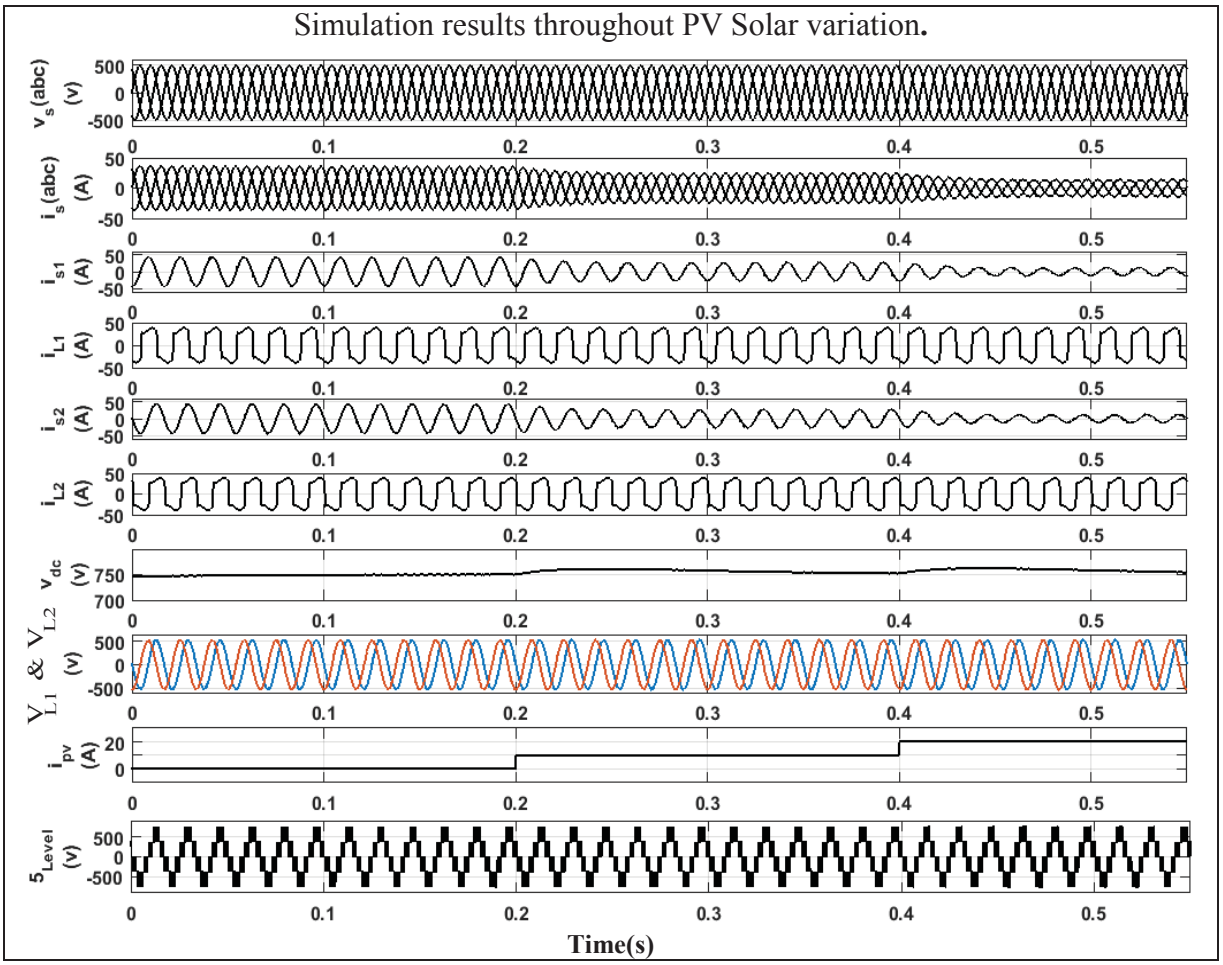

Figure 4.28 The dynamic response during PV connection and load variations

The Figure 4.28 shows the three-phase source currents (I_s abc) are balanced and decreased as the PV solar power increased in case. The obtained results also show the two single phase current source (i_S) and load (i_L), and the output of Leblanc transformer the two phases (V_1 & V_2) are in a good performance and shifted by 90º degree with the same amplitudes. We can also see the output of the multilevel inverter the signal of five levels is clear and in good performance. As a result the proposed model offers a good compensation performance at whatever the PV solar changes and while load current changes adapting and regulating the dc bus voltage, reactive power compensation and the THD for less than 5% as has been shown in the figure 4.29 .

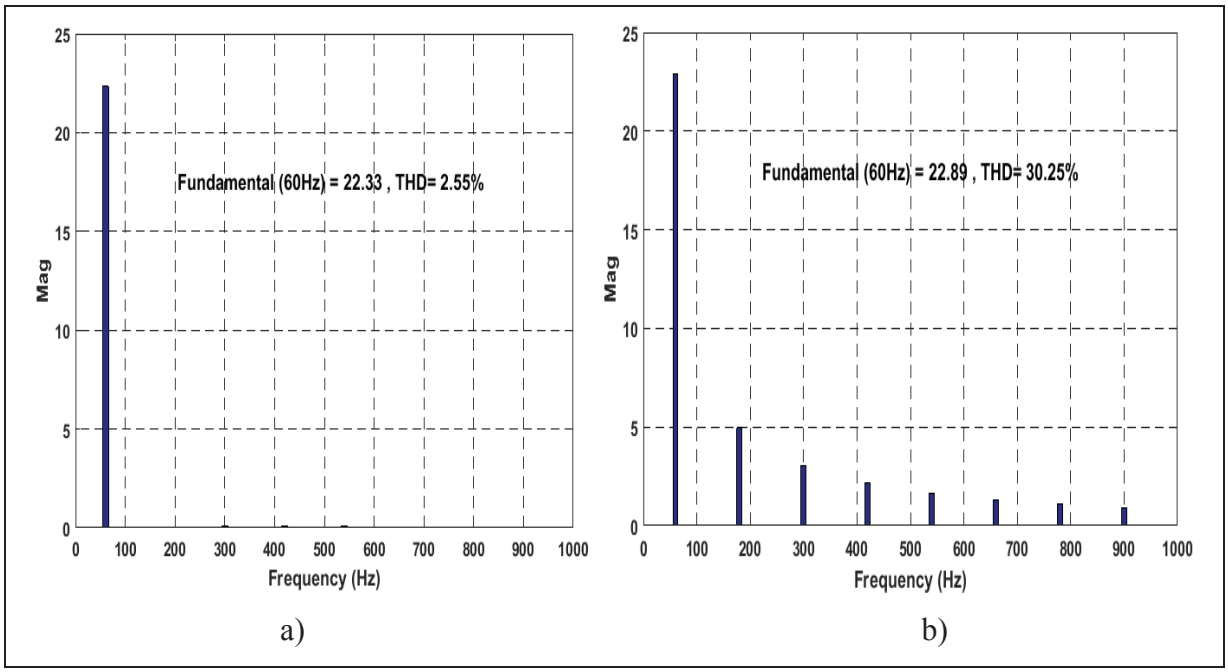

Figure 4.29 Harmonic spectrum a) Source current b) Load current

CONCLUSION

In this research, a study was dedicated to improve power quality problems.in a train railway traction and electric charging vehicles power supply. A proposed configuration combining a three-phase grid, Leblanc transformer, two single phases five levels inverters and a PV solar for multitasking use was proposed. The configuration is tested for two kinds of applications, namely the charging of electrical vehicle integrated with a group of residency. The simulation results give completely satisfactory, and the currents in the grid are fully compensated (current harmonics, unbalance load current, reactive power compensation). Also is tested the PV solar integration to reduce pressure on the grid side, especially during peak power demand.

Moreover, the proposed configuration is tested to supply a railway train by generating two single phase systems, each phase will supply the line, and the DC may be used to integrate a bank of energy storage battery systems or send this energy directly back to the grid during braking with recuperation.

To control the power converters, a sliding mode controller was adopted, the controllers were arranged in such way that the currents can flow between the two converters equally sharing the available power.

Two applications were targeted by this project namely the residential single phase one which necessitate having its own electric charging vehicle and the train railway traction to integrate solar energy to reduce the air pollution and to reduce the cost. Moreover, the main electrical aim of using the Le-Blanc transformer connection is to feed the single-phase power to electrical vehicles plug in from the general and perhaps weak three-phase system to keep the main grid currents balanced.

FUTURE WORK

Future work on finding more efficient means for optimizing the Power Quality while managing the peak power demand with the ultimate aim of building more stable and reliable energy supply system for single phase traction system is suitable. More efficient integration of renewable energy sources for railway systems should be the goal to be followed; mainly because of many advantages obtained by such approach instead of only limiting the effort on renewable energy for residential applications. Moreover, among the technical challenges one can find battery-charging systems for electric vehicles connected to single output side of Leblanc Transformer, this latter brings the difficulty of single supply stability on the double outputs available connection offered by the use of LeBlanc transformer, while the other output has no load. Furthermore, focus on the regulation of both converters in case of renewable energy injection into the DC bus while keeping the DC rail voltage constant. Finally, a thorough comparison between the proposed topology and other typologies aiming to have the best choice for such application. A second order sliding mode control along with chattering elimination problems should also be considered in future work.

BIBLIOGRAPHY

Akagi, H., Y. Kanazawa et A. Nabae. 1984. « Instantaneous Reactive Power Compensators Comprising Switching Devices without Energy Storage Components ». *IEEE Transactions on Industry Applications,* vol. IA-20, n^{o} 3, p. 625-630.

Veuillez sélectionner un type de document autre que « Generic » afin de faire afficher la référence bibliographique.

Veuillez sélectionner un type de document autre que « Generic » afin de faire afficher la référence bibliographique.

Bedford, Burnice Doyle, et Richard Gibson Hoft. 1964. « Principles of inverter circuits ».

Bin-Kwie, Chen, et Guo Bing-Song. 1996. « Three phase models of specially connected transformers ». *IEEE Transactions on Power Delivery,* vol. 11, n^{o} 1, p. 323-330.

Bor-Ren, Lin, et Wei Ta-Chang. 2004. « Space vector modulation strategy for an eight-switch three-phase NPC converter ». *IEEE Transactions on Aerospace and Electronic Systems,* vol. 40, n^{o} 2, p. 553-566.

Chaulagain, M., et B. Diong. 2016. « Forced redundant states of 5-level single-phase diode-clamped multilevel inverters ». In *SoutheastCon 2016*. (March 30 2016-April 3 2016), p. 1-7.

Chen, T. H., et H. Y. Kuo. 1995. « Network modeling of traction substation transformers for studying unbalance effects ». *IEE Proceedings - Generation, Transmission and Distribution,* vol. 142, n^{o} 2, p. 103-108.

Chen, Tsai-Hsiang. 1994. « Comparison of Scott and Leblanc transformers for supplying unbalanced electric railway demands ». *Electric Power Systems Research,* vol. 28, n^{o} 3, p. 235-240.

Dallinger, D., D. Krampe et M. Wietschel. 2011. « Vehicle-to-Grid Regulation Reserves Based on a Dynamic Simulation of Mobility Behavior ». *IEEE Transactions on Smart Grid,* vol. 2, n^{o} 2, p. 302-313.

Das, S., et G. Narayanan. 2012. « Novel Switching Sequences for a Space-Vector-Modulated Three-Level Inverter ». *IEEE Transactions on Industrial Electronics,* vol. 59, n^{o} 3, p. 1477-1487.

Dat, M. T., T. Wijnhoven et J. Driesen. 2012. « Fault-tolerant topology of a grid-connected PV inverter coupled by a Scott transformer ». In *2012 10th International Power & Energy Conference (IPEC)*. (12-14 Dec. 2012), p. 428-433.

Escalante, M. F., J. C. Vannier et A. Arzande. 2002. « Flying capacitor multilevel inverters and DTC motor drive applications ». *IEEE Transactions on Industrial Electronics,* vol. 49, n° 4, p. 809-815.

Franquelo, L. G., J. Rodriguez, J. I. Leon, S. Kouro, R. Portillo et M. A. M. Prats. 2008. « The age of multilevel converters arrives ». *IEEE Industrial Electronics Magazine,* vol. 2, n° 2, p. 28-39.

Guerrero, J. M., L. Garcia de Vicuna, J. Miret, J. Matas et M. Castilla. 2002. « A nonlinear feed-forward control technique for single-phase UPS inverters ». In *IEEE 2002 28th Annual Conference of the Industrial Electronics Society. IECON 02*. (5-8 Nov. 2002) Vol. 1, p. 257-261 vol.1.

Haddad, M., S. Rahmani, A. Hamadi et K. Al-Haddad. 2015. « New Single Phase Multilevel reduced count devices to Perform Active Power Filter ». In *SoutheastCon 2015*. (9-12 April 2015), p. 1-6.

He, Zhengyou, Zheng Zheng et Haitao Hu. 2016. « Power quality in high-speed railway systems ». *International Journal of Rail Transportation,* vol. 4, n° 2, p. 71-97.

Jinjun, Liu, Yang Jun et Wang Zhaoan. 1999. « A new approach for single-phase harmonic current detecting and its application in a hybrid active power filter ». In *Industrial Electronics Society, 1999. IECON '99 Proceedings. The 25th Annual Conference of the IEEE*. (1999) Vol. 2, p. 849-854 vol.2.

Khadkikar, V., et A. Chandra. 2008. « A New Control Philosophy for a Unified Power Quality Conditioner (UPQC) to Coordinate Load-Reactive Power Demand Between Shunt and Series Inverters ». *IEEE Transactions on Power Delivery,* vol. 23, n° 4, p. 2522-2534.

Khadkikar, V., et A. Chandra. 2012. « Control of single-phase UPQC in synchronous d-q reference frame ». In *2012 IEEE 15th International Conference on Harmonics and Quality of Power*. (17-20 June 2012), p. 378-383.

Khadkikar, V., A. Chandra et B. N. Singh. 2009. « Generalised single-phase p-q theory for active power filtering: simulation and DSP-based experimental investigation ». *IET Power Electronics,* vol. 2, n° 1, p. 67-78.

Khadkikar, V., M. Singh, A. Chandra et B. Singh. 2010. « Implementation of single-phase synchronous d-q reference frame controller for shunt active filter under distorted

voltage condition ». In *2010 Joint International Conference on Power Electronics, Drives and Energy Systems & 2010 Power India*. (20-23 Dec. 2010), p. 1-6.

Khajehoddin, S. A., M. Karimi-Ghartemani, A. Bakhshai et P. Jain. 2009. « A nonlinear approach to control instantaneous power for single-phase grid-connected photovoltaic systems ». In *2009 IEEE Energy Conversion Congress and Exposition*. (20-24 Sept. 2009), p. 2206-2212.

Khomfoi, Surin, et Leon M Tolbert. 2007. « Multilevel power converters ». *Power electronics handbook*, p. 451-482.

Kneschke, T. A. 1985. « Control of Utility System Unbalance Caused by Single-Phase Electric Traction ». *IEEE Transactions on Industry Applications,* vol. IA-21, n^{o} 6, p. 1559-1570.

Komurcugil, H. 2009. « Nonlinear control strategy for single-phase PWM current-source inverters ». In *2009 35th Annual Conference of IEEE Industrial Electronics*. (3-5 Nov. 2009), p. 682-687.

Kouro, S., M. Malinowski, K. Gopakumar, J. Pou, L. G. Franquelo, B. Wu, J. Rodriguez, M. A. Perez et J. I. Leon. 2010. « Recent Advances and Industrial Applications of Multilevel Converters ». *IEEE Transactions on Industrial Electronics,* vol. 57, n^{o} 8, p. 2553-2580.

Lewicki, A., Z. Krzeminski et H. Abu-Rub. 2011. « Space-Vector Pulsewidth Modulation for Three-Level NPC Converter With the Neutral Point Voltage Control ». *IEEE Transactions on Industrial Electronics,* vol. 58, n^{o} 11, p. 5076-5086.

Mahmud, M. A., H. R. Pota et M. J. Hossain. 2014. « Nonlinear Current Control Scheme for a Single-Phase Grid-Connected Photovoltaic System ». *IEEE Transactions on Sustainable Energy,* vol. 5, n^{o} 1, p. 218-227.

Malinowski, Mariusz, K Gopakumar, Jose Rodriguez et Marcelo A Perez. 2010. « A survey on cascaded multilevel inverters ». *IEEE transactions on industrial electronics,* vol. 57, n^{o} 7, p. 2197-2206.

Marra, Francesco, E Larsen et C Træholt. 2013. « Electric Vehicles Integration in the Electric Power System with Intermittent Energy Sources-The Charge/Discharge infrastructure ». PhD thesis, Technical University of DenmarkDanmarks Tekniske Universitet, Department of Electric Power EngineeringInstitut for Elteknik.

Martins, J., C. Martins et V. F. Pires. 2015. « A modeling scheme for the Le Blanc transformer ». In *2015 9th International Conference on Compatibility and Power Electronics (CPE)*. (24-26 June 2015), p. 25-30.

Mazin, H. E., et W. Xu. 2008. « An investigation on the effectiveness of Scott transformer on harmonic reduction ». In *2008 IEEE Power and Energy Society General Meeting - Conversion and Delivery of Electrical Energy in the 21st Century*. (20-24 July 2008), p. 1-4.

Mazin, Hooman Erfanian, et Joey Gallant. 2010. « A Probabilistic Analysis on the Harmonic Cancellation Characteristics of the Scott Transformer ». *Journal of Electromagnetic Analysis and Applications,* vol. 2, n° 01, p. 18.

Veuillez sélectionner un type de document autre que « Generic » afin de faire afficher la référence bibliographique.

Meynard, T. A., et H. Foch. 1992. « Multi-level conversion: high voltage choppers and voltage-source inverters ». In *Power Electronics Specialists Conference, 1992. PESC '92 Record., 23rd Annual IEEE*. (29 Jun-3 Jul 1992), p. 397-403 vol.1.

Mochinaga, Yoshifumi, Yoshio Akatsuka, Kohichi Arai et Masaru Ono. 1991. « Development of three-winding transformer for Shinkansen auto-transformer feeding system receiving extra-high voltage ». *IEEJ Transactions on Industry Applications,* vol. 111, n° 3, p. 237-244.

Nabae, A., I. Takahashi et H. Akagi. 1981. « A New Neutral-Point-Clamped PWM Inverter ». *IEEE Transactions on Industry Applications,* vol. IA-17, n° 5, p. 518-523.

Pires, V. F., M. Guerreiro, J. F. Martins et J. F. Silva. 2011. « Three-phase multilevel inverter based on LeBlanc transformer ». In *2011 7th International Conference-Workshop Compatibility and Power Electronics (CPE)*. (1-3 June 2011), p. 150-154.

Pires, Vitor, JF Martins, D Foito et Chen Hão. 2012. « A grid connected photovoltaic system with a multilevel inverter and a Le-Blanc transformer ». *International Journal of Renewable Energy Research (IJRER),* vol. 2, n° 1, p. 84-91.

Rodriguez, J., Lai Jih-Sheng et Peng Fang Zheng. 2002. « Multilevel inverters: a survey of topologies, controls, and applications ». *IEEE Transactions on Industrial Electronics,* vol. 49, n° 4, p. 724-738.

Rodriguez, Jose, Steffen Bernet, Peter K Steimer et Ignacio E Lizama. 2010. « A survey on neutral-point-clamped inverters ». *IEEE transactions on Industrial Electronics,* vol. 57, n° 7, p. 2219-2230.

Rojas, R., T. Ohnishi et T. Suzuki. 1995. « An improved voltage vector control method for neutral-point-clamped inverters ». *IEEE Transactions on Power Electronics,* vol. 10, n° 6, p. 666-672.

Salaet, J., S. Alepuz, A. Gilabert, J. Bordonau et J. Peracaula. 2002. « D-Q modeling and control of a single-phase three-level boost rectifier with power factor correction and neutral-point voltage balancing ». In *2002 IEEE 33rd Annual IEEE Power Electronics Specialists Conference. Proceedings (Cat. No.02CH37289)*. (2002) Vol. 2, p. 514-519 vol.2.

Santos, T., J. G. Pinto, P. Neves, D. Gonçalves et J. L. Afonso. 2009. « Comparison of three control theories for single-phase Active Power Filters ». In *2009 35th Annual Conference of IEEE Industrial Electronics*. (3-5 Nov. 2009), p. 3637-3642.

Sotoodeh, Pedram. 2014. *A single-phase multi-level D-STATCOM inverter using modular multi-level converter (MMC) topology for renewable energy sources*. Kansas State University.

Standard, IEC. 2004. « 61000-3-2: 2004, Limits for harmonic current emissions ». *International Electromechanical Commission. Geneva*.

Steimer, P. K., H. E. Gruning, J. Werninger, E. Carroll, S. Klaka et S. Linder. 1997. « IGCT-a new emerging technology for high power, low cost inverters ». In *Industry Applications Conference, 1997. Thirty-Second IAS Annual Meeting, IAS '97., Conference Record of the 1997 IEEE*. (5-9 Oct 1997) Vol. 2, p. 1592-1599 vol.2.

Tolbert, L. M., et F. Z. Peng. 2000. « Multilevel converters as a utility interface for renewable energy systems ». In *2000 Power Engineering Society Summer Meeting (Cat. No.00CH37134)*. (2000) Vol. 2, p. 1271-1274 vol. 2.

Vahedi, Hani. 2016. « Modeling, development and control of multilevel converters for power system application ». École de technologie supérieure.

Metri, Julie, Hani Vahedi, Hadi Kanaan et Kamal Al-Haddad. 2016. « Real-Time Implementation of Model Predictive Control on 7-Level Packed U-Cell Inverter ». IEEE Trans. Ind. Electron., vol. 63, no 7, p. 4180-4186.

Sebaaly, Fadia, Hani Vahedi, Hadi Kanaan, Nazih Moubayed et Kamal Al-Haddad. 2016. « Design and Implementation of Space Vector Modulation Based Sliding Mode Control for Grid-Connected 3L-NPC Inverter ». IEEE Trans. Ind. Electron., vol. 63, no 12, p. 7854-7863.

Vahedi, H., et K. Al-Haddad. 2016a. « Real-Time Implementation of a Seven-Level Packed U-Cell Inverter with a Low-Switching-Frequency Voltage Regulator ». IEEE Trans. Power Electron., vol. 31, no 8, p. 5967-5973.

Vahedi, H., P. Labbe et K. Al-Haddad. 2016. « Sensor-Less Five-Level Packed U-Cell (PUC5) Inverter Operating in Stand-Alone and Grid-Connected Modes ». IEEE Trans. Ind. Informat., vol. 12, no 1, p. 361-370.

Vahedi, H., A. Shojaei, A. Chandra et K. Al-Haddad. 2016. « Five-Level Reduced-Switch-Count Boost PFC Rectifier with Multicarrier PWM ». IEEE Trans. Ind. Applications, vol. 52, no 5, p. 4201-4207.

Vahedi, H., A. Shojaei, L-A. Dessaint et K. Al-Haddad. 2018. « Reduced DC Link Voltage Active Power Filter Using Modified PUC5 Converter ». IEEE Trans. Power Electron., vol. 33, no 2, p. 943-947.

Vahedi, Hani, et Kamal Al-Haddad. 2016b. « A Novel Multilevel Multi-Output Bidirectional Active Buck PFC Rectifier ». IEEE Trans. Ind. Electron., vol. 63, no 9, p. 5442 - 5450.

Vahedi, Hani, Sharifzadeh Mohammad et Kamal Al-Haddad. 2018. « Modified Seven-Level Pack U-Cell Inverter for Photovoltaic Applications ». IEEE Journal Emerg. and Select. Topics in Power Electron., vol. PP, no 99, p. 1.

Wu, B, High-Power Converters et AC Drives. 2006. « New York/Piscataway ». *NJ: Wiley/IEEE Press*, n^{o} 0.5, p. 1.

Zhang, R., M. Cardinal, P. Szczesny et M. Dame. 2002. « A grid simulator with control of single-phase power converters in D-Q rotating frame ». In *2002 IEEE 33rd Annual IEEE Power Electronics Specialists Conference. Proceedings (Cat. No.02CH37289)*. (2002) Vol. 3, p. 1431-1436 vol.3.